An investigation of eucalypt foliar oil gland chemistry

Allison M. Heskes

Submitted in total fulfilment of the requirements of the degree of

Doctor of Philosophy

School of Botany
THE UNIVERSITY OF MELBOURNE

September 2014

Produced on archival quality paper.

Abstract

Plants produce an extensive array of specialised metabolites, chemicals that are in addition to those that are essential for the basic functioning of the plant. These metabolites have evolved in response to the many selective pressures experienced by plants. Terpenoids form a large class of specialised metabolites and are important mediators of many ecological interactions. They can protect plants from pests and diseases, suppress competitors and attract pollinators. The work presented in this thesis focuses on the terpenoid chemistry of *Eucalyptus*, a genus with significant ecological and economic importance. Species in this genus produce an essential oil rich in mono- and sesquiterpenes (collectively termed terpenes). The oil is synthesised and stored in glands that are present throughout the plant but are particularly abundant in leaves. Until recently this was considered to be the only function of oil glands but new evidence suggests they may have a much broader role to play in terpenoid metabolism. The overall aim of this thesis is to explore this idea further with a focus on a specific group of terpenoids, the monoterpene-acid sugar esters (MSEs).

Firstly, the prevalence and diversity of MSEs in eucalypt oil glands was investigated using a high resolution LC-FTMS approach. Tandem MS experiments with three purified MSEs showed a characteristic fragmentation pattern. Along with accurate mass measurements, this was used to identify known and novel MSEs in the oil gland extracts of 18 species. Eight known and 10 novel MSEs were identified using this method. The use of the fragmentation pattern was validated with the structural elucidation by NMR of one of these novel compounds, named here as eucaglobulin B. The results of this study indicate that MSEs are common constituents of oil glands supporting the idea that these structures are a more general site of terpenoid accumulation and possibly biosynthesis in eucalypts. Interestingly, the non-volatile extract from oil glands of four species from the

subgenus *Eucalyptus* were dominated by flavonoids rather than MSEs, one of which was purified and identified with NMR as the defence compound pinocembrin. This finding indicates that oil glands are also involved in the storage of non-terpenoid constituents.

The next section of research set out to examine the relationship between MSEs and terpenes, two major groups of terpenoids present in oil glands. Firstly, essential oil and MSE variation was quantified across two populations of *E. polybractea*. Both groups of terpenoids were highly variable ranging between 27 and 161 mg g^{-1} DW and 4 and 25 mg g^{-1} DW for terpenes and MSEs, respectively. There was evidence of a strong positive relationship between MSE and terpene concentration with regression analysis of both populations returning r^2 values of >0.7.

To investigate the processes governing this relationship a plant was pulsed with $^{13}CO_2$ and the incorporation of ^{13}C into MSEs and terpenes was measured in both young expanding and mature leaves over five days. ^{13}C was rapidly incorporated into MSE, monoterpene and sesquiterpene pools in expanding leaves. Biosynthesis of monoterpenes and the major MSE, cuniloside B was also detected in mature leaves. Despite the large difference in concentration between different terpenoids (e.g. 664 μg leaf^{-1} 1,8-cineole compared to 110 μg leaf^{-1} cuniloside B) the ^{13}C enrichment of their respective pools was comparable in expanding leaves. This result is consistent with a model of regulation at this stage of development in which biosynthesis is the major determinant of pool composition, metabolites are being added to existing pools at a steady rate that is reflective of their pool size, with turnover and volatilisation having a relatively minor impact. The exception to this trend was the monoterpene, α-terpineol. ^{13}C enrichment followed a pattern consistent with this metabolite being turned-over. It is hypothesised that this monoterpene is further metabolised to oleuropeic acid and incorporated into MSEs.

The final section of research investigated the spatial organisation of metabolites within oil glands, specifically, the volatile essential oil and the immiscible, non-volatile component (NVC) comprised largely of MSEs. Because this type of oil gland is embedded in leaf tissue, previous investigations of eucalypt oil glands, and similar glands from other species, have used sectioned material. This has resulted in the loss

of cavity contents and as a consequence, it is not known if there is spatial segregation of metabolites within these structures. To overcome this problem a multiphoton fluorescence lifetime imaging method was developed. Intact enzymatically isolated oil glands from *E. polybractea* and *E. spathulata* were imaged to a depth of $\sim$80 μm. The NVC was shown to form a layer between the secretory cells lining the oil gland cavity and the essential oil. This finding could be indicative of a functional role of the NVC in providing a protective region of low diffusivity between the secretory cells of the oil gland and potentially autotoxic essential oil.

Through the investigation of the composition, ubiquity, localisation and regulation of oil gland metabolites, the work presented in this thesis provides new information on a major aspect of eucalypt chemistry. This research will hopefully pave the way for future investigations of terpenoid biosynthesis, regulation and function in this genus.

Declaration

This is to certify that:

i. the thesis comprises only my original work towards the PhD except where indicated in the Preface,

ii. due acknowledgement has been made in the text to all other material used,

iii. the thesis is less than 100,000 words in length, exclusive of tables, maps, references and appendices.

Allison M. Heskes, September 2014

Acknowledgements

I would like to thank my supervisors Prof Ian Woodrow, Dr Jason Goodger and Assoc. Prof Trevor Smith for all their support, advice and encouragement over the years.

To my lab mates Samanta, Wei Han, Marianne, Maddie, Victor, Sarah, Ed and Lizzie, thank you all so much for your friendship.

The School of Botany has been a fantastic place to study and work and I thank all of the people there that have helped me along the way. Special thanks to John Pederick for always being there to give both technical and emotional support. I would like to thank Damien Callahan and Berin Boughton for training me in all things LC-MS and also Berin for his incredible patience and good humour when faced with my many, many questions and requests. To Daniel Dias, who was always willing to run my samples on the GC-MS at short notice, thank you. Thank you to Spencer Williams and his group at Bio21 for helping with chemical structure elucidation, Lachlan McKimmie for help with the MP-FLIM work and to my mum for being a fantastic field assistant.

The School of Botany Foundation provided me with several scholarships over the years for which I am very grateful. The Holsworth Wildlife Research Endowment also provided my project with funding for three years and this enabled me to carry out essential field work and experiments that would otherwise have been difficult to undertake. This is an invaluable endowment that has helped many students through their postgraduate studies. Thank you.

I would also like to thank my lab group at the University of Copenhagen for welcoming me into their group and for helping to keep me sane through the final stages of my PhD. I am particularly grateful to Birger Lindberg Møller for inviting me to visit, but even more so for his infectious enthusiasm and energy for science that has helped me to think about my project in news ways.

Finally, thank you to my friends and family for always being there ready to lend a hand and enduring my ups and downs through this journey. To Flo, thank you for sitting with me and going over drafts when I got stuck, fixing my computer problems, your words of wisdom and your belief in me. It has meant a lot. To Lauren and Andrew, thank you for your understanding, your friendship and your kindness.

My mum and dad can not be thanked enough for their constant support throughout this PhD. And thank you to my brother Michael, who can always be relied on to put things in perspective.

Preface

The data presented in Chapter 2, terpene and MSE quantification data from Chapter 3, and fluorescence lifetime images of *E. polybractea* and *E. spathulata* secretory complexes from Chapter 4 have been published in:

> **Heskes AM, Goodger JQD, Tsegay S, Quach T, Williams SJ and Woodrow IE** (2012) Localization of oleuropeyl glucose esters and a flavanone to secretory cavities of Myrtaceae. PLoS ONE **7:** e40856

The quantification of cuniloside B and cypellocarpin C presented in Chapter 2 has been published in:

> **Hakki Z, Cao B, Heskes AM, Goodger JQD, Woodrow IE, Williams SJ** (2010) Synthesis of the monoterpene esters cypellocarpin C and cuniloside B and evidence for their widespread occurrence in *Eucalyptus*. Carbohydrate Research **345:** 2079-2084

Sections of Chapter 4 have been published in:

> **Heskes AM, Lincoln CN, Goodger JQD, Woodrow IE, Smith TA** (2012) Multiphoton fluorescence lifetime imaging shows spatial segregation of secondary metabolites in *Eucalyptus* secretory cavities. Journal of Microscopy **247:** 33-42

IR and NMR experiments and data analysis presented in Chapter 2 were carried out by Sammy Tsegay, Tim Quach and Spencer Williams at the Bio21 Institute, The University of Melbourne. Berin Boughton provided LC-MS technical support and Daniel Dias provided GC-MS technical support (Metabolomics Australia, The University of Melbourne). MP-FLIM data was aquired with the assistance of Lachlan McKimmie.

Contents

List of Figures

List of Tables

Chapter 1

Introduction- *Eucalyptus* terpenoid chemistry

1.1 The genus *Eucalyptus*

Eucalyptus is a species-rich tree genus that dominates the Australian landscape. It contains over 600 species divided across seven subgenera (Ladiges, 1997). The largest subgenus is *Symphyomyrtus*, consisting of over 300 species, followed by *Eucalyptus* with 120 species. The remaining subgenera are small and consist of 1-20 species (Brooker, 2000). There are also two closely related sister genera, *Corymbia* and *Angophora*, that some consider to be sub-genera within the *Eucalyptus* genus (Brooker, 2000; Ladiges and Udovicic, 2000).

Eucalypts are evergreen with the exception of some drought-deciduous species. They range in form from tall straight-boled taxa, including *E. regnans* the tallest flowering plant in the world, to smaller multi-stemmed trees and in a few instances shrubs. Members of this genus form the foundation species of the majority of wooded ecosystems in Australia and generally occupy the tallest vegetation stratum in a community (Kirkpatrick, 1997). Consequently, they have a significant impact on the water availability, nutrients and irradiance levels experienced by other species and are thus major determinants of community structure.

The drying out of the Australian climate after separation of the continent from Gondwana and an increase in fire frequency have been cited as the main drivers of eucalypt evolution and radiation (Crisp *et al.*, 2011; Crisp *et al.*, 2004; Gill, 1997; Wardell-Johnson *et al.*, 1997). As a result, eucalypts are characterised by sclerophyllous foliage

which is considered to be an adaptation to both low nutrients and water availability (Medina *et al.*, 1990; Salleo *et al.*, 1997). In addition, leaves are usually isobilateral and vertically oriented, particularly in arid and semi-arid regions and this morphology is likely an adaptation to high irradiance and low water availability as it reduces light interception resulting in reduced leaf temperatures (King, 1997; James and Bell, 2000). Furthermore, adaptations to fire include thick, insulative bark and the ability to resprout from epicormic buds and lignotubers (Gill, 1997).

In addition to these characteristic morphological and physiological traits, eucalypts have evolved a complex specialised chemistry in response to the many abiotic and biotic challenges faced over time. Along with a diverse array of phenolic compounds, terpenoids make up a major component of the secondary chemistry of this genus. Chemically complex mixtures of mono- and sesquiterpenes are commonly found in leaves in the form of volatile essential oils. A variety of non-volatile terpenoids are also present including triterpenoids, terpene-phloroglucinols and monoterpene-acid sugar esters. Aspects of the distribution and regulation of this latter group form the major focus of research presented in this thesis. To provide a context for this research, the remainder of this chapter aims to review the current state of knowledge on the chemistry, function and regulation of terpenoids in the genus *Eucalyptus*.

1.2 Terpenoids

Terpenoids are a ubiquitous class of chemicals in plants and are involved in both primary and secondary metabolism. They are built from five-carbon isoprene units that are combined to form different terpene subclasses: hemiterpenes contain one unit, while monoterpenes are composed of two units, sesquiterpenes of three units, diterpenes of four units, triterpenes of six units and so on up to polyterpenes such as those that make up rubber, consisting of thousands of isoprene units. These terpene backbones can be further rearranged and decorated with various functional groups to generate the diverse structures found in nature.

Terpenoids play an essential role in primary metabolism, for example as hormones and pigments (Fig. 1.1; Vranová *et al.*, 2013). Many however have no clear function in primary metabolism but are instead involved in, or are considered to be involved in, a plethora of ecological interactions. One of the major functions of these terpenoids is in plant defence (for example: Huang *et al.*, 2012; Miller *et al.*, 2005; Rasmann *et al.*, 2005). They can perform this function directly as toxins or by forming physical barriers to stop pests entering the plant (Becerra and Venable, 1990; Zulak and Bohlmann, 2010). For example, in some *Bursera* species a mixture of terpenoids are stored in pressurised canals that form a reticulated network in leaves. When insects bite through these canals they are squirted with the toxic resin and repelled (Becerra and Venable, 1990). Some plants release volatile terpenoids when damaged to attract predators or repel pests (Mumm *et al.*, 2003; Schnee *et al.*, 2007). For example, when maize is attacked by lepidopteran larvae, a mixture of sesquiterpenes is emitted from the damaged tissue attracting a parasitic wasp that oviposits in the larvae, eventually killing it (Schnee *et al.*, 2007). In this example, terpenes are induced in response to attack but many plants constitutively produce and store terpenoids in their tissue. Where terpenes are accumulated in plant tissue they are often stored in specialised structures such as resin ducts, oil cells, and glandular trichomes (Becerra and Venable, 1990; Turner *et al.*, 2000; Zulak and Bohlmann, 2010). This strategy enables plants to store defensively effective levels of compounds while avoiding self-toxicity.

A host of other ecologic interactions between plants and other organisms are mediated by terpenoids. For example, terpenes are emitted from flowers to attract pollinators (Dudareva *et al.*, 2006; Wright *et al.*, 2005) and released from roots where they are involved in interactions between mycorrhizal symbionts (Akiyama *et al.*, 2005). Furthermore, there is evidence that volatile terpenes are potentially involved in resistance to abiotic stress acting to protect photosynthetic machinery against heat induced oxidative stress (Loreto *et al.*, 2004).

Terpenoids are also harvested and utilised by humans and are used as solvents, food additives, fragrances, antibacterials and pharmaceuticals (Zwenger and Basu, 2008). Of particular recent interest are compounds with strong specific bioactivity towards a range

of human pathogens and diseases. Examples of pharmaceutically important terpenoids include the antimalarial sesquiterpene lactone artemisinin derived from *Artemisia annua* (Klayman, 1985) and the anti-cancer diterpene ester, ingenol-3-angelate from *Euphorbia peplus* (Ramsay *et al.*, 2011).

1.2.1 Terpenoid biosynthesis

The basic building blocks of terpenoids are isopentenyl diphosphate (IPP) and its isomer dimethylallyl diphosphate (DMAPP), also called isoprene units. IPP and DMAPP are both the products of two spatially separated pathways (Rodriguez-Concepcion and Boronat, 2002). The methylerythritol phosphate (MEP) pathway is plastid localised, whereas the mevalonic acid (MVA) pathway operates between the cytosol, peroxisomes and endoplasmic reticulum (Fig.1.1; Leivar *et al.*, 2005; Simkin *et al.*, 2011; Vranová *et al.*, 2013). The products of the MEP pathway provide the precursors of monoterpenes, diterpenes and tetraterpenes whereas products of the MVA pathway provide precursors for sesquiterpene and triterpene biosynthesis (Rodriguez-Concepcion and Boronat, 2002). Although this is the general rule, cross-talk between the pathways also occurs (Dudareva *et al.*, 2005; Hampel *et al.*, 2005; Hemmerlin *et al.*, 2012). For example, in snapdragon flowers, MEP pathway derived precursors are exported from the plastid to the cytosol and contribute to the cytosolic production of the sesquiterpene nerolidol (Dudareva *et al.*, 2005).

IPP and DMAPP are combined in head-to-head or head-to-tail condensation reactions catalysed by short-chain prenyltransferases. The resulting linear pyrophosphates form the direct precursor of the different terpene subclasses. Monoterpenes (C_{10}) are formed from geranyl pyrophosphate (GPP), sesquiterpenes (C_{15}) and triterpenes (C_{30}) are formed from farnesyl pyrophosphate (FPP), and diterpenes (C_{20}) and tetraterpenes (C_{40}) are formed from geranylgeranyl pyrophosphate (GGPP) (Liang *et al.*, 2002). Terpene synthases (TPSs) catalyse the conversion of these pyrophosphate precursors into a multitude of cyclic and acyclic terpene carbon skeletons (Chen *et al.*, 2011). Further diversification of terpenes occurs through the addition of functional groups to the terpene carbon backbone such as hydroxyl and carboxyl groups. In addition, these products can

then be glycosylated or incorporated into more complex chemicals that combine other classes of secondary metabolites such as monoterpene indole alkaloids.

1.3 Terpenoids in *Eucalyptus*

1.3.1 Mono- and sesquiterpenes

In terms of qualitative and quantitative abundance, the major classes of terpenoids present in eucalypts are mono- and sesquiterpenes (referred to collectively as essential oils). These are volatile lipophilic chemicals that are accumulated in specialised oil glands. There has been a considerable effort made to document the oil profile of the majority of the over 600 eucalypt species; the data from this extensive work has been summarised in Boland *et al.* (1991) and Brophy and Southwell (2002). The results reveal a great diversity in oil composition and quantity within and between species. The oil profile of individual plants generally contain over 30 components and are frequently dominated by one or two monoterpenes (Fig. 1.2). In particular, 1,8-cineole is a common component of eucalypt oils and is often present at high proportions of total oil ($> 50\%$) (Padovan *et al.*, 2013). In some species, oil profiles are dominated by sesquiterpenes (e.g. *E. pauciflora* and *E. sieberi*; Li *et al.*, 1995) with the oxygenated sesquiterpenes globulol and α, β and γ-eudesmols often present at higher proportions than other sesquiterpenes (Fig. 1.2).

Mono- and sesquiterpene composition and quantity is highly variable within species of this genus (Andrew *et al.*, 2013; Doran *et al.*, 1995; King *et al.*, 2004; O'Reilly-Wapstra *et al.*, 2013). For example, in a natural population of *E. polybractea* the proportion of 1,8-cineole of total oil ranged continuously from 49 to 95% and the yield of total oil between 14 and 65 mg g^{-1} DW (King *et al.*, 2004). In addition, many species show chemotypic variation in essential oil composition and are marked by distinct discontinuities in terpene variation both within and between terpene subclasses (Andrew *et al.*, 2013; Boland *et al.*, 1991; Padovan *et al.*, 2012). For instance, chemotypes either dominated by monoterpenes or sesquiterpenes occur in *E. melliodora* and *E. sideroxylon* populations and

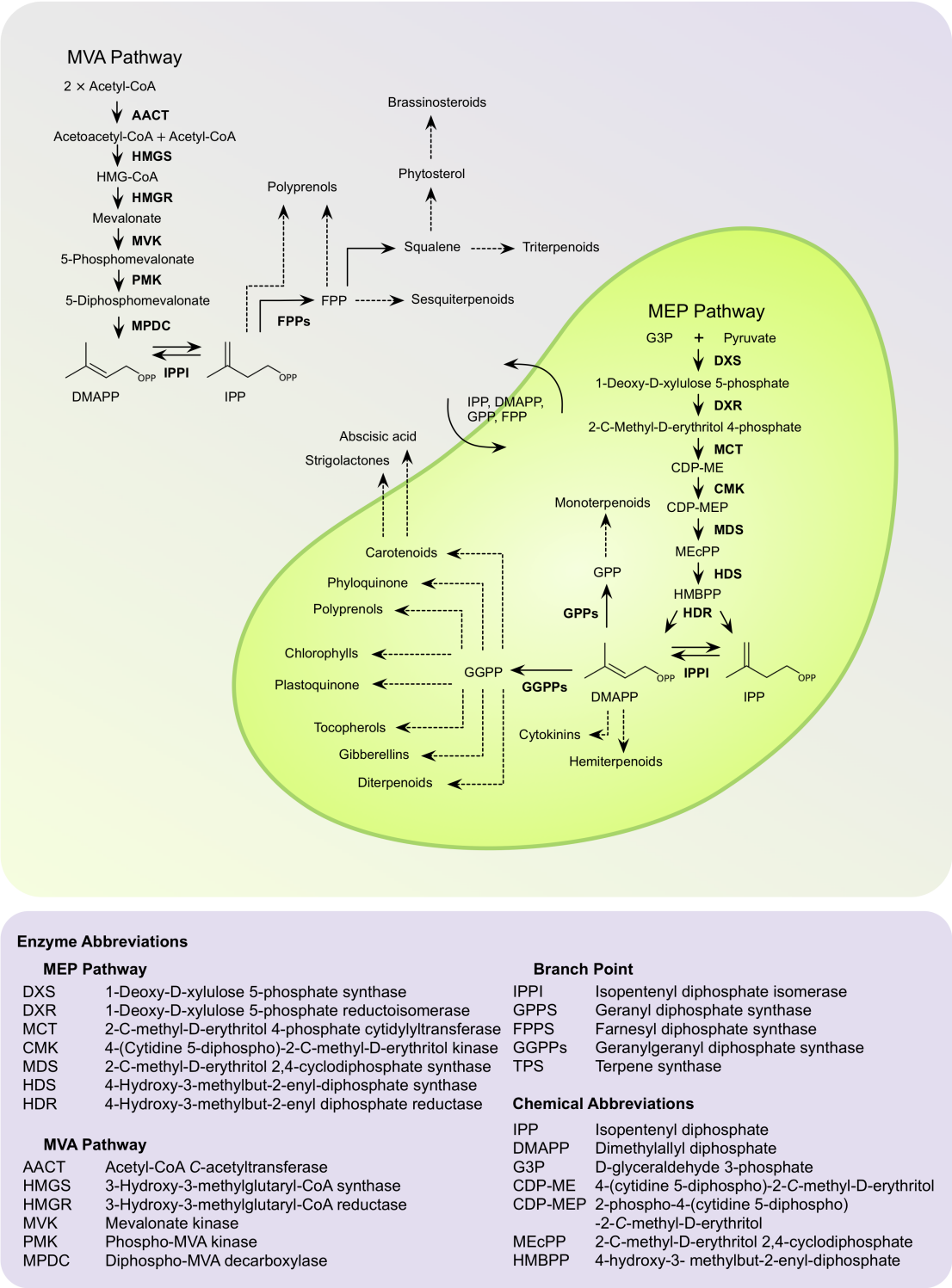

Enzyme Abbreviations

MEP Pathway

DXS	1-Deoxy-D-xylulose 5-phosphate synthase
DXR	1-Deoxy-D-xylulose 5-phosphate reductoisomerase
MCT	2-C-methyl-D-erythritol 4-phosphate cytidylyltransferase
CMK	4-(Cytidine 5-diphospho)-2-C-methyl-D-erythritol kinase
MDS	2-C-methyl-D-erythritol 2,4-cyclodiphosphate synthase
HDS	4-Hydroxy-3-methylbut-2-enyl-diphosphate synthase
HDR	4-Hydroxy-3-methylbut-2-enyl diphosphate reductase

MVA Pathway

AACT	Acetyl-CoA *C*-acetyltransferase
HMGS	3-Hydroxy-3-methylglutaryl-CoA synthase
HMGR	3-Hydroxy-3-methylglutaryl-CoA reductase
MVK	Mevalonate kinase
PMK	Phospho-MVA kinase
MPDC	Diphospho-MVA decarboxylase

Branch Point

IPPI	Isopentenyl diphosphate isomerase
GPPS	Geranyl diphosphate synthase
FPPS	Farnesyl diphosphate synthase
GGPPs	Geranylgeranyl diphosphate synthase
TPS	Terpene synthase

Chemical Abbreviations

IPP	Isopentenyl diphosphate
DMAPP	Dimethylallyl diphosphate
G3P	D-glyceraldehyde 3-phosphate
CDP-ME	4-(cytidine 5-diphospho)-2-*C*-methyl-D-erythritol
CDP-MEP	2-phospho-4-(cytidine 5-diphospho) -2-*C*-methyl-D-erythritol
MEcPP	2-C-methyl-D-erythritol 2,4-cyclodiphosphate
HMBPP	4-hydroxy-3- methylbut-2-enyl-diphosphate

Figure 1.1: Organization of terpenoid biosynthesis in the plant cell and examples of terpenoid metabolites. Arrows with solid lines indicate single enzymatic steps and arrows with dashed lines indicate multiple enzymatic steps. Names given in bold are enzymes. Figure adapted from Vranová *et al.*, 2013

were originally discovered due to marked differences in resistance to herbivorous beetles (Padovan *et al.*, 2012; Edwards *et al.*, 1993).

1.3.2 Triterpenoids

Triterpenoids have been isolated from many eucalypt species (Fig. 1.2; Begum *et al.*, 1997; Benyahia *et al.*, 2005; Li *et al.*, 1997; Pereira *et al.*, 2005; Sidana *et al.*, 2012; Wang and Fujimoto, 1993). Less is known about their diversity and distribution in this genus compared to mono- and sesquiterpenes, but they do appear to be relatively common constituents of epicuticular waxes (Horn and Lamberton, 1964; Li *et al.*, 1997; Pereira *et al.*, 2005). For example, the leaf waxes of all of the 17 symphyomyrtle species analysed by Li *et al.* (1997) contained a variety of pentacyclic triterpenoids including β-amyrin, methyl moronate, 11,12-dehydroursolic lactone acetate and several unidentified chemical species.

1.3.3 Terpene-phloroglucinols

A series of conjugated terpenoids that incorporate a phloroglucinol moiety have been isolated from eucalypts and are part of a large group of chemicals known as formylated phloroglucinol compounds (FPCs; Fig. 1.2; Ghisalberti, 1996). The terpene incorporating members of this group are split into macrocarpals and euglobals, the former incorporating sesquiterpenes and the latter incorporating either a monoterpene or sesquiterpene as well as a chroman ring in their structure (Singh and Bharate, 2006). Euglobals show the greatest structural diversity with at least 31 known compounds (Konoshima and Takasaki, 2002) while there have been at least 16 macrocarpals identified (Singh and Bharate, 2006). There is also chromatographic and mass spectral evidence from a number of species that many more macrocarpal and euglobal type compounds exist than have currently been fully structurally elucidated (Eschler *et al.*, 2000; Moore *et al.*, 2004a; Wallis *et al.*, 2010). In addition, Moore *et al.* (2004a) and Eyles *et al.* (2003) have both presented mass spectral evidence for the presence of tri- and sesterterpene-phloroglucinols in leaves and wound-wood of several species but the structure of these

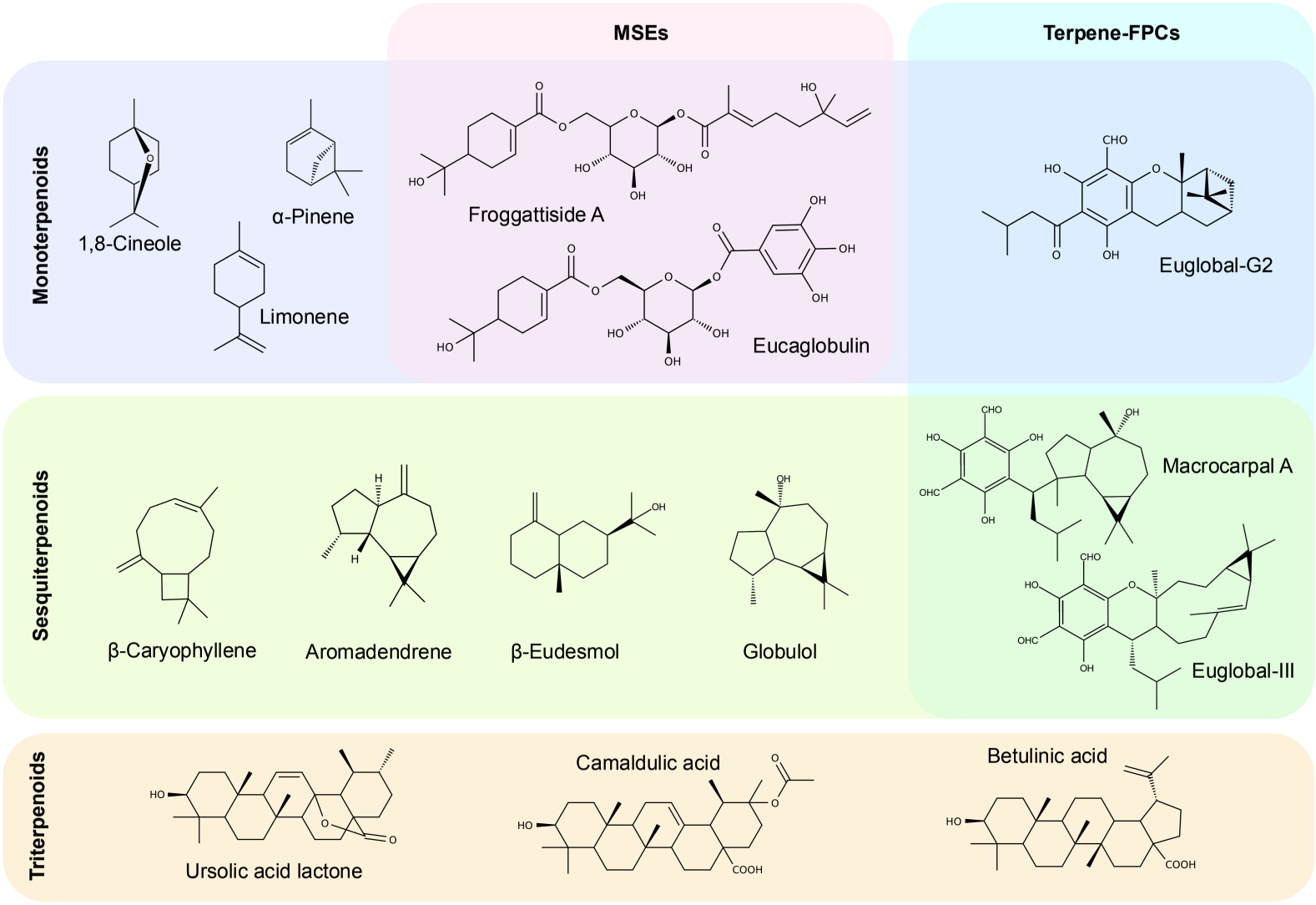

Figure 1.2: Examples of *Eucalyptus* terpenoids.

compounds has not been confirmed. Simple FPCs lacking the terpene adduct also occur (often in high concentrations), such as grandinol, jensenone and sideroxylonal (Eschler *et al.*, 2000; Ghisalberti, 1996; Moore *et al.*, 2004a).

The structural diversity of terpene-phloroglucinols stems mostly from variation in the terpene adduct. For instance, there are examples of monoterpene type euglobals incorporating α-pinene, β-pinene, γ-terpinene, α-terpinene, terpinolene, α-phellandrene and sabinene (Konoshima and Takasaki, 2002). Further structural variation arises from the substitution pattern of acyl functional groups attached to the phloroglucinol.

Macrocarpals and euglobals have a limited distribution in *Eucalyptus* and have thus far only been isolated from members of the *Symphyomyrtus* subgenus (Eschler *et al.*, 2000; Konoshima and Takasaki, 2002). While macrocarpals and euglobals are unique to *Eucalyptus*, it appears that terpene-phloroglucinols may be a feature of the Myrtaceae family with structurally similar compounds also isolated from taxa belonging to the myrtaceous genera *Kunzea* (Ito *et al.*, 2004), *Beackea* (Fujimoto *et al.*, 1996) and *Eugenia* (Faqueti *et al.*, 2013).

Like mono- and sesquiterpenes, the yield and composition of terpene-phloroglucinols is highly variable, both at the species and individual level (Moore *et al.*, 2004a; O'Reilly-Wapstra *et al.*, 2013; Wallis *et al.*, 2011). For example, the FPC content of *E. globulus*, *E. strzeleckii*, *E. ovata* and *E. viminalis* trees growing in a single community were found to vary significantly at both levels (Moore *et al.*, 2004a). Total FPC concentration ranged between zero and $\sim$60 mg g^{-1} DW. Macrocarpals were found to be qualitatively and quantitatively the largest group present in leaves of *E. globulus*, *E. viminalis* and *E. ovata*, with significant but smaller concentrations of euglobals and sideroxylonal also present. In contrast, the FPC profile of *E. strzeleckii* compared to the other species was almost completely lacking in macrocarpals and instead contained high levels of sideroxylonals and another FPC dimer, jensenal. Interestingly correlations between the concentration of both total FPCs and macrocarpals and terpenes were detected in several of these species.

1.3.4 Monoterpene-acid sugar esters

A second group of compounds incorporating terpenes are monoterpene-acid sugar esters (MSEs; Fig. 1.2; Goodger and Woodrow, 2011). MSEs are generally composed of two moieties, one or both of which are monoterpene acids, attached at the C-1 and C-6 positions of a central sugar moiety via an ester bond (commonly β-D-glucopyranose and rarely β-D-galactopyranose). The monoterpene acids are either an oleuropeic or menthiafolic acid, with the former occurring more commonly in *Eucalyptus*. In most cases the second moiety is not a monoterpene acid but a phenolic moiety, and may be bonded to the glucose via either an ester or O-linkage (Guo and Yang, 2006; Hasegawa *et al.*, 2008; Kasajima *et al.*, 2005; Tian *et al.*, 2009).

MSEs have been isolated from at least 10 eucalypt species, all of which belong to the *Symphyomyrtus* subgenus. To date, no systematic studies of MSE distribution in *Eucalyptus* have been done, so it is unknown how widely they occur in this genus. While the majority of MSEs have been found in eucalypt species, they have also been isolated from a range of species outside of this genus including *Cunila spicata* (Lamiaceae; Manns and Hartmann, 1994), *Portulaca oleracea* (Portulacaceae; Wu *et al.*, 2012) and *Jasminum hemsleyi* (Oleaceae; Tanahashi *et al.*, 1995).

1.4 Functions of terpenoids in *Eucalyptus*

Considering the prominence of terpenoids in eucalypt secondary metabolism, our understanding of their ecological and physiological functions is limited. Defining clear functions for specific terpenoids has been difficult due to the constitutive nature of their deployment, the generally complex chemistry of species, and the lack of molecular tools to artificially manipulate terpenoid biosynthesis. Nevertheless, feeding trials and correlative studies have shed some light on the defensive function of foliar mono- and sesquiterpenes, and macrocarpals. No work on elucidating the specific functions of triterpenes or MSEs has been undertaken.

1.4.1 Plant defence

Foliar monoterpenes in *Eucalyptus* and related species appear to act as insect antifeedants (Edwards *et al.*, 1993; Matsuki *et al.*, 2011; Padovan *et al.*, 2010). 1,8-Cineole concentration, in particular, has been identified as an important determinant of plant resistance to attack by some insects (Edwards *et al.*, 1993; Matsuki *et al.*, 2011; Padovan *et al.*, 2012; Stone and Bacon, 1994). For example, the ability of *E. melliodora* and *E. sideroxylon* trees to resist insect attack was shown to correlate with 1,8-cineole concentration (Padovan *et al.*, 2012). Specifically, high total oil concentration alone did not provide resistance unless trees had a high proportion of 1,8-cineole. Trees with either high proportions of sesquiterpenes or high proportions of other monoterpenes were shown to be susceptible. However, other lower abundant monoterpenes often covary with 1,8-cineole (Andrew *et al.*, 2013; Edwards *et al.*, 1993), so that the role of other monoterpenes in these interactions can not be excluded.

1,8-Cineole has also been shown to have a negative effect on marsupial browsing (Wiggins *et al.*, 2003). In controlled feeding trials, 1,8-cineole reduced foliage intake by the common brushtail possum (*Trichosurus vulpecula*) in a concentration dependent manner. In addition, feeding periods were shorter when 1,8-cineole was present in the food (Wiggins *et al.*, 2003). In addition to monoterpenes, other factors appear to be important determinants of susceptibility to attack by both insects and marsupials including the presence of other secondary metabolites and foliar nitrogen levels (Jones *et al.*, 2002; Moore and Foley, 2005; O'Reilly-Wapstra *et al.*, 2005).

The antifeedant effects of selected terpene-phloroglucinols on marsupial folivores has been well documented (Lawler *et al.*, 1999; Moore and Foley, 2005; Youngentob *et al.*, 2011). Originally, bioguided fractionation using the feeding response of the marsupial folivore and *Eucalyptus* specialist *Pseudocheirus peregrinus* (common ringtail possum) identified the terpene-phloroglucinol, macrocarpal G, as a key feeding deterrent (Pass *et al.*, 1998). A range of terpene-phloroglucinols and also simple FPCs have since been shown to have similar affects on other marsupial folivores such as *Phascolarctos cinereus* (koala), *Petauroides volans* (greater glider) and *T. vulpecula* (Moore and Foley, 2005; O'Reilly-Wapstra *et al.*, 2004; Youngentob *et al.*, 2011).

In contrast to marsupials, the role of terpene-phloroglucinols, and FPCs in general, in mediating interactions with insects is less clear. They do not appear to be an effective defence against *Paropsis* species, a genus of leaf eating beetles which are eucalypt specialists (Henery *et al.*, 2008a), but the non-terpene-FPC, sideroxylonal was shown to be effective against another group of leaf eating beetles, *Anoplognathus* species. In *E. sideroxylon* and *E. melliodora* foliar sideroxylonal concentration was negatively correlated with rates of leaf consumption of these beetles (Matsuki *et al.*, 2011). Artificial manipulation of sideroxylonal levels confirmed the importance of this secondary metabolite as a feeding deterrent.

1.4.2 Terpene emission

Eucalypts emit moderate to high levels of monoterpenes and also low to moderate levels of the hemiterpene, isoprene, from their leaves (Guenther *et al.*, 1991; He *et al.*, 2000; Winters *et al.*, 2009; Street *et al.*, 1997). A recent field based study of terpene emission from *E. globulus*, *E. grandis*, *E. camaldulensis* and *E. viminalis* reported mean monoterpene emission rates of between 175 and 375 nmol m^{-2} min^{-1} (Winters *et al.*, 2009). By comparison, emission rates of conifers that also store monoterpenes in their leaves were found to be between 30 and 150 nmol m^{-2} min^{-1} (Ghirardo *et al.*, 2010). The main emitted terpenes for all four species of eucalypt were 1,8-cineole, *p*-cymene and α-pinene. Most terpenes were emitted in a temperature dependent manner consistent with their origin being from constitutive foliar pools. The exceptions in this experiment were *cis*-ocimene and *trans*-caryophyllene which were emitted in both a temperature and light dependent manner suggesting these terpenes were being synthesised and emitted *de novo* (Winters, 2010).

The biological significance of terpene emissions from eucalypts is not understood. Some non-terpene storing species, such as various oaks, synthesise and emit terpenes in a temperature and light dependent manner (Staudt and Bertin, 1998). By inhibiting terpene production in these species and also fumigating species that do not naturally emit terpenes researchers have shown that both isoprene and monoterpenes increase the thermotolerance of plants (Loreto *et al.*, 1998, 2001, 2004). It is thought that this works

in two ways: the terpenes act as antioxidants, counteracting the reactive oxygen species that form due to heat and water stress and also by stabilising chloroplast membranes allowing photosynthesis to operate effectively under higher temperatures (Loreto and Schnitzler, 2010). Given the frequent occurrence of high temperatures paired with high solar irradiance levels and low water availability in many regions of Australia, it is conceivable that the accumulation of volatile terpenes in leaves of eucalypts may fulfil a similar function.

1.5 Terpenoid regulation in *Eucalyptus*

1.5.1 Developmental regulation of terpenoids

Terpenoid production is often under strong developmental regulation particularly in species that constitutively accumulate these compounds in their tissue. This is because the development of the specialised structures in which they are biosynthesised and stored is tied to the development of the whole organ (Majdi *et al.*, 2011; Turner *et al.*, 2000; Wang *et al.*, 2008), while changes in terpenoid profile through development has been linked to changes in enzyme activity (Bouwmeester *et al.*, 1998; McConkey *et al.*, 2000). There has been relatively few studies on eucalypt species examining how terpenoid deployment is developmentally regulated. Nevertheless, essential oil production has been the most extensively studied in this regard, and the results indicate that both amount and composition is highly regulated by development.

Essential oil concentration has been shown to increase as plants develop from seedlings to mature trees (Goodger and Woodrow, 2009; McArthur *et al.*, 2010). This is potentially a consequence of the expected high cost of oil gland formation and maintenance (Goodger and Woodrow, 2012). Oil glands occupy space in leaves that would otherwise be devoted to photosynthesis. At early stages of development it may be more beneficial for seedlings to maximise photosynthetic area rather than produce high levels of mono- and/or sesquiterpenes; however, as seedlings become established and their ability to acquire resources increases the cost of producing these terpenes is outweighed by their benefits to plant fitness (Goodger *et al.*, 2013a). This pattern of

increasing oil concentration is mirrored through leaf development (Goodger *et al.*, 2013b); however, leaf expansion seems to be the driving factor behind this increase: as leaves expand, cavities also expand and, in addition, new oil glands are initiated until leaves reach maturation (Goodger and Woodrow, 2012; List *et al.*, 1995).

Complex developmental patterns in mono and sesquiterpene composition have been noted in multiple species both at the whole plant and leaf development level (Goodger *et al.*, 2008, 2009, 2013a; McArthur *et al.*, 2010). For example, McArthur *et al.* (2010) found that monoterpenes in *E. nitens* leaves had contrasting ontogenetic trajectories. 1,8-Cineole concentration increased with seedling age but α-pinene peaked early at 50 days after sowing, declined and peaked again at around 150 days. Similar to whole plant ontogeny, developing leaves of *E. polybractea* also exhibited interesting changes in oil composition (Goodger *et al.*, 2013b). Expanding apical leaves were found to contain high proportions of the sesquiterpene β-eudesmol at $\sim$50% of total oil but this dropped to $\sim$1% by leaf maturity. In contrast, the main monoterpene, 1,8-cineole increased from 30 to 80% of total oil from apical to basal leaves. Together, these results indicate a fine scale developmental regulation of terpenoid biosynthesis in eucalypts.

Some eucalypt species exhibit heteroblasty having morphologically distinct juvenile and adult foliage types. In such species, juvenile foliage transitions to adult foliage as the whole tree develops but regrowth (i.e. coppice) after foliage loss also takes the juvenile form in mature trees. Given the relationship between oil glands and leaf morphology we might expect differences in terpenoid concentration between these leaf types. Indeed, some species such as *E. globulus* show distinct differences in chemistry between juvenile and adult foliage (O'Reilly-Wapstra *et al.*, 2007), whereas, in many others no chemical difference has been detected (Gras *et al.*, 2005; Loney *et al.*, 2006). O'Reilly-Wapstra *et al.* (2007) found that *E. globulus* coppice regrowth had significantly higher concentrations of 1,8-cineole and total oil. In contrast, there was no significant difference detected in total oil concentration between juvenile and adult leaves in either *E. nitens* or *E. regnans* (Gras *et al.*, 2005).

A detailed analysis of the developmental regulation of terpenoids other than mono- and sesquiterpenes is currently lacking. The study by O'Reilly-Wapstra *et al.* (2007)

examining coppice and adult foliage of *E. globulus* represents one of the very few reports where the ontogenetic regulation of terpene-phloroglucinols has been investigated. In contrast, to 1,8-cineole and total oil concentration, macrocarpal G was found to differ marginally between coppice and adult foliage of *E. globulus*. There is a strong relationship between sesquiterpene and macrocarpal chemistry in this and other species (Moore *et al.*, 2004a; Wallis *et al.*, 2011), supporting the idea that the same terpene synthases that give rise to the sesquiterpenes also supply the terpene adducts for macrocarpals (discussed further in section 1.6.1). The sesquiterpene chemistry was not reported in this study but such comparisons between biosynthetically related groups could provide information on how terpenoid diversity is generated and also regulated. This information could be invaluable when addressing questions regarding when macrocarpal/euglobal/MSEs are produced relative to their sesquiterpene and monoterpene precursors and how the pools of potential precursors are affected.

1.5.2 Environmental regulation of terpenoids

Abiotic

Both quantity and composition of mono- and sesquiterpenes and terpene-phloroglucinols in eucalypts are known to be under strong genetic control (Barton *et al.*, 1991; Doran and Matheson, 1994; O'Reilly-Wapstra *et al.*, 2013). Nevertheless, environmental factors do contribute a small amount to the observed variation within a species. Both King *et al.* (2006b) and O'Reilly-Wapstra *et al.* (2005) found that terpene concentration increased with fertilisation in *E. polybractea* and *E. globulus*, respectively. Furthermore, in *E. microcorys*, concentration of the main monoterpene, 1,8-cineole, was positively correlated with foliar nitrogen levels and better site quality more generally (Moore *et al.*, 2004b). Importantly for understanding terpenoid regulation, there was no genotype by environment effect detected for any terpene related trait in a common garden trial of *E. globulus* plants sourced from a wide geographic area (O'Reilly-Wapstra *et al.*, 2013). This lends support to the idea that the observed changes in terpene concentration in response to environ-

ment are the indirect result of changes in leaf traits that affect oil gland size or number and not due to changes in terpenoid regulation, *per se*.

Biotic

In many species terpenoid production is induced in response to attack by pests (Danner *et al.*, 2011; Litvak and Monson, 1998; Schnee *et al.*, 2002). There have been few studies examining the induction of terpenoids in leaves of eucalypts but it seems that terpenoid deployment is not strongly altered in response to leaf damage (Henery *et al.*, 2008b; Martins and Zarbin, 2013; Rapley *et al.*, 2007). No significant change in FPC or essential oil concentration was detected in leaves either treated with methyl jasmonate or fed upon by insects compared to controls (Henery *et al.*, 2008b; Rapley *et al.*, 2007). However, a recent study that measured volatile emissions after leaf damage in a eucalypt species did detect an increase in volatile terpene emissions after insect feeding suggesting induction in this tissue may occur (Martins and Zarbin, 2013). In contrast to foliar terpenoids, wounding of woody tissue induces the formation of traumatic oil glands and this is accompanied by an increase in FPC and essential oil concentration (Eyles *et al.*, 2003; 2004). Relatively minor differences in oil composition between wounded and unwounded woody tissues were observed in the study of Eyles *et al.* (2004) suggesting that the same terpene synthases induced by wounding are also involved in the constitutive formation of terpenoids.

1.6 Understanding terpenoid regulation at the genetic and molecular level

A significant body of work exists examining the molecular and genetic underpinnings of terpenoid concentration and composition in plants. Upstream steps in the MEP and MVA pathways have been identified as key regulatory points of terpene production through the modulation of precursor supply (Enfissi *et al.*, 2005; Rodríguez-Concepción, 2006), while the activity of terpene synthases and later acting enzymes are important determinants of terpenoid composition (Lücker *et al.*, 2004; Lucker *et al.*, 2004). Yet despite the ecological and economic importance of eucalypt terpenoids, we currently have a very

poor understanding of the specific molecular mechanisms that regulate their formation, concentration and composition in this genus. Given what we know of the complex terpenoid chemistry of many species as well as the spatial and developmental control, we can expect the presence of complex, multi-layered regulatory networks controlling terpenoid chemistry.

1.6.1 Terpene synthases

As terpene synthases are a major point where structural diversity is introduced in the terpenoid biosynthetic pathway, identifying and characterising these enzymes has been the main focus of work so far in this genus. The economically important essential oils extracted from eucalypts are also the direct products of these enzymes. Characterisation of the *Eucalyptus* terpene synthase gene family is currently underway and analysis of the *E. grandis* genome has revealed the presence of at least 120 loci with similarity to terpene synthases (Kulheim *et al.*, 2011). Of these, 53 have been assigned to the TPSa subfamily (sesquiterpene synthases) and 38 to TPSb (monoterpene synthases). Based on the analysis of grape terpene synthases (Martin *et al.*, 2010), it is possible that many of these loci do not represent functional genes in *E. grandis*. Nonetheless, this is the largest terpene synthase family yet reported from a single plant species and recent work profiling the expression of terpene synthases in different tissues of *E. grandis* indicates that a large number are indeed expressed (as cited in: Padovan *et al.*, 2013). Furthermore, Keszei *et al.* (2010) specifically looked at the expression of terpene synthases in expanding leaves of 17 species of eucalypts and found that between zero and four unique transcripts with similarity to monoterpene synthases and between one and six with similarity to sesquiterpene synthases were expressed. It can be expected based on essential oil developmental profiles that other terpene synthases may also be expressed during different stages of leaf and also whole plant ontogeny (Goodger *et al.*, 2013a; Goodger *et al.*, 2013b).

No genes directly involved in the biosynthesis of either MSEs or terpene-phloroglucinols have been identified. Interestingly, both Moore *et al.* (2004a) and Wallis *et al.* (2011) noted the presence of sesquiterpene/macrocarpal chemotypes in

E. globulus. Chemotype 1 was characterised by aromadendrene type sesquiterpenes whereas chemotype 2 contained eudesmol type sesquiterpenes (Moore *et al.*, 2004a). There was also a third chemotype where both groups of sesquiterpenes occurred in roughly equal amounts. The macrocarpals which occurred in each chemotype reflected the sesquiterpenes found in the oil profile, i.e. chemotype 1 contained aromadendrene type macrocarpals. Thus, it seems that the composition of terpene-phloroglucinols in an individual may be strongly dependent on the activity of the same terpene synthases whose products contribute to the essential oil.

1.6.2 Genetic determinants of terpenoid yield

Through a combination of association mapping and quantitative trait loci (QTL) studies, some progress has been made towards understanding the genetic basis of quantitative variation in foliar monoterpenes, sesquiterpenes and selected FPCs including macrocarpal G (Freeman *et al.*, 2008; Henery *et al.*, 2007; Külheim *et al.*, 2011; O'Reilly-Wapstra *et al.*, 2011; Shepherd *et al.*, 1999). Both O'Reilly-Wapstra *et al.* (2011) and Henery *et al.* (2007) identified multiple QTL affecting terpenoid levels in the genome of *E. globulus* and *E. nitens*, respectively. Several regions of chromosome were found to contain high numbers of overlapping QTL for different terpenoids making them the focus for future work on gene identification. For example, in *E. globulus*, loci affecting six of the seven sesquiterpenes included in the study co-located to the same genomic region (O'Reilly-Wapstra *et al.*, 2011). Similarly, multiple monoterpenes also shared QTL in both *E. nitens* and *E. globulus*. Such colocation of biosynthetically related terpenoids suggests these loci contain genes encoding either multi-product terpene synthases or potentially genes regulating the availability of the prenyldiphosphate substrates of these enzymes.

In contrast, terpenoids that require further enzymatic steps downstream of the terpene synthase for their formation were affected by separate QTL (Henery *et al.*, 2007; O'Reilly-Wapstra *et al.*, 2011). In particular, pinocarveol and trans-pinocarvone, two oxidised monoterpenoids colocalised to two unlinked QTL in the *E. nitens* genome. Pinocarveol is thought to be derived from the oxidation of α-pinene and *trans*-pinocarvone is the result of further oxidisation of this alcohol to a ketone (Henery *et al.*,

2007). Based on this biosynthetic scheme, these loci may represent the location of the enzymes responsible for these conversions. This finding highlights the potential for QTL analyses to aid in the identification of downstream enzymes such as those involved in the biosynthesis of macrocarpals, euglobals and MSEs for which there are expected to be numerous potential candidates and where information on homologous pathways in other species are lacking.

1.7 Thesis focus

One of the characteristic features of *Eucalyptus* is the presence of oil glands embedded either wholly or partially in tissues (Fig. 1.3). They are formed of multiple layers of overlapping outer cells, notable for their thickened walls at maturity, and an inner layer of epithelial cells that surround a central cavity (Bohte and Drinnan, 2011; Carr and Carr, 1970). Oil glands occur throughout the leaf lamina and are also present in woody tissues, including bark, roots and floral tissues (Bohte and Drinnan, 2011; Eyles *et al.*, 2004).

The functions of eucalypt oil glands have historically only been thought to involve the biosynthesis and storage of essential oil. This idea was turned on its head with the localisation of two MSEs, cuniloside B and froggattiside A, to oil glands of *E. polybractea*, *E. froggattii* and *E. globulus* (Goodger *et al.*, 2009). These two MSEs, were shown to be the major constituents of a non-volatile component (NVC) whose existence had not been previously reported despite an estimated 50% of cavity volume being occupied by this secretion (Goodger *et al.*, 2010). Furthermore, evidence from sesquiterpene/macrocarpal chemotypes indicates there is a direct biosynthetic link between these two groups of terpenoids (Moore *et al.*, 2004a; Wallis *et al.*, 2011), raising the prospect that terpene-phloroglucinols are also localised to these structures. Thus, it appears that, with the exception of triterpenes, oil glands may be the general site of terpenoid metabolism in eucalypts.

The goal of this thesis is to explore this idea further with a focus on MSE metabolism. In Chapter 2 the presence and composition of MSEs is examined from a diverse cross

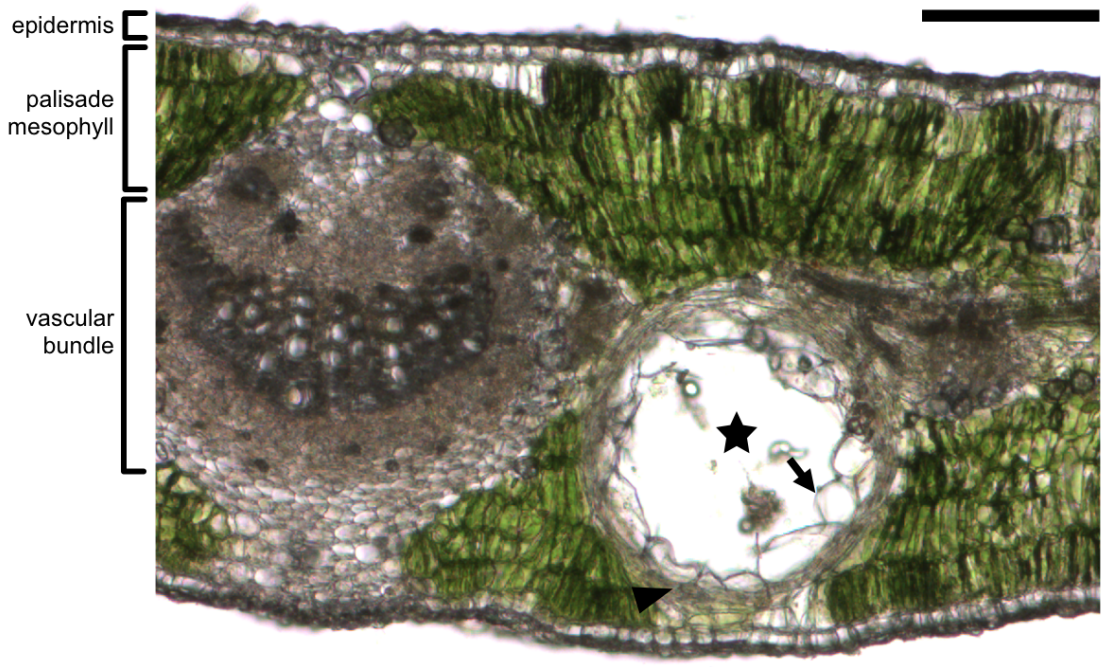

Figure 1.3: Transverse section of a *Eucalyptus polybractea* leaf with an oil gland. The oil gland is made up of a central cavity (star) bounded by a layer of epithelial cells (arrow) which is further surrounded by several layers of flattened cells (arrowhead). Scalebar = 100 μm.

section of eucalypts. This survey examines the non-volatile chemistry of oil glands and establishes the general localisation of MSEs to these structures. Following on from this study, Chapter 3 examines the relationship between MSEs and terpenes in the model eucalypt species *E. polybractea*. The aim of this chapter is to develop a better understanding of the relationship between the co-accumulated classes of terpenoids. In the first section of this chapter, the variation in MSE concentration at a population level is examined and compared with the variation in mono- and sesquiterpenes. The second part of this chapter explores the mechanistic links between terpene and MSE biosynthesis. Finally, Chapter 4 examines the localisation and interaction between the volatile terpene component and the non-volatile component (NVC) found in oil gland cavities, of which MSEs are a constituent.

.

Chapter 2

Survey of non-volatile oil gland metabolites in eucalypt species

2.1 Introduction

Monoterpene-acid sugar esters (MSEs) were first isolated from *Eucalyptus* by Hyodo *et al.* (1992). They reported the presence of two flavonol glycosides, resinoside A and resinoside B (Fig. 2.2) in the leaves of *E. resinifera*. Following this discovery, other MSEs incorporating flavonoid moieties were isolated from leaves of four more species; another three flavonol glycosides were isolated from *E. cypellocarpa*, cypellogins A, B and C (Kasajima *et al.*, 2005), and one from *E. madenii*, eucalmaidin D (Tian *et al.*, 2009). In addition, the MSE incorporating chromanone glycosides cypellocarpin B and C (Ito *et al.*, 2000) and eucamalduside A, B and C (Begum *et al.*, 2011) were isolated from *E. cypellocarpa* and *E. camaldulensis*, respectively. MSEs incorporating gallic acid derivatives have also been reported from *E. cypellocarpa* (cypellocarpin A; Ito *et al.*, 2000), *E. madienii* (eucalmaidin B and C; Tian *et al.*, 2009), and *E. globulus* (eucaglobulin and globulusin B; Hasegawa *et al.*, 2008; Hou *et al.*, 2000).

With few exceptions, oleuropeic acid is the moiety attached at the C-6 position of β-D-glucopyranose (or in rare cases, β-D-galactopyranose) in MSEs. One exception is eucamalduside A in which the monoterpenoid unit is a menthiafolic acid (Begum *et al.*, 2011) and the other is globulusin B in which gallic acid is attached via an ester bond at this position and oleuropeic acid is attached at the anomeric carbon of glucose (Hasegawa *et al.*, 2008). Three MSEs where both aglycones are monoterpene acids have also been reported: the diastereoisomers cuniloside A and B and froggattiside A. Cuniloside A

has been isolated from *E. globulus* (Hasegawa *et al.*, 2008) but was first reported in leaf extracts from *Cunila spicata* (Manns and Hartmann, 1994). Cuniloside B and froggattiside A were isolated from *E. polybractea*, *E. froggattii*, *E. globulus*, *E. cypellocarpa* and *E. beheriana* (Goodger *et al.*, 2009). Eucalmaidin A is the only example in which there is no second moiety bonded at the C-1 position of the sugar (Tian *et al.*, 2009). There are also reports of compounds incorporating 1,8-cineole as the monoterpenoid moiety (Hasegawa *et al.*, 2008). Although not MSEs by the definition used here, as the terpene moiety is O-linked to the sugar, these compounds are nonetheless structurally very similar and the precursors are derived from the same biosynthetic pathways as MSEs.

The *in planta* functions of MSEs are not known. However, some have been shown to have specific bioactivities (Hasegawa *et al.*, 2008; Hou *et al.*, 2000; Hyodo *et al.*, 1992; Sidana *et al.*, 2012; Tian *et al.*, 2009). For example, resinoside A is an inhibitor of blue mussel (*Mytilus edulis*) attachment. Interestingly, the components of resinoside A, oleuropeic acid and kaempferol, had much lower inhibitory activity, leading to the conclusion that the overall structure of the compound is important for activity (Hyodo *et al.*, 1992). Eucalmaidins A, B, C and cuniloside A were tested for their anti-herpes simplex virus type 1 (HSV-1) activity and Vero cell cytotoxicity (Tian *et al.*, 2009). None of the MSEs tested were active against HSV-1 but cuniloside A was found to be relatively cytotoxic. Similar to the findings of Hyodo *et al.* (1992), the intact compound was found to be far more bioactive than its components; cuniloside A had a maximal noncytotoxic concentration against Vero cells of 0.2 mM compared to 1.09 mM for oleuropeic acid. Other MSEs have also been shown to have anti-inflammatory and anti-cancer properties which may relate to their proven antioxidant activity (Hasegawa *et al.*, 2008). This latter activity is potentially important for their function *in planta* as a recent study reported the induction of two MSEs in *Portulaca oleracea* in response to copper toxicity (Wu *et al.*, 2012). The activity (in this case as antioxidants) of the MSEs was much greater than their components, again indicating their structure is important for activity.

Eucalyptus is a diverse genus of more than 600 species. These species are divided across seven subgenera which are further subdivided into numerous sections and series (Brooker, 2000; Ladiges, 1997). All reports of MSEs have so far been from members

of the largest subgenus, *Symphyomyrtus*, and only from a limited number of sections. Furthermore, only one report has localised MSEs to a specific tissue: Goodger *et al.* (2009) reported the isolation of cuniloside B and froggattiside A from the oil glands of three eucalypt species. It is thus unclear how widespread MSEs are in this genus and also whether other MSEs are also associated with oil glands. The aims of this chapter are to address these uncertainties by analysing the oil gland extracts from a diverse range of eucalypt species.

Extracts harvested directly from oil glands were analysed by high resolution tandem mass spectrometry for MSEs. After establishing the prevalence, structural diversity and localisation of MSEs a broader analysis of three of the most common MSEs was undertaken using bulk leaf extracts. This allowed the inclusion of those species from which a non-volatile component (NVC) could not be collected from cavities and also allowed a quantitative measure of MSEs. The significance of the findings are discussed in light of phylogenetic relationships as well as the significance of their localisation to oil glands.

2.2 Materials and Methods

2.2.1 Plant material

Species were selected using a combination of three criteria: published descriptions of large foliar oil glands, high essential oil yield, and representation of different subgenera of the genus *Eucalyptus*. Bulk samples of fully expanded leaves were collected in April 2009 from *Eucalyptus* trees growing in the Peter Francis Points Arboretum (Coleraine, Australia, 37°36.57′ S, 141°41.05′ E; permission for sample collection was gained from the arboretum curator Ray Clay). Collected samples were stored at −80°C until analysis.

2.2.2 Collection of non-volatile fractions from oil glands

With the aid of a stereomicroscope, individual leaves from each species were cut into ∼2 mm wide strips. The strips were held under water with forceps and the NVC

physically removed from the oil gland cavities that were exposed along the cut edges of the leaf strips using a microprobe with a 1 μm tip (World Precision Instruments, Sarasota, USA). The microprobe tip was then rinsed in a vial of MeCN (50%) to dissolve the collected non-volatile material. This process was continued until sufficient NVC was collected for analysis. Each MeCN collection was dried under a constant stream of N_2, re-dissolved in MeCN (50%), passed through a 0.45 μm filter and analysed using the LC-MS system described below.

2.2.3 Oil gland extract analysis and accurate mass measurements

The liquid chromatography-mass spectrometry (LC-MS) system used for fractionation and accurate mass measurements was composed of a Finnigan Surveyor LC Pump, Surveyor AutoSampler, electrospray ionisation (ESI) source and a linear ion trap coupled to a Fourier transform ion cyclotron resonance (FT-ICR) mass spectrometer (LC-ESI-FTICR-MS in full; Finnigan MAT, Bremen, Germany). The instrument was calibrated weekly with Agilent G2421A solution (Agilent Technologies, Santa Clara, USA) for positive and negative ion mode. Samples were separated on a Gemini C18 analytical column (150 $\times$ 4.6 mm, 5 μm; Phenomenex, Torrance, USA) with a flow rate of 0.5 mL min^{-1} and column temperature of 23°C. The mobile phase consisted of 0.1% (v/v) formic acid in water (solvent A) and 0.1% (v/v) formic acid in MeCN (solvent B). The LC gradient method was as follows: solvent B was ramped from 20 to 35% over 2 min followed by an increase to 65% over 14 min, followed by an increase to 100% where it was held for 3 min. The column was then re-equilibrated at 20% solvent B for 10 min. The following MS source conditions were used in positive ion mode: sheath gas, 60 arbitrary units; spray voltage, 5.3 kV; capillary temperature, 250°C; capillary voltage, 33 V; and tube lens voltage, 80 V. In negative ion mode: sheath gas, 60 arbitrary units; spray voltage, 2.7 kV; capillary temperature, 250°C; capillary voltage, -12 V; and tube lens voltage, -140 V. In both positive and negative mode a scan range of 200-1000 m/z was used and collision induced dissociation (CID) carried out at 35% normalised collision energy. Mass spectra were analysed with Xcalibur software (Thermo Electron, San Jose, USA). Identification of cuniloside B and froggattiside A was based on spectral similarity, UV

absorbance and retention time of natural standards purified from *E. froggattii* (Goodger *et al.*, 2009). Identification of cypellocarpin C was based on spectral similarity and retention time of a synthetic standard (provided by Spencer Williams, The University of Melbourne; Hakki *et al.*, 2010).

2.2.4 Infrared and nuclear magnetic resonance spectroscopy

Nuclear magnetic resonance (NMR) spectra were recorded on a Varian 500, Bruker AV 600 (600, 150 MHz), or Bruker Biospin-Avance 800 (Bruker Corporation, Billerica, USA). Chemical shifts (δ) for ^{1}H NMR spectra are reported in parts per million and are followed by multiplicity, coupling constant(s) (J, Hz), integration and assignments. The following abbreviations are used in reporting multiplicities: s, singlet; d, doublet; ABq, AB quartet; br, broad. Residual solvent signals were used for reference: δ 7.26 for ^{1}H NMR in $CHCl_3$, δ 2.05 for ^{1}H NMR and δ 29.84 for ^{13}C NMR in d_6-acetone. Infrared spectra were obtained on a Perkin-Elmer Spectrum One FT-IR spectrometer (Perkin Elmer, Melbourne, Australia) with a zinc selenide/diamond Universal ATR sampling accessory as a thin film.

2.2.5 Structural elucidation of eucaglobulin B

Eucaglobulin B was purified for structural elucidation from bulk leaf extracts of *E. platypus*. Leaf samples were ground under liquid N_2 to a fine powder and extracted in 70% acetone for 24 h at 25°C. The extract was loaded onto a 200 mg Strata-X reverse phase cartridge (Phenomenex) for solid-phase extraction and eluted successively with 10, 20 and 30% MeCN. The 20% fraction was dried under a stream of N_2 and then redissolved in 50% MeCN acidified with 0.1% formic acid. Purification of eucaglobulin B from this fraction was carried out on a LC system composed of a Shimadzu LC-20AT pump, SIL-20A HT autosampler, SPD-M20A detector and FRC-10A fraction collector (Shimadzu Corporation, Kyoto, Japan). The sample was separated on a Gemini C18 analytical column (150 $\times$ 4.6 mm, 5 μm; Phenomenex) with a flow rate 1 mL min^{-1} and column temperature of 23°C. The mobile phase consisted of 0.1% (v/v) formic acid in

water (solvent A) and 0.1% (v/v) formic acid in MeCN (solvent B). The LC gradient method was as follows: solvent B was ramped from 20 to 36% over 15 min. The column was then re-equilibrated at 20% solvent B for 5 min.

2.2.6 Structural elucidation of (−)-(S)-pinocembrin

Pinocembrin was purified for structure elucidation from cavity extracts of *E. olsenii*. Purification of pinocembrin was carried out on the Shimadzu LC system under the same conditions described for eucaglobulin B, except that the LC gradient method was as follows: solvent B was ramped from 65-100% over 5 min which was then dropped back to 65% over 0.1 min and held for 5 min.

2.2.7 Cuniloside B, froggattiside A and cypellocarpin C quantification

Freeze dried leaf samples composed of five randomly selected leaves were ground to a fine powder in an IKA Labortechnic A10 analytical mill (Janke and Kunkel GmbH Co, Staufen, Germany). Duplicate 100 mg subsamples were extracted with acetone in water (70%, 3 mL) for 24 h at 25°C. A 1 mL aliquot of acetone extract was then extracted successively with petroleum ether (60-80°C fraction; 1 mL × 4) and ethyl acetate (1 mL × 4). The combined ethyl acetate fraction was air-dried, re-dissolved in MeCN in water (50%) and analysed by LC-MS. LC-MS was carried out on an Agilent 1200 series with a triple-quadrupole mass spectrometer (Agilent). The sample was separated on a Gemini C18 analytical column (150 × 4.6 mm, 5 μm; Phenomenex) with a flow rate 0.5 mL min^{-1} and column temperature of 23°C. The mobile phase consisted of 0.1% (v/v) formic acid in water (solvent A) and 0.1% (v/v) formic acid in MeCN (solvent B). The LC gradient method was as follows: solvent B was ramped from 30 to 45% over 2 min then to 65% over 8 min followed by an increase to 100% over 4 min. The column was then re-equilibrated at 30% solvent B for 5 min. The source conditions were as follows: nebuliser pressure of 45 psi, gas flow rate of 10 L min^{-1}, gas temperature 315°C and capillary voltage of 4000 V. Quantification of cuniloside B, froggattiside A and cypellocarpin C was carried out by comparison of the response integral for the most abundant ion transition

of each compound (m/z 530 $>$ 329 for cuniloside B and froggattiside A and $m/$ z 521 $>$ 503 for cypellocarpin C) to standard series of synthesised cuniloside B and cypellocarpin C run under optimal conditions. The optimised conditions were: fragmentor energy 100 V, collision energy 30 V and dwell time 75 ms. Peak integration of product ion chromatograms was performed using MassHunter Quantitative Analysis (Agilent).

2.3 Results

2.3.1 Species selection

The primary aim of this study was to investigate the occurrence and diversity of MSEs and the general occurrence and composition of NVCs in oil glands of eucalypts. Therefore, the major consideration for initial species selection was ease of direct non-volatile collection from cavities. Accordingly, species with published descriptions of large or numerous cavities were favoured, as they would hopefully prove more amenable to direct collection of non-volatiles. Additional taxa were selected to represent different lineages within the eucalypt group. The final species selection consisted of 27 representatives from *Eucalyptus* and two species from the sister genus *Corymbia* (Table 2.1). Within the genus *Eucalyptus*, five of the seven subgenera were represented. Twenty species were selected from the largest subgenus *Symphyomyrtus* (∼500 taxa) and four from subgenus *Eucalyptus* (∼110 taxa). In addition, *E. microcorys* and *E. cloeziana* from the monotypic subgenera *Alveolata* and *Idiogenes*, respectively, were included along with *E. erythrocorys* from the small subgenus *Eudesmia* (20 taxa).

2.3.2 Localisation of MSEs to oil glands of *Eucalyptus*

In all 29 species an NVC was observed in oil gland cavities. Of these, 18 species contained large and abundant enough cavities for the NVC to be physically collected. The collected extracts were separated and analysed by LC-ESI-FTICR-MS with UV absorbance detection (Table 2.2). The NVC extracts contained a complex array of compounds with absorbance spectra consistent with oleuropeyl esters (absorbance

Table 2.1: List of *Eucalyptus* species surveyed in this study.

#	Species	Subgenus	Section	Series	Authority
1	*Corymbia intermedia*	*Corymbia*	*Rufaria*		R. Baker
2	*C. eximia*		*Septentrionales*	*Naviculares*	Schauer
3	*Eucalyptus microcorys*	*Alveolata*		*Alveolatae*	F. Muell.
4	*E. erythrocorys*	*Eudesmia*			F. Muell.
5	*E. cloeziana*	*Idiogenes*			F. Muell.
6	*E. froggattii*	*Symphyomyrtus*	*Adnataria*	*Buxeales*	Blakely
7	*E. polybractea*			*Buxeales*	R. Baker
8	*E. sideroxylon*			*Melliodorae*	A. Cunn. ex Woolls
9	*E. dielsii*		*Bisectae*	*Elongatae*	C.A. Gardner
10	*E. platypus*			*Erectae*	Hook
11	*E. spathulata*			*Erectae*	Hook
12	*E. halophila*			*Halophilae*	D.J. Carr & S.G.M Carr
13	*E. gracilis*			*Heterostemones*	F. Muell.
14	*E. loxophleba ssp. lissophloia*			*Loxophlebae*	L.A.S. Johnson & Blaxell
15	*E. leptophylla*			*Porantherae*	F. Muell. ex Miq.
16	*E. kochii*			*Subulatae*	Maiden & Blakely
17	*E. myriadena*		*Dumaria*	*Ovulares*	Brooker
18	*E. torquate*			*Torquatae*	Luehm.
19	*E. camaldulensis*		*Exsertaria*	*Rostratae*	Dehnh.
20	*E. resinifera*		*Latoangulatae*	*Annulares*	Smith
21	*E. cinerea*		*Maidenaria*	*Argyrophyllae*	F. Muell. ex Benth.
22	*E. cypellocarpa*			*Globulares*	L.A.S. Johnson
23	*E. globulus*			*Globulares*	Labill.
24	*E. pulverulenta*			*Orbiculares*	Sims
25	*E. dalrympleana*			*Viminales*	Maiden
26	*E. meulleriana*	*Eucalyptus*	*Capillulus*	*Pachyphloius*	A.W.Howitt
27	*E. gregsoniana*		*Cineracceae*	*Pauciflorae*	L.A.S. Johnson & Blaxell
28	*E. pauciflora*			*Pauciflorae*	Sieber ex Sprengel
29	*E. olsenii*		*Eucalyptus*	*Regnantes*	L.A.S. Johnson & Blaxell

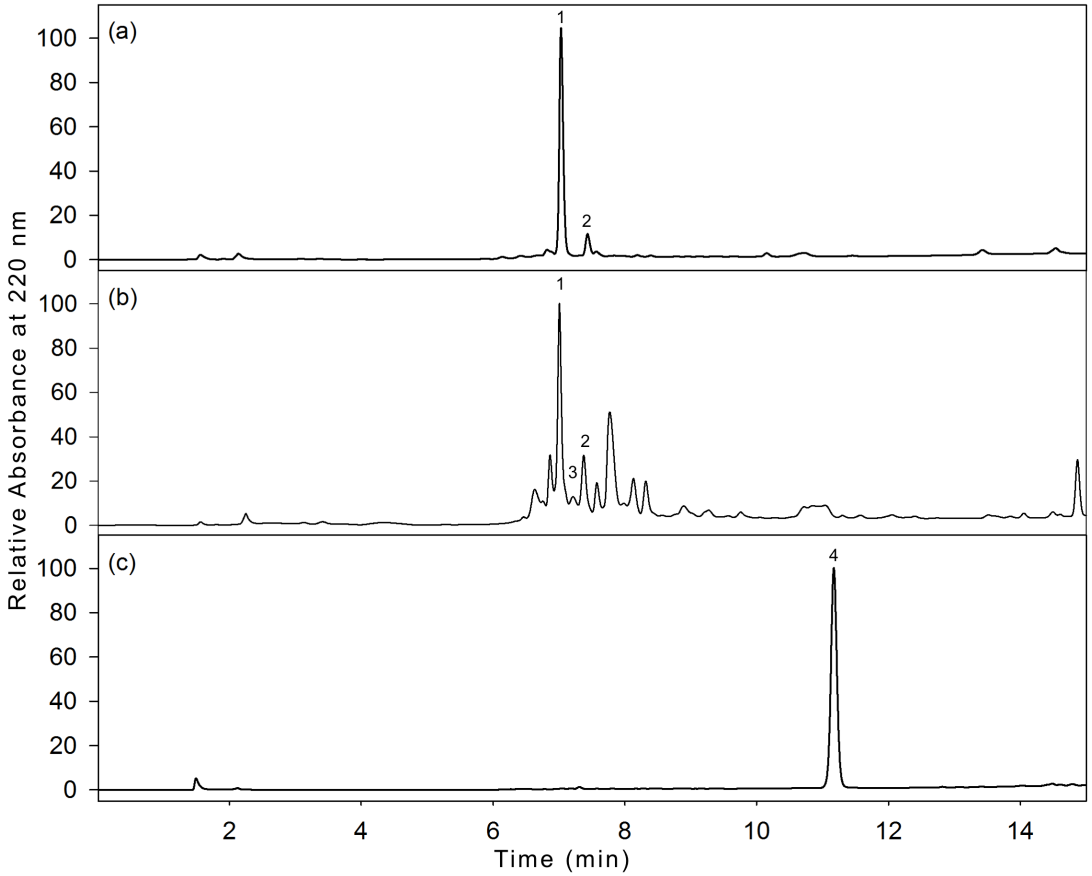

Figure 2.1: LC-UV absorbance chromatograms of oil gland extracts from *Eucalyptus froggattii* (a) *E. dielsii* (b) and *E. olsenii* (c). Peak numbers indicate cuniloside B (1), froggattiside A (2), cypellocarpin C (3) and pinocembrin (4).

maxima of 220 nm) and phenolics (absorbance maxima of 280-420 nm). The majority of species had extracts dominated by compounds eluting between 30 and 50% MeCN such as *E. dielsii* and *E. froggattii* (Fig. 2.1, a & b). A small subset of species belonging to the subgenus *Eucalytpus* were dominated by later eluting compounds (Fig. 2.1c). Comparison of MS spectra, UV absorbance and retention times with standards showed the cavities of all 18 species of eucalypts contained cuniloside B and froggattiside A, whereas cypellocarpin C was detected in 15 species (Table 2.2).

2.3.3 Collision induced dissociation of MSEs

Both cuniloside B and froggattiside A share a distinctive fragmentation pattern with the production of two highly abundant C_{16} fragments of m/z 329.1593 and 311.1488. These ions correspond to an oleuropeic acid linked to glucose via an ester bond, with the loss of one or two water molecules, respectively (Fig. 2.3 & 2.4a; Goodger *et al.*, 2009). A lower abundance C_{16} fragment of m/z 347.1699 was also observed, corresponding to an oleuropeyl glucose ester with no loss of water. The fragmentation of cypellocarpin C resulted in the production of an m/z 311.1492 ion, also consistent with its structure containing an oleuropeyl glucose ester (Fig. 2.2). The characteristic fragmentation pattern of the oleuropeyl glucose ester moiety was used as a means to search for other structurally-related compounds in the NVC extracts (Fig. 2.4). Species from the section *Bisectaria* (subgenus *Symphyomyrtus*) were particularly abundant in MSEs compared to species from other sections. For example, *E. dielsii* contained at least 10 peaks with the signature 311/329 product ions (Fig. 2.4b).

Of the 20 MSEs previously reported from eucalypts, mass spectral data matching eight of these were detected in cavity extracts (Table 2 & Fig. 2.2). For example, a pseudo-molecular ion peak $[M+H]^+$ at m/z 615.2061 and $[M+Na]^+$ at m/z 637.1880, corresponding to the molecular formula $C_{31}H_{34}O_{13}$, matched published data for resinoside A (Hyodo *et al.*, 1992). Furthermore, fragmentation of the $[M+H]^+$ ion resulted in the fragments m/z 287.0550 and 311.1490, consistent with the presence of a kaempferol moiety and an oleuropeyl glucose ester, respectively. Similarly diagnostic fragmentation patterns of an ion matching eucalmaidin C (Tian *et al.*, 2009) were also observed. A series of putative MSEs with the molecular formula $C_{23}H_{30}O_{12}$ were found to elute between 4 and 6 min in five of the species. Fragmentation of the $[M-H]^-$ ion gave a product ion of m/z 169.0136 consistent with a gallic acid group matching published data for eucaglobulin (Hou *et al.*, 2000), cypellocarpin A (Ito *et al.*, 2000) and eucalmaidin B (Tian *et al.*, 2009; Table 2.2 & Fig. 2.2).

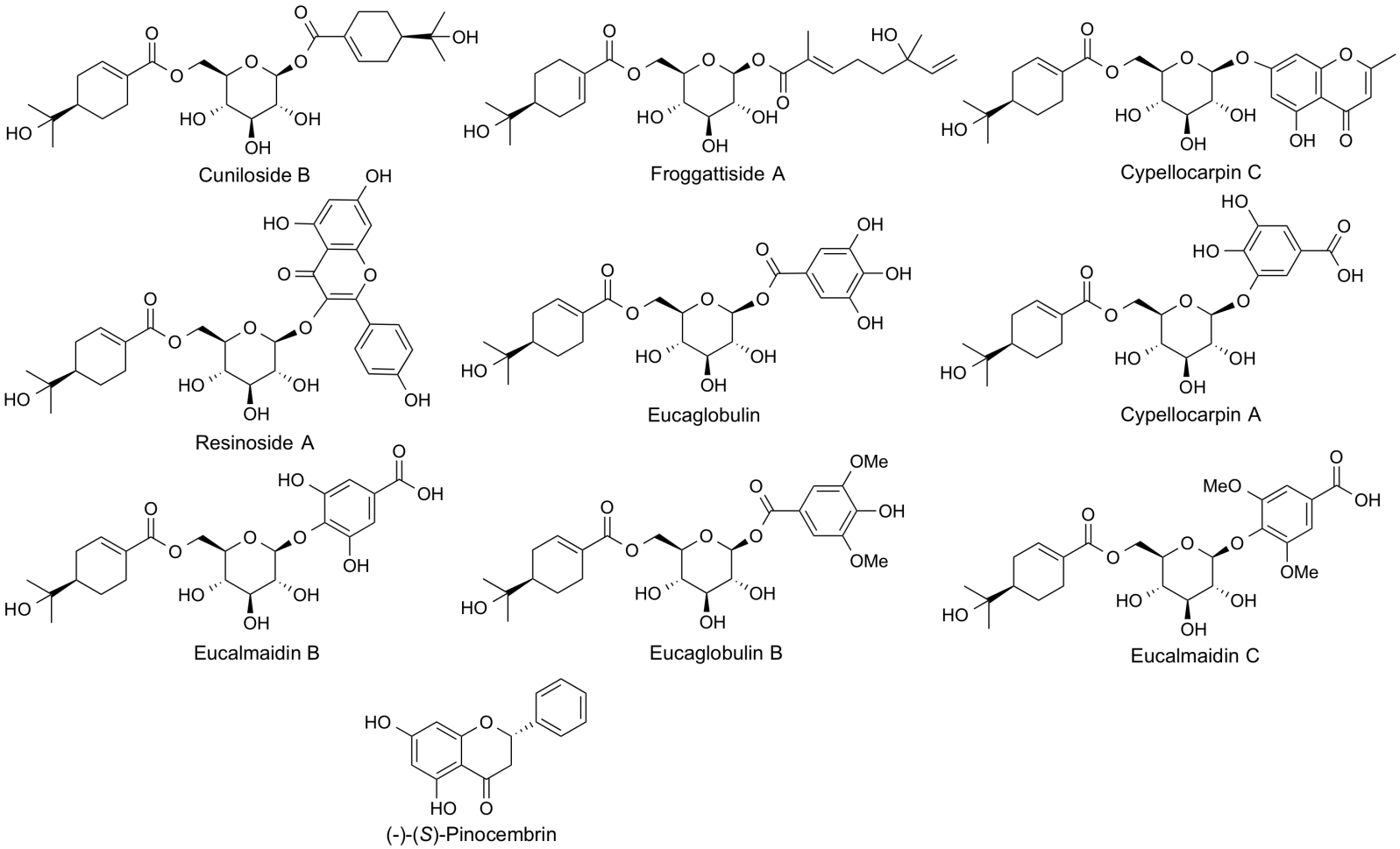

Figure 2.2: Structures of non-volatile compounds localised to foliar oil glands of *Eucalyptus* species.

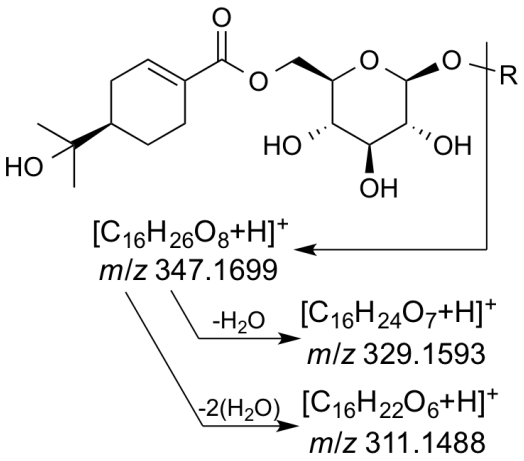

Figure 2.3: MS^2 fragmentation of oleuropeyl glucose esters resulting in diagnostic C_{16} fragments.

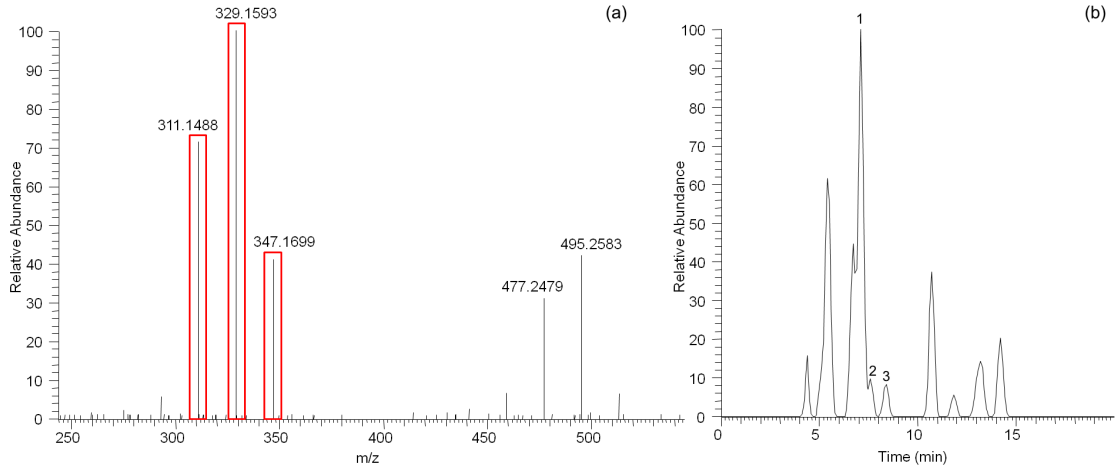

Figure 2.4: MS^2 spectrum of cuniloside B showing diagnostic oleuropeyl-glucose product ions highlighted in red boxes (a) and extracted ion chromatogram of the m/z 329 ion from a *Eucalyptus dielsii* cavity extract (b). Peak numbers in panel (b) indicate cuniloside B (1), eucaglobulin B (2) and froggattiside A (3).

Table 2.2: Electrospray ionisation Fourier transform ion cyclotron mass spectral analysis of *Eucalyptus* oil gland extracts. Ions in bold type were fragmented to give the listed product ions.

RT (min)	Pseudo-molecular ion	Formula	Product ions	Compound	Species No.[a]
5.25	**516.2067** $[\mathbf{M}+\mathbf{NH_4}]^+$	$C_{23}H_{30}O_{12}$	329.1594 (100)	eucaglobulin, cypellocarpin A, or eucalmaidin B	9,22-25
	521.1624 $[M+Na]^+$		311.1488 (80)		
			481.1703 (24)		
			293.1383 (13)		
			463.1597 (12)		
5.61	**546.2899** $[\mathbf{M}+\mathbf{NH_4}]^+$	$C_{26}H_{40}O_{11}$	511.2536 (100)	unknown 1	16,14
	551.2456 $[M+Na]^+$		493.2430 (45)		
	529.2637		329.1594 (35)		
			347.1700 (21)		
			311.1490 (19)		
			475.2321 (14)		
6.75	**544.2378** $[\mathbf{M}+\mathbf{NH_4}]^+$	$C_{25}H_{34}O_{12}$	329.1593 (100)	eucalmaidin C	9-11,18
	549.1935 $[M+Na]^+$		311.1488 (98)		
			509.2018 (29)		
6.77	**546.2899** $[\mathbf{M}+\mathbf{NH_4}]^+$	$C_{26}H_{40}O_{11}$	511.2535 (100)	unknown 2	6,9,14,25
	551.2457 $[M+Na]^+$		329.1594 (59)		
	529.2637 $[M+H]^+$		493.2430 (29)		
			311.1488 (14)		
			347.1699 (13)		
7.2	**530.2951** $[\mathbf{M}+\mathbf{NH_4}]^+$	$C_{26}H_{40}O_{10}$	329.1593 (100)	cuniloside B	All species
	535.2505 $[M+Na]^+$		311.1488 (81)		
	513.2687 $[M+H]^+$		495.2583 (36)		
			477.2479 (14)		
			347.1699 (13)		
7.77	**544.2378** $[\mathbf{M}+\mathbf{NH_4}]^+$	$C_{25}H_{34}O_{12}$	311.1488 (100)	eucaglobulin B	9-11
	549.1935 $[M+Na]^+$		509.2015 (53)		
	527.2114 $[M+H]^+$		491.1909 (39)		
			329.1595 (21)		
			347.1490 (7)		
			275.1278 (6)		
			293.1383 (6)		
			167.1066 (6)		

continued on next page

[a] See Table 2.1

RT (min)	Pseudo-molecular ion	Formula	Product ions	Compound	Species No.
8	**615.2061** $[\mathbf{M}+\mathbf{H}]^+$	$C_{31}H_{34}O_{13}$	287.0550 (100)	resinoside A/B	14,22,23
	637.1880 $[M+Na]^+$		311.1490 (92)		
8.06	**521.2009** $[\mathbf{M}+\mathbf{H}]^+$	$C_{26}H_{32}O_{11}$	503.1904 (100)	cypellocarpin C	4,6,7,9,10-12,
			311.1492 (1)		14,15,17,20,
					22-25,27
8.23	**505.2635** $[\mathbf{M}+\mathbf{H}]^+$	$C_{24}H_{40}O_{11}$	193.0495 (100)	unknown 3	3,4,9,10,11,
	522.2900 $[M+NH_4]^+$		311.1488 (86)		17,18,20
	527.2453 $[M+Na]^+$				
	487.2529 $[M-H_2O+H]^+$				
8.39	**530.2950** $[\mathbf{M}+\mathbf{NH_4}]^+$	$C_{26}H_{40}O_{10}$	329.1593 (100)	froggattiside A	6,7,9,10-12,
	535.2505 $[M+Na]^+$		311.1488 (71)		14,15,17,18,
	513.2685 $[M+H]^+$		495.2583 (42)		22-25,27,28
			347.1699 (41)		
			477.2479 (31)		
			459.2378 (7)		
9.27	**602.3884** $[\mathbf{M}+\mathbf{NH_4}]^+$	$C_{31}H_{52}O_{10}$	329.1594 (100)	unknown 4	9-11,17,22
	607.3439 $[M+Na]^+$		549.3417 (82)		
	585.3621 $[M+H]^+$		311.1487 (32)		
			347.1699 (21)		
			567.3525 (19)		
			531.3312 (11)		
9.37	**521.2009** $[\mathbf{M}+\mathbf{H}]^+$	$C_{26}H_{32}O_{11}$	503.1904 (100)	unknown 5	9,11,12,15,
			485.1809 (2)		17,23-25,
			467.1702 (1)		27-29
			311.1492 (1)		
9.56	**556.2744** $[\mathbf{M}+\mathbf{NH_4}]^+$	$C_{27}H_{38}O_{11}$	521.2378 (100)	unknown 6	11,14,23,25
	561.2296 $[M+Na]^+$		311.1489 (23)		
	539.2480 $[M+H]^+$		539.2488 (14)		
			503.2272 (11)		
			329.1595 (5)		
9.66	**522.2900** $[\mathbf{M}+\mathbf{NH_4}]^+$	$C_{24}H_{40}O_{11}$	487.2535 (100)	unknown 7	9-11,17
	527.2453 $[M+Na]^+$		469.2431 (43)		
	505.2635 $[M+H]^+$		311.1489 (31)		
	487.2530 $[M-H_2O+H]^+$		451.2325 (16)		
			321.1542 (4)		

continued on next page

RT (min)	Pseudo-molecular ion	Formula	Product ions	Compound	Species No.
10.79	**602.3885** $[\mathbf{M}+\mathbf{NH_4}]^+$	$C_{31}H_{52}O_{10}$	549.3419 (100)	unknown 8	9-11
	607.3441 $[M+Na]^+$		531.3314 (95)		
	585.3625 $[M+H]^+$		329.1594 (77)		
			567.3527 (58)		
			311.1489 (35)		
			347.1698 (9)		
13.27	**553.2635** $[\mathbf{M}+\mathbf{H}]^+$	$C_{28}H_{40}O_{11}$	535.2537 (100)	unknown 9	9-11,14,22,
			517.2427 (28)		23,25
			311.1487 (24)		
17.06	**255.0661** $[\mathbf{M}-\mathbf{H}]^-$	$C_{15}H_{12}O_4$	213.0551 (100)	pinocembrin	26-29
	511.1386 $[2M-H]^-$		151.0032 (97)		
			187.0761 (48)		
			211.0760 (35)		
			169.0655 (30)		
			183.0813 (21)		

2.3.4 Novel monoterpene-acid sugar esters

The cavity extracts of many species also contained putative MSEs which did not match any of the published mass spectral data (Table 2.2). The subgenus *Symphyomyrtus* was particularly rich in novel MSEs with *E. dielsii* (Fig. 2.4b) and *E. spathulata* containing eight, and *E. platypus* containing six of these compounds. One such compound was present in three species and was particularly abundant in the cavity extract from *E. platypus*. The compound was purified from that species, subjected to MS and NMR analyses and identified as a new compound, named here as eucaglobulin B, owing to its close structural relationship to eucaglobulin (Fig. 2.2; Hou *et al.*, 2000).

The molecular formula of eucaglobulin B was established by LC-ESI-FTICR-MS (m/z 544.2378 $[M+NH_4]^+$; 549.1935 $[M+Na]^+$; 527.2114 $[M+H]^+$) as $C_{25}H_{34}O_{12}$. Fragmentation of the $[M+NH_4]^+$ ion resulted in the characteristic 311, 329 and 347 product ions, consistent with the putative presence of an oleuropeyl glucose ester. Fragmentation of the $[M-H]^-$ ion gave a product ion of m/z 197.0448 consistent with a dimethylgallic acid group. The presence of this group and an oleuropeyl group suggested structural similarity or identity with the known compound eucalmaidin C. The ^{1}H NMR

spectrum appeared almost identical to that reported for eucalmaidin C, supporting the presence of oleuropeyl and 3,5-dimethylgallyl esters, with the exception of the anomeric proton being present at δ 5.67 ppm (rather than δ 4.88 as reported for eucalmaidin C). In particular, the downfield shifts of both H1' and H6'a and H6'b are consistent with ester bonds at these positions. HMBC spectroscopy revealed correlations between H2 and C7 of the 3,5-dimethylgallyl fragment, and between C7 of the 3,5-dimethylgallyl fragment and the glucopyranose H1', confirming that the 3,5-dimethylgallic acid group was attached to the anomeric position of the glucose (C1'), and the oleuropeic acid group at C6'. Based on these analyses, the structure of eucaglobulin B was proposed (Fig. 2.2, for full NMR and IR results see Appendix A).

2.3.5 Localisation of the flavanone pinocembrin to oil glands

Based on the LC-UV and MS total ion current data, the NVC extracted from oil gland cavities of four species belonging to the subgenus *Eucalyptus* (*E. meulleriana*, *E. pauciflora*, *E. gregsoniana* and *E. olsenii*) were dominated by a later eluting compound with an absorbance spectrum consistent with a flavonoid. LC-ESI-FTICR-MS analysis gave a pseudo-molecular ion peak $[M-H]^-$ at m/z 255.0661, corresponding to the molecular formula $C_{15}H_{12}O_4$. ^1H and ^{13}C NMR analysis and optical rotation identified this compound as (−)-(*S*)-pinocembrin (Fig. 2.2; for NMR and IR results see Appendix A).

2.3.6 Cuniloside B, froggattiside A and cypellocarpin C quantification

The extraction of non-volatiles directly from cavities is a purely qualitative method. To get an idea of the quantity of MSEs present in leaves cuniloside B, froggattiside A and cypellocarpin C were quantified from bulk leaf extracts. These MSEs were chosen due to their prevalence in cavity extracts and the availability of standards for cuniloside B and cypellocarpin C. Consequently, the ethyl acetate-soluble fraction of acetone/water leaf extracts from 28 species were analysed by LC-MS. Cuniloside B was detected in all species examined, froggattiside A and cypellocarpin C were detected in 24 and 23 species, respectively (Table 2.3). Cuniloside B was present at low levels ($<$0.08 mg g^{-1}

DW) in *E. halophila*, *E. intermedia* and *E. olsenii*, but ranged to over 28 mg g^{-1} DW in *E. polybractea* and *E. froggattii*. In the species where froggattiside A and cypellocarpin C were detected their levels were consistently lower in abundance than cuniloside B (Table 2.3). The concentration of froggattiside A and cypellocarpin C ranged from undetectable in four and five of the examined species, respectively, to a maximum of 8.19 mg g^{-1} DW and 1.38 mg g^{-1} DW in *E. froggattii*.

Table 2.3: Quantification of monoterpene-acid glucose esters in *Eucalyptus* bulk leaf extracts in mg g^{-1} leaf DW.

Species No.	Cuniloside B	Froggattiside A	Cypellocarpin C
1	0.03	0	0
2	0.13	0.02	0
3	3.8	0.65	0.02
4	0.1	0	0
5	0.1	0.06	0
6	30.63	8.19	1.37
7	28.56	6.31	0.75
8	2.02	0.56	0.22
9	2.62	1.21	0.05
10	0.63	0.02	0.16
11	2.06	0.65	0.17
12	0.07	0.01	0.04
13	9.63	6.6	0.39
14	7.82	0.81	0.02
15	6.1	0.28	0.14
16	6.12	0.57	0.06
17	17.03	6.17	0.34
18	0.92	0.13	0
19	6.24	0.33	1.12
20	0.5	0.04	0.01
21	0.19	0.04	0.02
22	0.41	0.03	0.05
23	0.47	0.04	0.1
24	0.06	0.01	0.03
25	1.07	0.17	0.22
27	0.34	0.05	0.01
28	0.1	0	0
29	0.02	0	0.01

2.4 Discussion

The results of this study show that the oil glands of *Eucalyptus* are composed of a complex array of metabolites. Alongside the well characterised terpenes exists an abundant non-volatile component whose composition includes a variety of MSEs.

2.4.1 Diagnostic fragmentation of MSEs

The characteristic fragmentation pattern of cuniloside B, froggattiside A and cypellocarpin C proved to be an indispensable tool in the detection of other structurally related compounds. Importantly, the sensitivity of the LC-ESI-FTICR-MS analysis provided a means to search for novel esters in extracts from tissues of limited size. This resulted in the localisation and identification of the new compound eucaglobulin B, which was initially targeted because of the presence of the characteristic m/z 311 and 329 product ions (Fig. 2.3).

It is important to acknowledge that this method is only intended as an initial screening tool to identify putative MSEs as it gives no information on the specific identity of either the monoterpene-acid or sugar. Nonetheless, based on the structures of known eucalypt MSEs it is likely that many of the putative compounds identified in this study also follow the general theme where oleuropeic acid (either *R* or *S* isomer) is linked via an ester bond at the C-6 position of glucose. There are only 2 compounds known from eucalypts where this position is occupied by a different aglycone (Begum *et al.*, 2011; Hasegawa *et al.*, 2008) and only three compounds where the sugar moiety is not a β-D-glucopyranose: cypellogin B and resinoside B and C, all of which contain β-D-galactopyranose (Kasajima *et al.*, 2005; Hyodo *et al.*, 1992). Full structural elucidation would require ^{1}H and ^{13}C NMR (as was the case for eucaglobulin B); however, these techniques require purified compound which is not always feasible due to the chemical complexity of the extracts.

2.4.2 Sequestration and biological activity

It is possible MSEs are defence chemicals as their structure indicates the potential for significant biological activity. A common structural theme shared among them is the presence of at least one α,β-unsaturated carbonyl group in the monoterpene-acid moieties, and often another in the phenolic moieties (Fig. 2.2; Goodger and Woodrow, 2011). The electrophilic nature of the β carbon means it can be attacked by nucleophiles in the cell, such as the thiol and amine groups of amino acid residues (Mueller and Berger, 2009). In some bioactive compounds the α,β-unsaturated carbonyl group has been shown to be key to their reactivity (Alméras *et al.*, 2003; Groll *et al.*, 2008). For example, the proteasome inhibiting activity of the bacterial virulence factor, syringolin A, is due to the binding of its α,β-unsaturated carbonyl to the threonine residue in the enzyme complex active site (Groll *et al.*, 2008). The presence of such biologically active compounds in the leaves of eucalypts may serve as effective defences against a variety of herbivores and pathogens.

There is a risk MSEs identified in cavity extracts were due to contamination from surrounding tissue when leaves were sliced into strips. However, Goodger and Woodrow (2011) demonstrated that 99% of the cuniloside B and froggattiside A in *E. polybractea* was cavity localised, with only small fractions detected in the cuticle, mesophyll and vasculature. Assuming that the MSEs identified in this study are in fact cavity localised, this localisation is consistent with their putative reactivity. The sequestration of defence chemicals to extracellular spaces is a strategy to allow the accumulation of high concentrations of defence chemicals while avoiding auto-toxicity (Sirikantaramas *et al.*, 2007). Examples include the accumulation of monoterpenes and diterpene acids in conifer resin ducts (Zulak and Bohlmann, 2010) and the accumulation of terpenes, cannabinoids and polyketides in the GSTs of species in the Cannabaceae family (Sirikantaramas *et al.*, 2005; Wang *et al.*, 2008). The importance of such segregation to plant health is highlighted by the damage caused in *Citrus* fruits when oil glands collapse and essential oil subsequently leaks into surrounding tissue (Knight *et al.*, 2002). Indeed, it is interesting to note that many species from which MSEs have been isolated from bulk leaf extracts produce essential oils and, with the exception of *Olea*

europea, store essential oils in specialised storage structures (Manns and Hartmann, 1994; Nakanishi *et al.*, 2005; Scarpati and Trogolo, 1966). This correlation suggests that in other species MSEs may also be sequestered to extracellular spaces.

The sequestration of pinocembrin to oil glands is also likely due to its potential for autotoxicity. It is known to be biologically activity and is an effective antibacterial, antifungal and antifeedant agent (Diaz Napal *et al.*, 2009; Hanawa *et al.*, 2001; Shain and Miller, 1982) making a role in eucalypt defence likely. It has been identified in the resinous exudates of leaf glands (including glandular trichomes) of several species including *Populus deltoides* (Salicaceae; Shain and Miller, 1982), *Lychnophora ericoides* (Asteraceae; Gobbo-Neto *et al.*, 2008), *Adenostoma sparsifolium* (Rosaceae; Proksch *et al.*, 1985) and *Acacia neovernicosa* (Fabaceae; Wollenweber and Seigler, 1982). There is only a single confirmed report of its isolation from the leaves of a eucalypt, *E. sieberi* from subgenus *Eucalyptus* (Bick *et al.*, 1972), but it has recently been putatively identified in the leaf extracts of other species from this subgenus (Tucker *et al.*, 2010).

2.4.3 Chemotaxonomy and ecology

Although only a small sample of eucalypts was examined in this study some phylogenetic trends were observed. Based on the fractionation and detection conditions used, the extracts from species in subgenus *Symphyomyrtus* were generally dominated by MSEs and contained both the highest levels and greatest variety of the different taxonomic groups appraised (Tables 2.2 & 2.3). The bulk leaf extract from *E. microcorys*, phylogenetically closely related to the symphyomyrts (Steane *et al.*, 2002), was also found to have relatively high levels of cuniloside B and froggattiside A compared to the other subgenera. In support of this trend, all reports of MSEs have thus far come from species belonging to subgenus *Symphyomyrtus*.

Species from subgenera *Eucalyptus* (henceforth referred to informally as monocalyptus), *Idiogenes* and *Eudesmia*, as well as from the sister genus *Corymbia* had low levels of all quantified compounds. It is possible the NVCs of cavities from these species are dominated by compounds other than MSEs (like the monocalypts) or are dominated by non-quantified MSEs such as in *E. halophila*. However, the NVC of one species outside of

the two major *Eucalyptus* lineages, *E. erythrocorys* (subgenus *Eudesmia*), was collected and had limited diversity of MSEs with only cuniloside B and cypellocarpin C detected (the latter of which was below the detection limit in the bulk leaf extract; Tables 2.2 & 2.3). The detection of cuniloside B in the bulk leaf extracts of all species, including those in the sister genus *Corymbia*, does indicate that the ability to produce MSEs is an ancestral trait.

In contrast to symphyomyrt species, the NVC extracted from oil glands of the four monocalypt species sampled were dominated by the flavanone pinocembrin (Fig. 2.2; Table 2.2). Such distinct differences in biochemistry between the two subgenera have been demonstrated previously. For example, FPCs and cyanogenic glycosides are present in symphyomyrts but are not found in monocalypts (Eschler *et al.*, 2000; Gleadow *et al.*, 2008). Interestingly, where symphyomyrts and monocalypts are compared directly under the same growing conditions the former appear to show a greater capacity to adapt to a range of abiotic factors such as water availability (Anekonda *et al.*, 1999; Merchant *et al.*, 2006), while the latter are less attacked by herbivores and pathogens (Anekonda *et al.*, 1999; Stone *et al.*, 1998). Tucker *et al.* (2010) attempted to use a non-targeted metabolomics approach to identify whether underlying differences in chemistry are responsible for some of these differences. In agreement with the present study, they found that leaf extracts from monocalypts were characterised by the presence of flavanones with unsubstituted B-rings. However, whether this influences herbivore species choice has not been established.

2.5 Concluding remarks

The work presented in this chapter provides evidence of the widespread occurrence of MSEs in the oil glands of eucalypts. The di-monoterpene ester cuniloside B was identified in all extracts and, in addition, many known and novel phenolic MSEs were putatively identified. Unconjugated flavanones dominated the NVC extracts from the four species sampled from the subgenus *Eucalyptus*. This apparent marked difference in oil gland chemistry is interesting from both an oil gland metabolism and an ecological point of view and warrants further investigation.

2.5.1 Food for thought

So far the discussion has focused on the specific composition of the NVC, but perhaps it is the NVC as a total entity which serves a function also. Thus the markedly differing composition between the two subgenera could reflect a different solution to the same problem. Pinocembrin is bioactive and, based on evidence from other species, holds a defensive role in eucalypts. It has also been argued that MSEs are likely to hold a defensive function based on localisation, structure, and bioactivity. However, both classes of compounds also have structures which lend themselves towards amphiphilic properties (Fig. 2.2). This would allow them to interact with both co-stored lipophilic and volatile terpenes as well as the hydrophilic domains associated with the cell wall of secretory cells. This aspect of the proposed function of the NVC forms the research basis of Chapter 4.

Chapter 3

Relationships between terpenes and MSEs in the leaves of *Eucalyptus polybractea*

3.1 Introduction

Eucalyptus polybractea R.T. Baker is a species characterised by high concentrations of foliar mono- and sesquiterpenes (collectively referred to as terpenes in this chapter). It is particularly rich in 1,8-cineole with the oil from some genotypes containing over 90% of this monoterpene on a dry weight (DW) basis (Goodger and Woodrow, 2008). The high yield and composition of *E. polybractea* terpenes has made this species a key source of pharmaceutical grade oil in Australia (Goodger *et al.*, 2008). Other than 1,8-cineole, the oil also contains lower levels of a range of mono- and sesquiterpenes including α-pinene, limonene, myrcene, β-elemene and β-caryophyllene (Goodger *et al.*, 2010; King *et al.*, 2006a).

At a population level, foliar terpene deployment is highly variable, ranging from 14.4 to 64.4 mg g^{-1} DW in a single population (King *et al.*, 2004). As for other *Eucalyptus* species, the terpene profile and concentration is under strong genetic control (Andrew *et al.*, 2005; Doran and Matheson, 1994; Goodger and Woodrow, 2008). For example, 1,8-cineole percentage in a clonal line of *E. polybractea* ranged between 90 and 92% compared to a range of 48 to 91% in the half-sib family of the ortet (Goodger and Woodrow, 2008). In addition, terpene deployment is little impacted by abiotic factors including nitrogen availability and water stress (King *et al.*, 2006a).

Terpene concentration is developmentally regulated and is closely linked with leaf expansion; as leaves expand the terpene concentration increases (Goodger and Woodrow, 2012). Like other species that store terpenes in specialised structures, this pattern of deployment is due to the initiation and expansion of oil glands during leaf development (Goodger and Woodrow, 2012). Early on in leaf development a large number of glands are initiated, this is followed by enlargement of the glands concurrent with leaf expansion resulting in a drop in density but an overall increase in total cavity volume and oil concentration (Goodger and Woodrow, 2012). The site of terpene biosynthesis is unknown in eucalypts. However, based on evidence from terpene accumulating oil glands and ducts in citrus and conifer species, it is likely to be the secretory cells which bound the cavity of oil glands (Abbott *et al.*, 2010; Voo *et al.*, 2012).

It was from *E. polybractea* and a closely related species, *E. froggattii*, that the monoterpene-acid sugar esters (MSEs) cuniloside B and froggattiside A were first isolated (Fig. 2.2; Goodger *et al.*, 2009). It was also shown that these compounds accumulate exclusively in oil glands (Goodger and Woodrow, 2011). In Chapter 2 the chemical diversity of MSEs and their localisation to oil glands was explored. MSEs were found to be both chemically diverse and present in all species examined. In addition, there were clear differences between phylogenetic groups in terms of both quality and quantity. For example, species belonging to the sections *Adnataria*, *Bisectae* and *Dumaria* tended to have higher quantities and a greater diversity of MSEs than species from other groups.

To begin to understand the regulation of oil gland terpenoids the research presented in this chapter aims to investigate the deployment of MSEs and terpenes using *E. polybractea* as a model species. The first aim was to test whether MSEs and terpenes always co-occur and how variable the ratio between the two groups is. To test this aim the variation in MSEs and terpenes was quantified in two natural populations of *E. polybractea*. The two groups were found to covary and so a second ^{13}C pulse-chase study was undertaken to look in finer detail at the relationship between individual MSEs and terpenes. Specifically the aim of this experiment is to test the coordination of MSE and terpene biosynthesis and accumulation.

3.2 Materials and Methods

3.2.1 Population survey

Plant material

Bulk samples of fully expanded leaves were collected in February 2011 from two natural populations of *Eucalyptus polybractea* R.T. Baker from north-western Victoria, Australia (population A: 36°31.87 S, 143°44.68 E, population B: 36°32.78 S, 143°44.93 E) located on public land approximately 2 km apart (Parks Victoria collection permit: 10004785). The plants had been subjected to short rotation coppicing for many years (Goodger *et al.*, 2007). At the time of harvesting the coppice was 18 months of age. Samples were collected along a 30 m north-south transect with only fully expanded leaves from the current season's growth harvested. Leaves were kept on ice for no longer than 5 h before being transferred to a -80 °C freezer.

Mono- and sesquiterpene analysis

Two leaves from each tree were combined and ground to a fine powder in liquid nitrogen in a mortar. The leaves were extracted in 3 mL of hexane containing 100 μg mL^{-1} tridecane as an internal standard in glass vials. Samples were incubated at 50°C for 4 days on an orbital shaker (Ratek Instruments Pty Ltd, Boronia, Australia) operating at 150 rpm. After this time, the hexane extracts were dehydrated with Na_2SO_4, vortexed for 1 min, centrifuged for 10 min at 20000 g, and the supernatant transferred into 2 mL GC vials. The mono- and sesquiterpene content of the hexane extracts was quantified using gas chromatography with flame ionisation detection (GC-FID). The system consisted of a Perkin Elmer Autosystem XC GC-FID (Perkin Elmer, Melbourne, Australia) fitted with a Zebron-5 column (30 m $\times$ 0.25 mm i.d. $\times$ 0.25 μm film; Phenomenex, Torrance, USA). The carrier gas was He and had a flow rate of 1 mL min^{-1}. The temperature gradient was as follows: 70°C for 4 min, 10°C min^{-1} ramp to 250°C where it was held for 4 min. Terpenes were identified by comparison to the following standards: 1,8-cineole, *p*-cymene, limonene, sabinene, α-terpineol, terpinen-4-ol, myrcene, β-pinene and

α-pinene, aromadendrene, caryophyllene (Sigma-Aldrich, St Louis, USA). Terpenes were quantified by comparison to response curves of these standards.

MSE analysis

Tissue extracted for oil was allowed to dry and then re-extracted with 3 mL 70% acetone in water at 25°C for 24 h. Following this step, 180 μL aliquots of acetone extract were made up to 1.2 mL with water and then fractionated using 30 mg Strata-X reverse phase cartridges (Phenomenex) that had been preconditioned with 100% MeOH followed by water. Cartridges were washed with 1 mL 30% MeOH in water. The fraction containing cuniloside B and froggattiside A was then eluted with 3 mL 80% MeOH in water. This fraction was further separated by high-performance liquid chromatography (HPLC) using a Shimadzu HPLC system comprised of a Shimadzu LC-20AT pump, SIL-20A HT autosampler and SPD-M20A detector (Shimadzu Corporation, Kyoto, Japan). The samples were separated on a Gemini C18 analytical column (150 $\times$ 4.6 mm, 5 μm; Phenomenex) with a flow rate of 1 mL min^{-1} and column temperature of 23°C. The mobile phase consisted of 0.1% (v/v) formic acid in water (solvent A) and 0.1% (v/v) formic acid in MeCN (solvent B). The LC gradient method was as follows: solvent B was ramped from 30 to 45% over 2 min then increased to 65% over 8 min followed by an increase to 100% over 1 min and held for 1 min. The column was then re-equilibrated at 30% solvent B for 7 min. Cuniloside B was quantified based on absorbance at 220 nm compared to a standard series of synthetic cuniloside B (provided by Spencer Williams, The University of Melbourne; Hakki *et al.*, 2010). Froggattiside A was also quantified using this same standard series of cuniloside B and it was assumed the optical density of froggattiside A was equivalent to cuniloside B due to the shared oleuropeic acid and glucose moieties.

3.2.2 ^{13}C labelling

Plant material and sampling strategy

A *E. polybractea* clone growing in the System Garden at the University of Melbourne (Parkville, Australia 37°47.81′ S, 144°57.53′ E) was used in this experiment. The plant was micropropagated in 2008 and planted in the ground on the 5th April 2009. It was coppiced to ground level on 17th May 2012 and left to resprout for 6 months. After 6 months the coppice growth was approximately 0.5 m in height with numerous branches of the same age and at the same developmental stage (Fig. 3.1).

Harvests were made immediately before labelling and then at 4 and 8 h post-labelling and then each day for the next five days. At each harvest three branches with leaves ranging in developmental stage from newly emerged to ∼5.5 months of age were collected onto ice. Leaves were imaged with a flat bed scanner, weighed for fresh weight and then stored at −80°C until analysis. Leaf area was calculated from images of scanned leaves using ImageJ (Version 1.44; Schneider *et al.*, 2012)

^{13}C labelling

The plant was pulsed with ^{13}C by enclosing it in an acrylic chamber and generating an atmosphere enriched in $^{13}CO_2$. This was done by combining H_2SO_4 with $Na_2^{13}CO_3$ (99% ^{13}C; Cambridge Isotope Laboratories, Andover, MA, USA) in the chamber causing the evolution of $^{13}CO_2$. The chamber was constructed out of clear 4.5 mm polymethyl methacrylate and was custom built for this experiment by Plastics for Industry Pty Ltd (Keysorough, Australia). The chamber was 0.7 × 0.3 × 0.3 m with an internal volume of 0.059 m^3. The chamber consisted of two halves that when fitted together overlapped to create a seal. The edge of the chamber was also rimmed with rubber tape to improve gas tightness. A semi-circle was cut in the end of each chamber half to create a hole that would allow the chamber to be fitted over rooted plants. Rubber pipe insulation was used to protect the plant from damage while at the same time creating a close seal around the trunk. To this a clear plastic skirt was attached that was then sealed around

Figure 3.1: Coppiced *E. polybractea* plant used in $^{13}CO_2$ labelling study.

the chamber. Air inside the chamber was circulated with four 12 V fans (50 × 50 × 15 mm) fastened to the sides of the chamber. Each fan had an airflow of 7 m^3 h^{-1} .

To monitor CO_2 concentration and relative humidity, chamber air was drawn through a LICOR Portable Photosynthesis System (LI-6400, Lincoln, Nebraska, USA) at a rate of 0.01 m^3 h^{-1}. Air that would normally be exhausted from the system after analysis was redirected back into the chamber to avoid loss of $^{13}CO_2$.

The chamber was tested for gas leaks by setting up the chamber as for the field but without the plant. CO_2 was generated by adding 5 mL of 0.5 M H_2SO_4 to 100 mg of Na_2CO_3 through a syringe port in the side of the chamber. CO_2 increased from 397 to 735 μmol mol^{-1} in 2 min then gradually climbed to a maximum of 750 μmol mol^{-1} after 35 min. The chamber was found to be relatively airtight with the CO_2 concentration dropping by 42 μmol mol^{-1} over two hours.

The LICOR system was not ideal for measuring $^{13}CO_2$ concentration as the gas analyser is calibrated for detecting $^{12}CO_2$ resulting in an underestimation of $^{13}CO_2$ concentration (McDermitt *et al.*, 1993). To test the approximate length of time it would take for the plant to draw down the supplied $^{13}CO_2$ a preliminary test was carried out using $^{12}CO_2$ and a coppiced plant comparable to the specimen to be labelled and growing in the same garden plot. This time 5 mL of 0.5 M H_2SO_4 was added to 180 mg of Na_2CO_3 increasing CO_2 by 502 μmol mol^{-1}. CO_2 concentration dropped to 74 μmol mol^{-1} over the next 50 min and the temperature inside the chamber increased from 21 to 28°C (Fig. 3.2). The experiment was repeated under similar conditions with the labelled plant using $Na_2{}^{13}CO_3$. Based on the above measurements the plant was held in the chamber for 50 min to allow the $^{13}CO_2$ to be assimilated. The labelling experiment took place at the beginning of November 2012 on a partly cloudy day at ∼10:30 am.

Tissue extraction and sample preparation

The following metabolites were extracted from expanding and mature leaves and analysed for ^{13}C incorporation: monoterpenes and sesquiterpenes, cuniloside B, cypellocarpin C and froggattiside A. Mean values at each time point are the average of three leaves harvested from different branches.

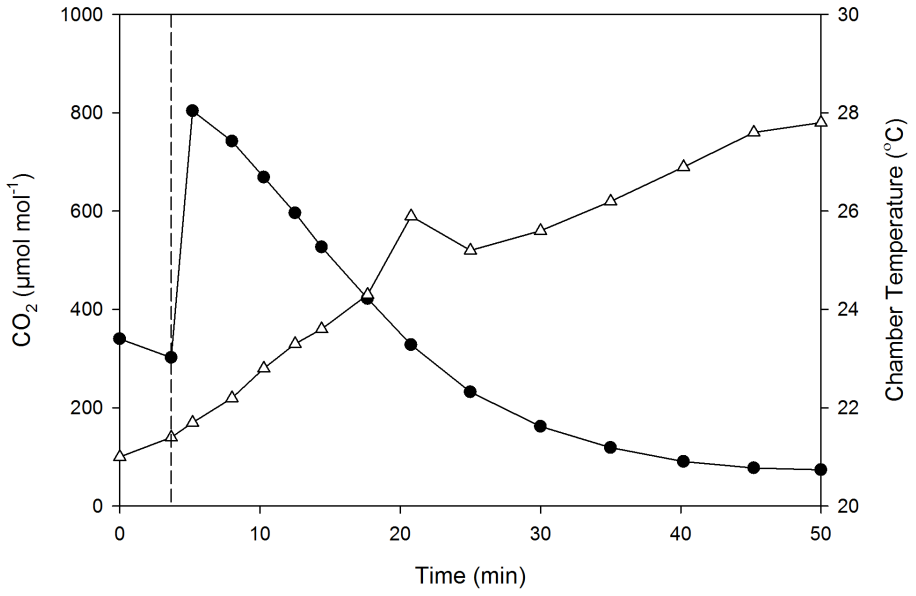

Figure 3.2: Validation of labelling experimental setup: $^{12}CO_2$ draw down by a *Eucalyptus polybractea* plant in the labelling chamber. Trace of chamber $^{12}CO_2$ concentration (black dots) and chamber temperature (white triangles) during labelling period. Dashed vertical line is where acid was added to Na_2CO_3 to generate $^{12}CO_2$. The experiment was carried out under natural light.

Pre-weighed and scanned leaves were ground to a fine powder in liquid nitrogen in a mortar. The homogenised frozen leaf powder was divided between two pre-weighed glass vials and weighed. One sample of tissue was analysed for terpene content and received 0.5 mL hexane with 100 μg mL^{-1} tridecane (Sigma) as an internal standard. Hexane extracts were prepared for GC analysis as per the population study (Section 3.2.1), except that each extract was split between two 2 mL GC vials. The terpene content of one vial was quantified with GC-FID and the other vial was analysed by GC-MS for ^{13}C isotope content.

The other half of ground leaf samples were used for MSE analysis and were extracted in 0.5 mL 30% MeCN in water. These samples were incubated for 24 h at 25°C on an orbital shaker operating at 150 rpm. The extracts were then transferred into 2 mL Eppendorf tubes and centrifuged for 5 min at 20000 g. The supernatant was transferred to HPLC vials and stored as a stock of raw extract at −20°C. Samples were prepared for HPLC analysis by diluting the raw extracts by a factor of 10 with 0.1% (v/v) formic acid in MeOH. Extracted tissue was dried at 50°C for two days and weighed for tissue dry weight.

3.2.3 Terpene quantification and isotope analysis

Terpenes were quantified using the same GC-FID system described for the population study (Section 3.2.1).

The ^{13}C abundance of terpenes was measured using GC-MS. The GC-MS system was comprised of Gerstel 2.5.2 autosampler, a 7890A Agilent gas chromatograph and a 5975C Agilent quadrupole mass spectrometer (Agilent Technologies, Santa Clara, USA). The mass spectrometer was tuned according to the manufacturers recommendations using *tris*-(perfluorobutyl)-amine. Gas chromatography was performed on a VF-5MS column (30 m × 0.25 mm i.d. × 0.25 μm film) with a 10 m Integra guard column (Varian, Inc, Victoria, Australia). Initial temperatures were as follows: injection temperatures, 250°C; MS transfer line, 280°C; ion source, 250°C and quadrupole, 150°C. Helium was used as the carrier gas at a flow rate of 0.8 mL min^{-1}. The gradient method was as follows: samples were injected onto a column at 40°C which was held for a further 1 min, followed

by a 10°C min^{-1} oven temperature ramp to 250°C with a final hold of 5 min. Mass spectra were recorded at 2 scans s^{-1} with a scanning range of m/z 50-600. Isotope data was extracted using MassHunter software (Agilent). Mass spectra of eluting compounds were identified using the commercial mass spectra library NIST (http://www.nist.gov).

3.2.4 MSE quantification and isotope analysis

Cuniloside B and froggattiside A were quantified as per section 3.2.1. Cypellocarpin C, noreugenin and oleuropeic acid were quantified by comparison to standard series of these compounds (provided by Spencer Williams, The University of Melbourne) and using the LC-MS system described below.

Isotope analysis was carried out using an LC-MS system consisting of an Agilent 1200 LC system coupled to an Agilent 6520 Electrospray Ionisation-Quadrupole-Time of Flight MS (Agilent). The following MS source conditions were used in positive ion mode: capillary voltage, 3500 V; gas temperature, 225°C; gas flow 10 L min^{-1}; nebuliser pressure, 35 psi; sheath gas temperature, 325°C; fragmentor voltage, 150 V; skimmer, 65 V. Samples were separated on a Zorbax Eclipse XDB-C18 Rapid Resolution HT column (2.1 $\times$ 100 mm, 1.8 μm; Agilent) with a flow rate of 0.8 mL min^{-1} and column temperature of 45°C. The mobile phase consisted of 0.1% (v/v) formic acid in water (solvent A) and 0.1% (v/v) formic acid in MeCN (solvent B). The LC gradient method was as follows: solvent B was held at 10% for 1 min then ramped to 60% over 5 min followed by an increase to 100% over 0.1 min and held for 1 min. The column was then re-equilibrated at 10% for 3.8 min. Isotope data was extracted using MassHunter software (Agilent).

3.2.5 ^{13}C incorporation into phenylalanine

Analysis of ^{13}C incorporation into phenylalanine followed the method of (Boughton *et al.*, 2011). Tissue samples extracted with hexane for terpene analysis were re-extracted with 75% MeOH by vortexing for 30 s. Samples were then centrifuged at 20000 g for 10 min. The supernatant was transferred to a fresh vial and amines were derivatised by 6-aminoquinolyl-N-hydroxysuccinimidylcarbamate (Aqc) with the following procedure.

A 10 μL aliquot of each sample was added to 70 μL of borate buffer (200 mM, pH = 8.8) containing 2-aminobutyric acid (25 μM) as internal standard. The resulting solution was vortexed and then 20 μL of Aqc reagent (10 mM dissolved in 100% MeCN) was added and immediately vortexed. The samples were heated with shaking at 55°C for 10 minutes then centrifuged and transferred to HPLC vials.

Samples were analysed on an Agilent 1200 LC-system coupled to an Agilent 6420 Electrospray Ionization-Triple Quadrupole MS (Agilent). The following MS source conditions were used in positive ion mode: capillary voltage, 3500 V; gas temperature, 325°C; gas flow 10 L min^{-1}; nebuliser pressure, 45 psi; sheath gas temperature, 325°C; fragmentor voltage, 145 V; skimmer, 65 V. A Zorbax Eclipse XDB-C18 Rapid Resolution HT column (2.1 $\times$ 100 mm, 1.8 μm; Agilent) was used to separate analytes with a flow rate of 0.3 mL min^{-1} and column temperature of 30°C. The mobile phase consisted of 0.1% (v/v) formic acid in water (solvent A) and 0.1% (v/v) formic acid in MeCN (solvent B). The LC gradient method was as follows: solvent B was held at 1% for 2 min then ramped to 15% over 7 min followed by an increase to 30% over 5 min. The column was then re-equilibrated at 1% solvent B for 5 min. Isotope data was extracted using MassHunter software (Agilent). Amino acids were identified based on mass comparisons with derivatised standards.

3.2.6 Calculations and statistical analyses

The ^{13}C incorporation into each metabolite was expressed as the ^{13}C atom fraction ($x(^{13}C)$) of a given metabolite and was calculated using Equation 3.1:

$$x(^{13}C)_P = \frac{n(^{13}C)_P}{n(^{12}C)_P + n(^{13}C)_P} \tag{3.1}$$

where n is the molar amount of the given isotope in compound, P.

Statistical analyses were performed using SPSS version 21.0 (SPSS Inc., Chicago, USA). Data were tested for normality using the Shapiro-Wilk test and homogeneity of variance between groups was measured using Levene's test. Where variances were non-homogenous, Welch ANOVA was used to compare sample means. Terpene data

for expanding and mature leaves of the labelled plant were not normally distributed. This could not be corrected by transforming the data and so the non-parametric Mann-Whitney *U* test was used to test differences between means.

3.3 Results

3.3.1 Intraspecific variation of MSEs and terpene concentration

The intra- and interpopulation variation of the two most abundant MSEs in *E. polybractea*, cuniloside B and froggattiside A, and terpenes was examined in two populations *E. polybractea*. Terpene content in population A ranged between 33.5 and 160.6 mg g^{-1} DW with an average ($\pm$ 1 SE) of 89.7 $\pm$ 6.5 mg g^{-1} DW. Similarly, terpene content ranged between 27.2 and 150.9 mg g^{-1} DW with an average ($\pm$ 1 SE) of 76.7 $\pm$ 6.2 mg g^{-1} DW in population B. Terpene concentration was normally distributed in both populations (Fig. 3.3) and was not significantly different between the populations (Welch ANOVA (unequal variance): $F(1, 52.5) = 2.84$, $P = 0.10$). The terpene profile was dominated by the monoterpene 1,8-cineole which made up, on average ($\pm$ 1 SE), 78.5% $\pm$ 0.8 of total terpenes in population A and 72.0% $\pm$ 1.5 in population B (Fig. 3.4). Many other components were present at low levels, in particular, the monoterpenes α-pinene, sabinene and limonene, and the sesquiterpenes β-elemene and cadinene.

The concentration of MSEs ranged between 6.7 and 26.0 mg g^{-1} DW with an average ($\pm$ 1 SE) of 16.4 $\pm$ 1.1 mg g^{-1} DW in population A and between 4.4 and 24.6 mg g^{-1} DW with an average ($\pm$ 1 SE) of 13.2 $\pm$ 1.03 mg g^{-1} DW in population B. MSE concentration was normally distributed in both populations (Fig. 3.5) and mean MSE concentration was significantly different between the populations (independent *t*-test: $t(53) = -2.16$, $P = 0.04$). Cuniloside B was present in far greater quantities than froggattiside A, making up, on average ($\pm$ 1 SE), 90.69 $\pm$ 0.78% and 87.61 $\pm$ 1.21% of the combined total in population A and B, respectively (Fig. 3.6).

MSE concentration and terpene concentration were regressed against each other and found to have a significant linear relationship in both populations ($P < 0.001$, Fig. 3.7). Variation in terpene concentration accounted for 80% and 73% of the variation in MSE

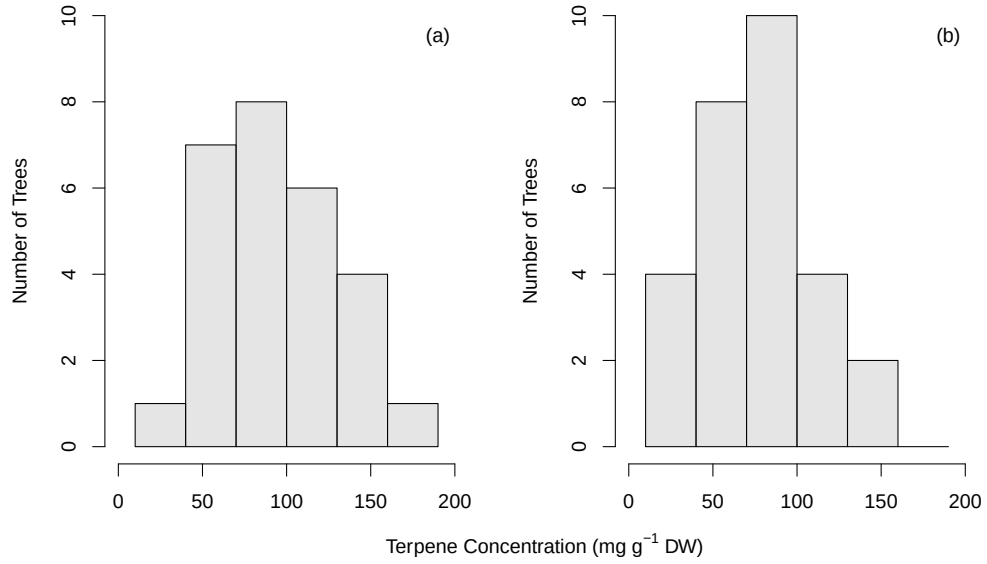

Figure 3.3: Foliar terpene concentration in two populations of *Eucalyptus polybractea*. Terpene concentration (mono- and sesquiterpenes) was normally distributed in both populations as assessed with a Shapiro-Wilk test (population A: $W(27) = 0.97$, $P = 0.54$; population B: $W(28) = 0.97$, $P = 0.48$). Figure panels: population A (a) and B (b).

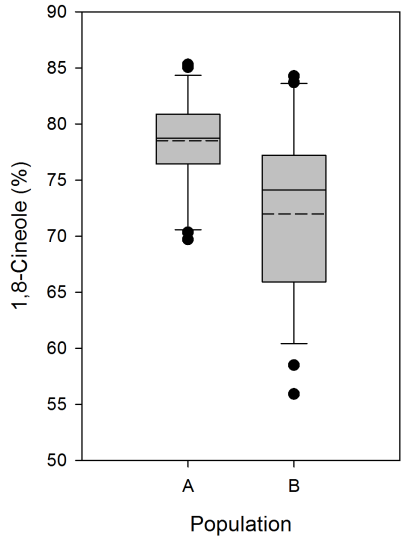

Figure 3.4: Percent 1,8-cineole of total terpenes (mono- and sesquiterpenes) in two *Eucalyptus polybractea* populations. Population A, $n = 27$. Population B, $n = 28$. Dashed and solid lines correspond to mean and median, respectively.

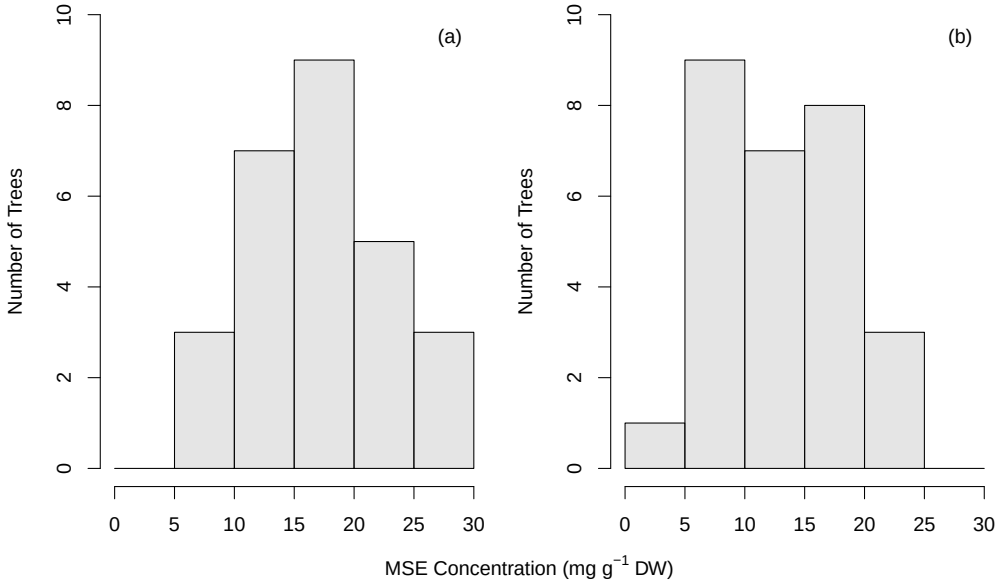

Figure 3.5: MSE concentration in two populations of *Eucalyptus polybractea*. MSE concentration (cuniloside B and froggattiside A) was normally distributed in both populations as assessed with a Shapiro-Wilk test (population A: $W(27) = 0.96$, $P = 0.34$; population B: $W(28) = 0.97$, $P = 0.51$). Figure panels: population A (a) and B (b).

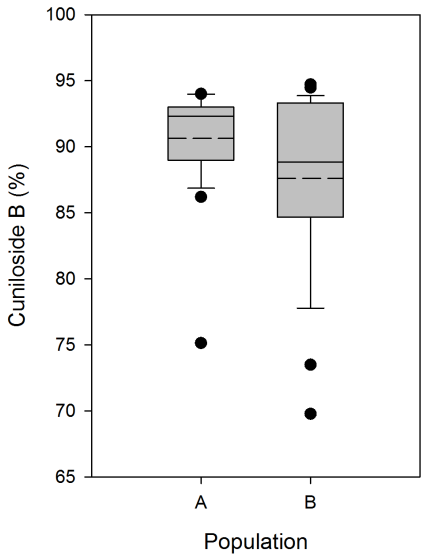

Figure 3.6: Percent cuniloside B of total MSEs in two *Eucalyptus polybractea* populations. Population A, $n = 27$. Population B, $n = 28$. Dashed and solid lines corresspond to mean and median, respectively.

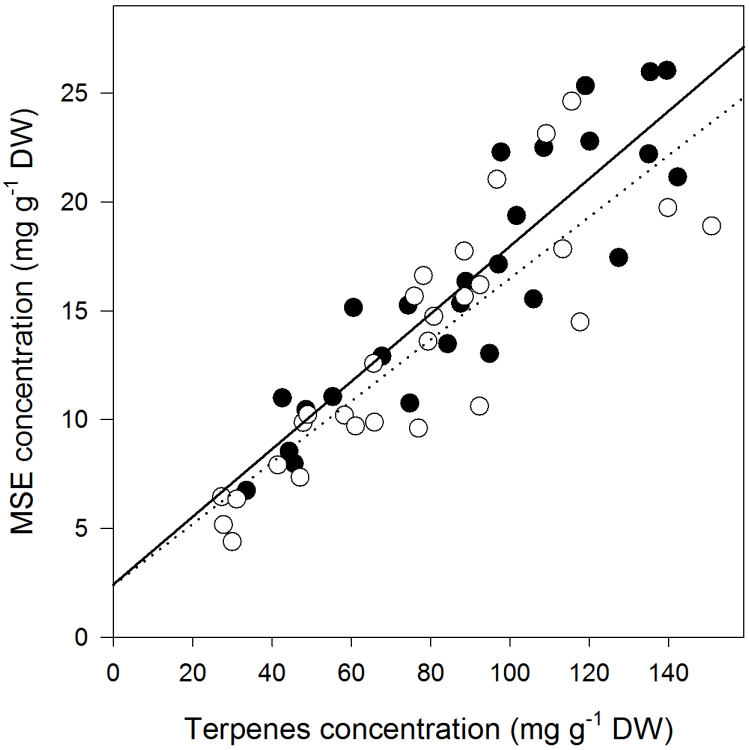

Figure 3.7: Relationship between terpene and MSE concentration in *Eucalyptus polybractea* leaves in two populations. Population A is represented with black dots and a solid regression line, and population B is represented with white dots and a dotted regression line. Population A regression equation: $y = 0.15x + 2.44$, $r^2 = 0.80$ $(F(1,26) = 96.23, P < 0.001)$; population B regression equation: $y = 0.14x + 2.40$, $r^2 = 0.73$ $(F(1,27) = 70.99, P < 0.001)$.

concentration in populations A and B respectively. The slopes of the regression lines were also consistent between populations with an ANOVA unable to detect a significant difference between the two ($F(1,52) = 0.58$, $P = 0.45$). There was no relationship between MSE concentration and percentage composition of any mono- or sesquiterpene (data not shown).

3.3.2 ^{13}C incorporation into terpenoids

To gain a more detailed understanding of the relationship between terpenes and MSEs, an *E. polybractea* plant was pulsed with $^{13}CO_2$ and the timing and extent of terpene and MSE labelling was examined.

Sampled leaves

A three year old plant of *E. polybractea* was coppiced 6 months prior to pulsing. This provided multiple even aged stems with leaves ranging in age from ∼5.5 months to just initiated (Fig. 3.8a). Leaves ranged in size from an ∼80 mm^2 for the youngest leaves to ∼350 for the oldest leaves. Expanding leaves, 3rd from the branch apex and with a mean area of (±1 SE) of 214.23 ± 9.50 mm^2, and mature leaves, 7th from the branch apex with a mean (±1 SE) of 352.61 ± 13.63 mm^2, were selected for analysis. This provided information on terpene and MSE regulation during leaf growth when oil glands are developing and when leaves are fully expanded (Fig. 3.8 a & b).

Leaf chemistry

The terpene and MSE profile of both expanding and mature leaves were qualitatively similar. Relative concentration (on a dry weight basis) of total MSEs, cuniloside B, total terpenes and total monoterpenes increased significantly from expanding to mature leaves (Fig. 3.9). In contrast, froggattiside A and total sesquiterpene concentration were not significantly different in mature compared to expanding leaves and cypellocarpin C had a significantly lower concentration in mature compared to expanding leaves (Fig. 3.9).

In a similar manner to the population study, there was a significant relationship between MSE and terpene concentration in expanding leaves with 37% of the variation in MSEs explained by variation in monoterpene concentration (Fig. 3.10). However, there was no significant relationship detected in mature leaves.

It was of interest whether specific terpenoids continued to be biosynthesised during leaf expansion, however, concentration measurements made on a per unit leaf mass basis are not suitable for this analysis. This is because the absolute amount of a metabolite may increase between ontogenetic stages but this does not necessarily translate into higher concentrations on a per unit leaf mass basis if the leaf mass has increased by a greater proportion than the metabolite mass. For this reason, metabolites were also compared on an absolute (per leaf) basis. All monoterpenes and MSEs were significantly higher in mature compared to expanding leaves indicating that these metabolites were still

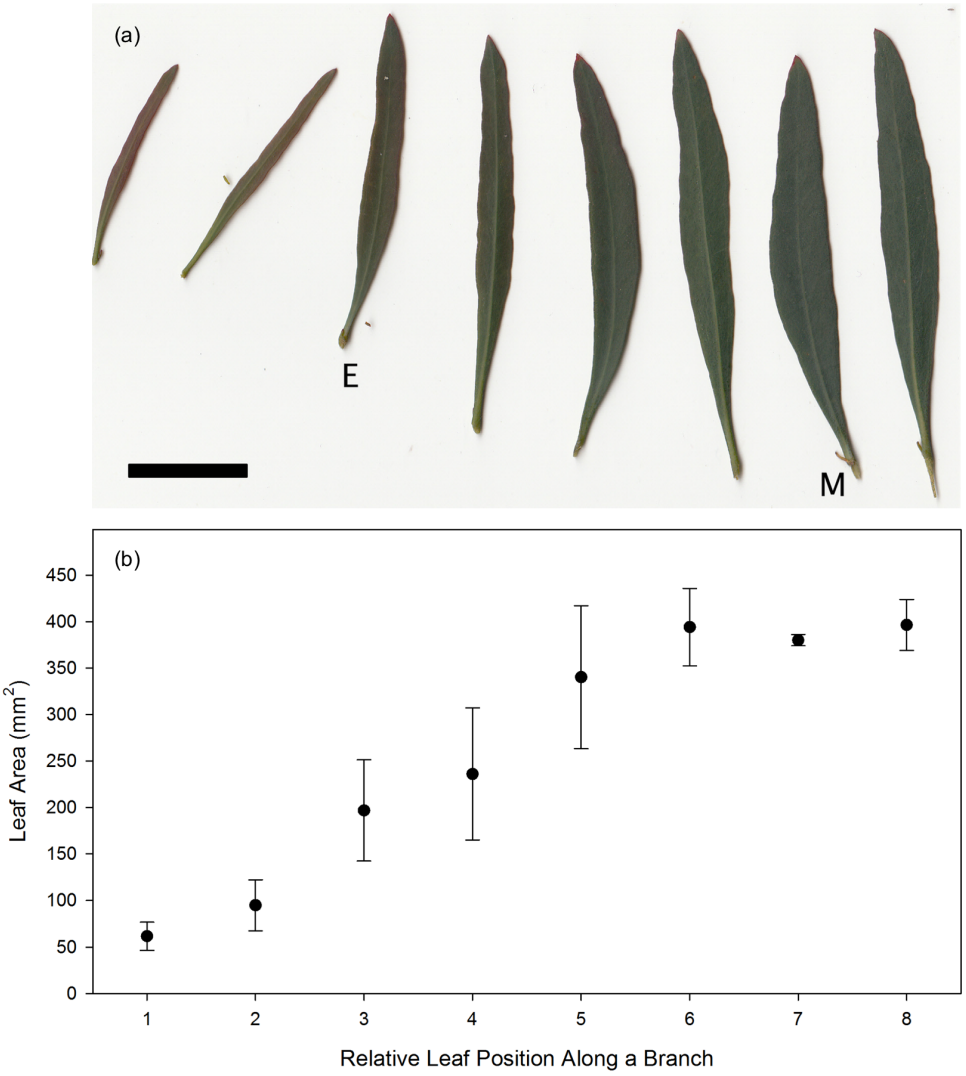

Figure 3.8: (a) Representative leaf series along a *Eucalyptus polybractea* branch. Analysed leaf classes indicated by letters: expanding (E) and mature (M). Scale bar = 20 mm. (b) Mean leaf area ($n = 3$) with error bars representing ± 1 SE at each node of three replicate branches from the first harvest.

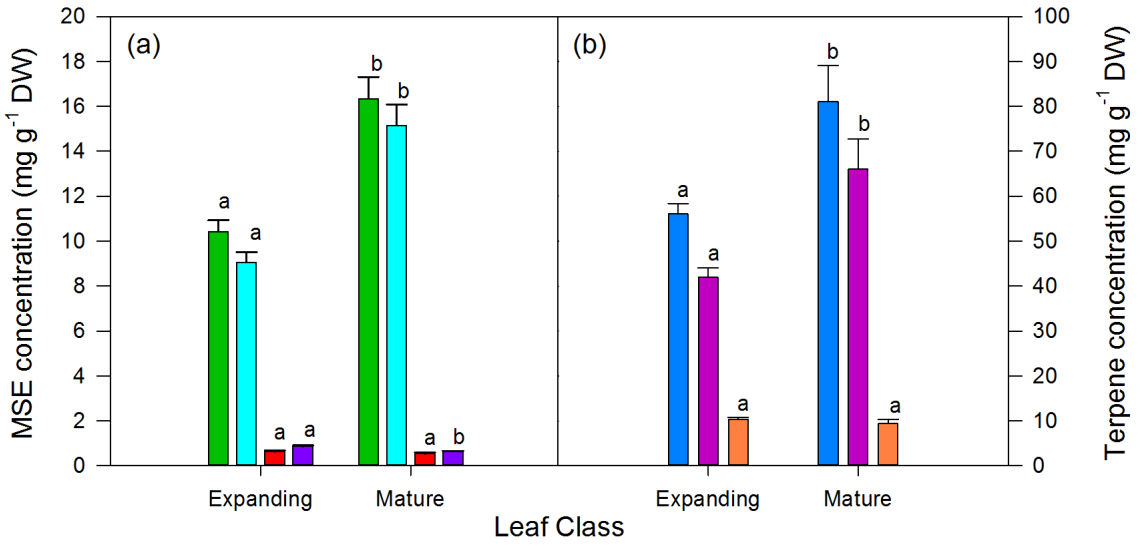

Figure 3.9: Mean terpenoid concentration in expanding and mature leaves. The concentration of different terpenoids was averaged across all harvests for each leaf class (expanding: $n = 27$, mature: $n = 20$). (a) MSEs: green = total MSEs, aqua = cuniloside B, red = froggattiside A and purple = cypellocarpin C. (b) Terpenes: blue = total terpenes, magenta = monoterpenes and orange = sesquiterpenes. Different letters above bars indicate expanding and mature means are significantly different at $P < 0.05$, as assessed by a Mann-Whitney U test.

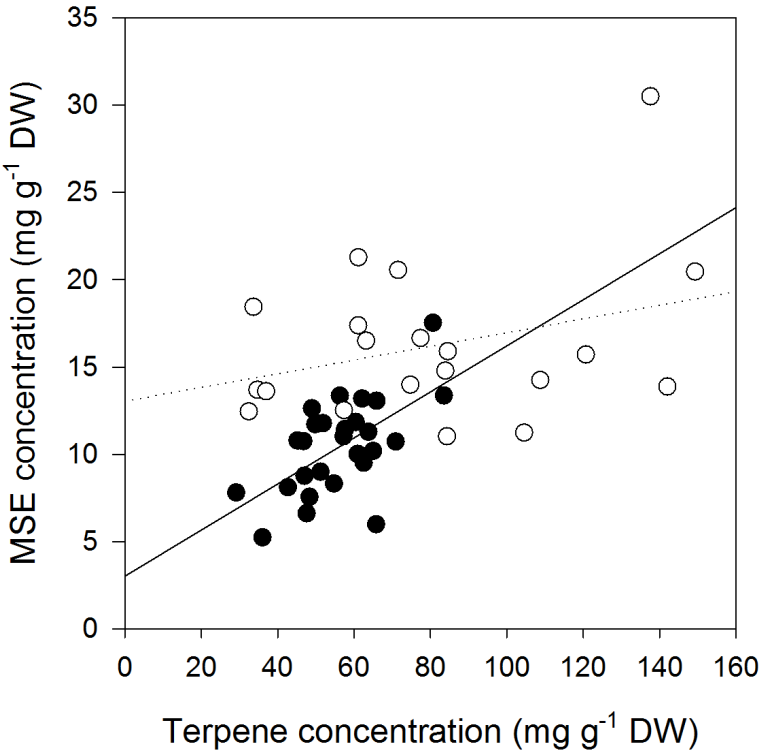

Figure 3.10: Relationship between terpene and MSE concentration in expanding and mature leaves. Expanding leaves are represented with black dots and a solid regression line and mature leaves are represented with white dots and a dotted regression line. Regression equations: expanding leaves, $y = 0.13x + 3.03$, $r^2 = 0.37$ $(F(1,25) = 14.22, P < 0.01)$; mature leaves - no significant relationship.

Table 3.1: Mean terpene and MSE concentrations in expanding and mature leaves expressed in μg leaf^{-1}. The concentration of different terpenoids was averaged across all harvests for each leaf class (expanding: n = 27, mature: n = 20). Mann-Whitney *U* tests were used to test for significant differences of means between expanding and mature leaves.

	Expanding		**Mature**		
Terpenoid	Mean	SE	Mean	SE	*P*
Monoterpenes					
Total Monoterpenes	770.6	75.7	1782.7	202.9	< 0.01
1,8-Cineole	663.9	65.2	1523.7	172.8	< 0.01
Sabinene	37.1	3.7	89.8	10.5	< 0.01
Limonene	32.5	3.1	77.9	9.0	< 0.01
α-Pinene	17.0	1.5	32.6	3.8	< 0.01
Myrcene	12.6	1.2	30.5	3.5	< 0.01
α-Terpineol	4.3	0.4	20.4	2.9	< 0.01
β-Pinene	2.8	0.3	7.4	0.8	< 0.01
Sesquiterpenes					
Total sesquiterpenes	179.5	10.7	255.7	27.3	0.03
β-Elemene	77.6	4.4	98.6	10.5	**0.26**
trans-Caryophyllene	49.0	3.3	72.7	7.8	0.02
Cadinene	34.6	2.2	55.5	5.8	< 0.01
α-Humulene	7.3	0.5	13.8	2.0	< 0.01
Globulol	4.7	0.3	4.3	0.7	**0.12**
Selinene	3.4	0.2	4.6	0.5	**0.16**
α-Eudesmol	2.5	0.3	5.8	1.0	< 0.01
MSEs					
Total MSEs	128.6	11.4	332.0	22.2	< 0.01
Cuniloside B	110.3	10.2	307.9	21.3	< 0.01
Cypellocarpin C	10.7	0.8	13.1	0.6	0.02
Froggattiside A	7.5	0.7	11.0	0.8	< 0.01

being accumulated at later stages of leaf expansion (Table 3.1). The sesquiterpenes, *trans*-caryophyllene, cadinene, α-humulene and α-eudesmol also showed the same ontogenetic pattern as MSEs and monoterpenes. In contrast, the absolute concentration of β-elemene, globulol and selinene did not change significantly between leaf classes indicating that accumulation of these sesquiterpenes occurs early in leaf development (Table 3.1). Samples were also analysed for the concentration of the MSE aglycones oleuropeic acid and noreugenin (the phenolic group of cypellocarpin C) which were present in trace amounts in both leaf classes.

Incorporation of ^{13}C into an amino acid

The incorporation of ^{13}C into the amino acid phenylalanine was measured in expanding leaves. As a primary metabolite, phenylalanine is likely to be turned over relatively rapidly in the cell and is a point of comparison for the incorporation pattern observed for MSEs and terpenes. ^{13}C was rapidly incorporated into this amino acid reaching a peak between 0 and 4 h after the pulse, returning to pre-pulse levels by 50 h, consistent with the expected rapid turnover of this metabolite (Fig. 3.11).

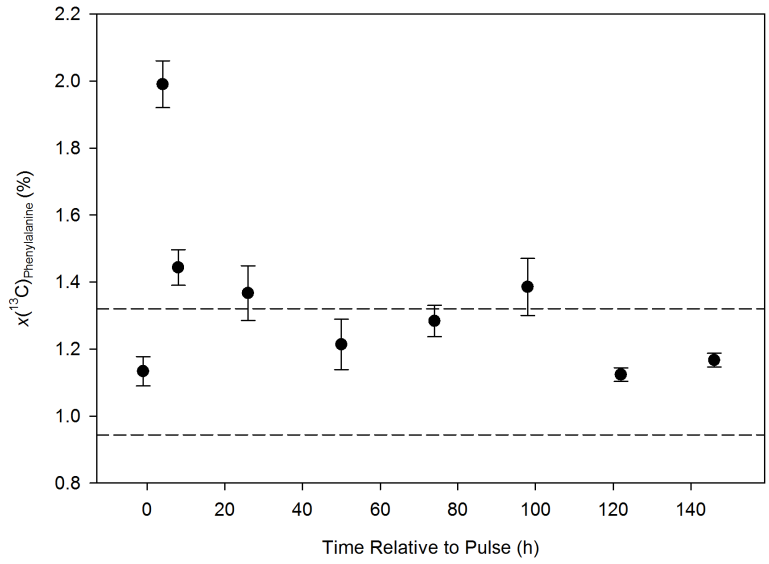

Figure 3.11: Incorporation of ^{13}C into phenylalanine in expanding leaves. The dashed lines indicate the upper and lower limits of the 95% confidence interval of the mean ($n = 3$) natural ^{13}C atom fraction at t = -1 h.

Incorporation of ^{13}C into MSEs

The ^{13}C enrichment of cuniloside B, froggattiside A and cypellocarpin C pools was measured over the course of the experiment. The ^{13}C atom fraction of all MSE pools increased in expanding leaves (Fig. 3.12 a, c & e). Incorporation followed a similar trajectory in all compounds: a lag of at least 4 h and then gradual incorporation reaching

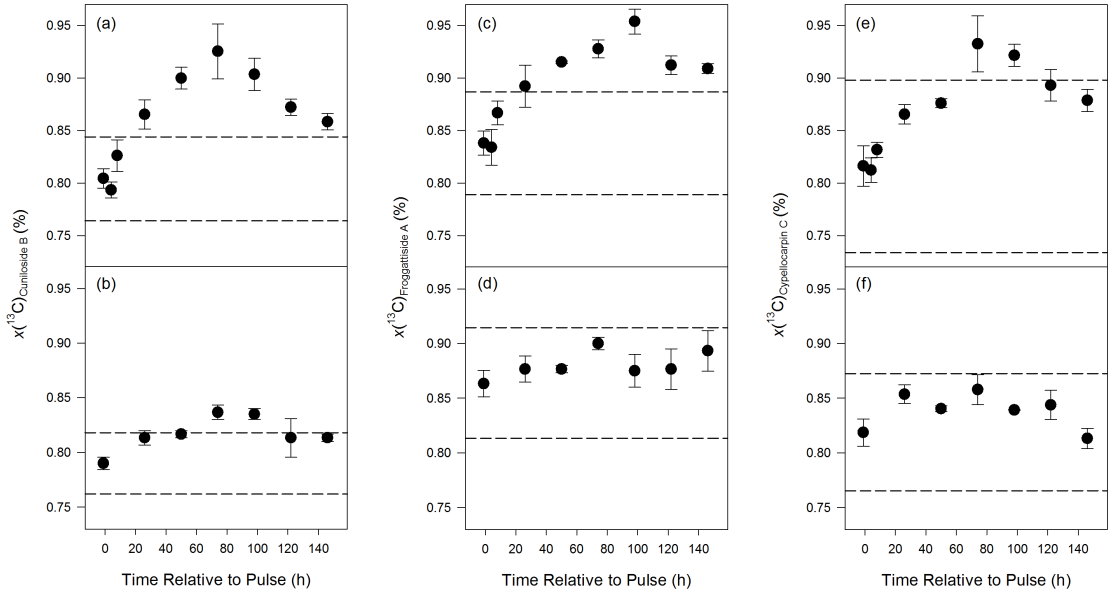

Figure 3.12: Incorporation of ^{13}C into cuniloside B, froggattiside A and cypellocarpin C expressed as ^{13}C atom fraction. Panels (a), (c) and (e) show incorporation into expanding leaves and (b), (d) and (f) show incorporation into mature leaves. The dashed lines indicate the upper and lower limits of the 95% confidence interval of the mean ($n = 3$) natural ^{13}C atom fraction at t = -1 h.

a peak between 74 and 98 h. After this point the ^{13}C atom fraction gradually declined to the end of the chase period at 146 h (Fig. 3.12 a, c & e). The data for mature leaves is less clear and suffers from the low sample number and high variability which made it difficult to detect lower levels of ^{13}C incorporation likely to occur in mature leaves. The data at each time point for cuniloside B was the least variable of the MSEs (due to higher concentrations of this compound in samples) and showed a similar pattern of ^{13}C incorporation as found for expanding leaves but with a lower peak value (Fig. 3.12 b).

Incorporation of ^{13}C into terpenes

^{13}C incorporation into all terpenes could not be determined because the GC-MS technique used in this study was not ideal for looking at isotope information. Specifically, the low mass resolution and hard ionisation technique gave many fragment ions for which reliable isotope data could not be extracted. Consequently, the molecular ion

was used to calculate ^{13}C atom fraction values; however, these ions had low abundances so incorporation data for many terpenes could not be collected. A second issue which arose was that the aliphatic monoterpenes were poorly separated chromatographically. This was problematic as aliphatic monoterpenes do not have unique ions which could be used to separate compounds. As a consequence, carbon isotope information for these monoterpenes was not obtained. In contrast, 1,8-cineole and α-terpineol are both oxygenated and so produce ions not present in aliphatic monoterpene spectra and were also chromatographically well separated from each other. This meant carbon isotope data could be extracted for both compounds.

Incorporation of ^{13}C into 1,8-cineole and α-terpineol occurred slightly faster than for MSEs, showing an increase in ^{13}C abundance by 4 h in expanding leaves (Fig. 3.13 a & c). ^{13}C enrichment of the 1,8-cineole pool increased by a slightly greater magnitude than observed for MSEs in expanding leaves. It peaked between 50 and 74 h, then gradually declined until the end of the chase period (Fig. 3.13a). In contrast to 1,8-cineole, the initial pattern and magnitude of ^{13}C enrichment of the α-terpineol pool was similar to phenylalanine (Fig. 3.11), increasing by a magnitude of $\sim$1% and reaching a peak between 8 and 24 h before declining to pre-pulse levels by 98 h (Fig. 3.13c). Both monoterpene pools in mature leaves increased in ^{13}C enrichment although the percent increase was less than that observed in expanding leaves (Fig. 3.13 b & d).

Information on ^{13}C incorporation into the sesquiterpenes *trans*-caryophyllene, cadinene and globulol was extracted from the GC-MS data. Incorporation of label into globulol was not detected in expanding or mature leaves (Fig. 3.14 e & f). In contrast, *trans*-caryophyllene and cadinene showed a similar pattern of ^{13}C enrichment in expanding leaves as found for 1,8-cineole and MSEs (Fig. 3.14 a & c). No incorporation of label was detected in mature leaves for any of the sesquiterpenes (Fig. 3.14 b & d).

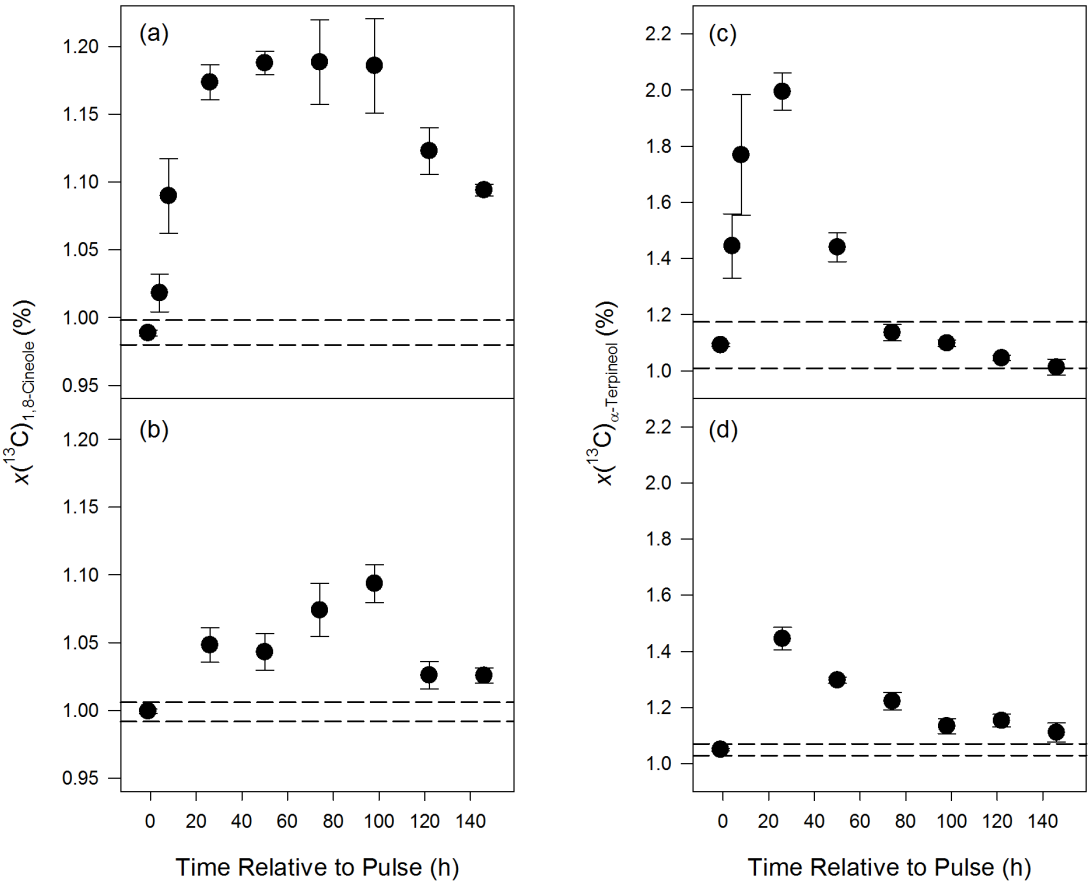

Figure 3.13: Incorporation of ^{13}C into 1,8-cineole and α-terpineol expressed as ^{13}C atom fraction. Panels (a) and (c) show incorporation into expanding leaves and (b) and (d) show incorporation into mature leaves. The dashed lines indicate the upper and lower limits of the 95% confidence interval of the mean ($n = 3$) natural ^{13}C atom fraction at t = -1 h. Note different Y-axis scale between 1,8-cineole and α-terpineol.

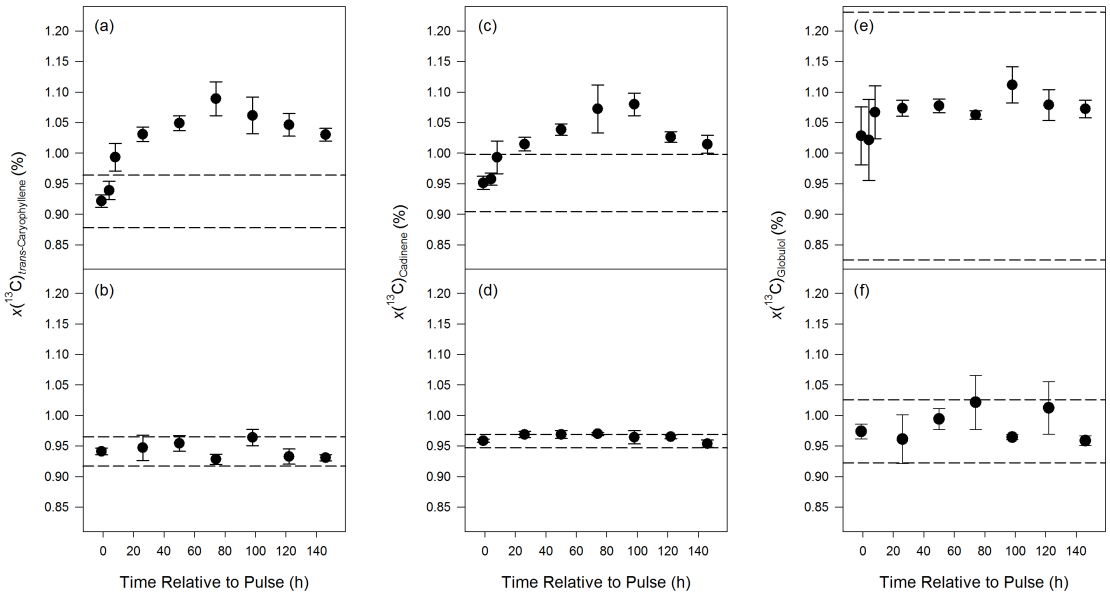

Figure 3.14: Incorporation of ^{13}C into *trans*-caryophyllene, cadinene and globulol expressed as ^{13}C atom fraction. Panels (a), (c) and (e) show incorporation into expanding leaves and (b), (d) and (f) show incorporation into mature leaves. The dashed lines indicate the upper and lower limits of the 95% confidence interval of the mean ($n = 3$) natural ^{13}C atom fraction at t = -1 h.

Regression analysis of ^{13}C incorporation into terpenoids

With the exception of α-terpineol and globulol (which did not incorporate detectable levels of pulse ^{13}C), enrichment of each individual terpenoid pool followed a similar pattern and reached a similar magnitude in expanding leaves. To investigate the coordination of terpenoid regulation in expanding leaves, linear regression analyses were performed on ^{13}C atom fraction data comparing metabolites both within and between terpenoid groups. In this analysis a significant correlation between two metabolites indicates that the pattern of enrichment and depletion of ^{13}C in the respective metabolite pools follows the same pattern; whereas the regression coefficient gives a measure of the relative magnitude of pool enrichment/depletion between the two metabolites (a slope of 1 indicates both pools are equally enriched/depleted). ^{13}C enrichment correlated well between terpenoids of the same group and between groups (Fig. 3.15, Table 3.2). The ^{13}C atom fraction of cuniloside B was regressed with froggattiside A and cypellocarpin C resulting in highly significant positive relationships (Table. 3.2). The regression coefficients were estimated to be between 0.64 and 1.02 (95% CI), and between 0.59 and 0.97 (95% CI), respectively. These results indicate that at this confidence level the enrichment of cuniloside B and cypellocarpin C were not significantly different from 1, and cuniloside B and froggattiside A were marginally different. The two sesquiterpenes which incorporated ^{13}C, *trans*-caryophyllene and cadinene, were also regressed and similarly found to have a highly significant positive relationship and with a regression coefficient estimated to be between 0.54 and 0.92 (95% CI; Table. 3.2), indicating the two sesquiterpenes were not equally enriched. As expected, 1,8-cineole ^{13}C atom fraction did not have a significant relationship with α-terpineol, but did with cuniloside B and *trans*-caryophyllene. Estimates of regression coefficients were between 0.46 and 0.66 (95% CI), and between 0.54 and 0.82 (95% CI), respectively (Table 3.2), indicating that the pool of 1,8-cineole was more enriched than any of the MSEs or sesquiterpenes.

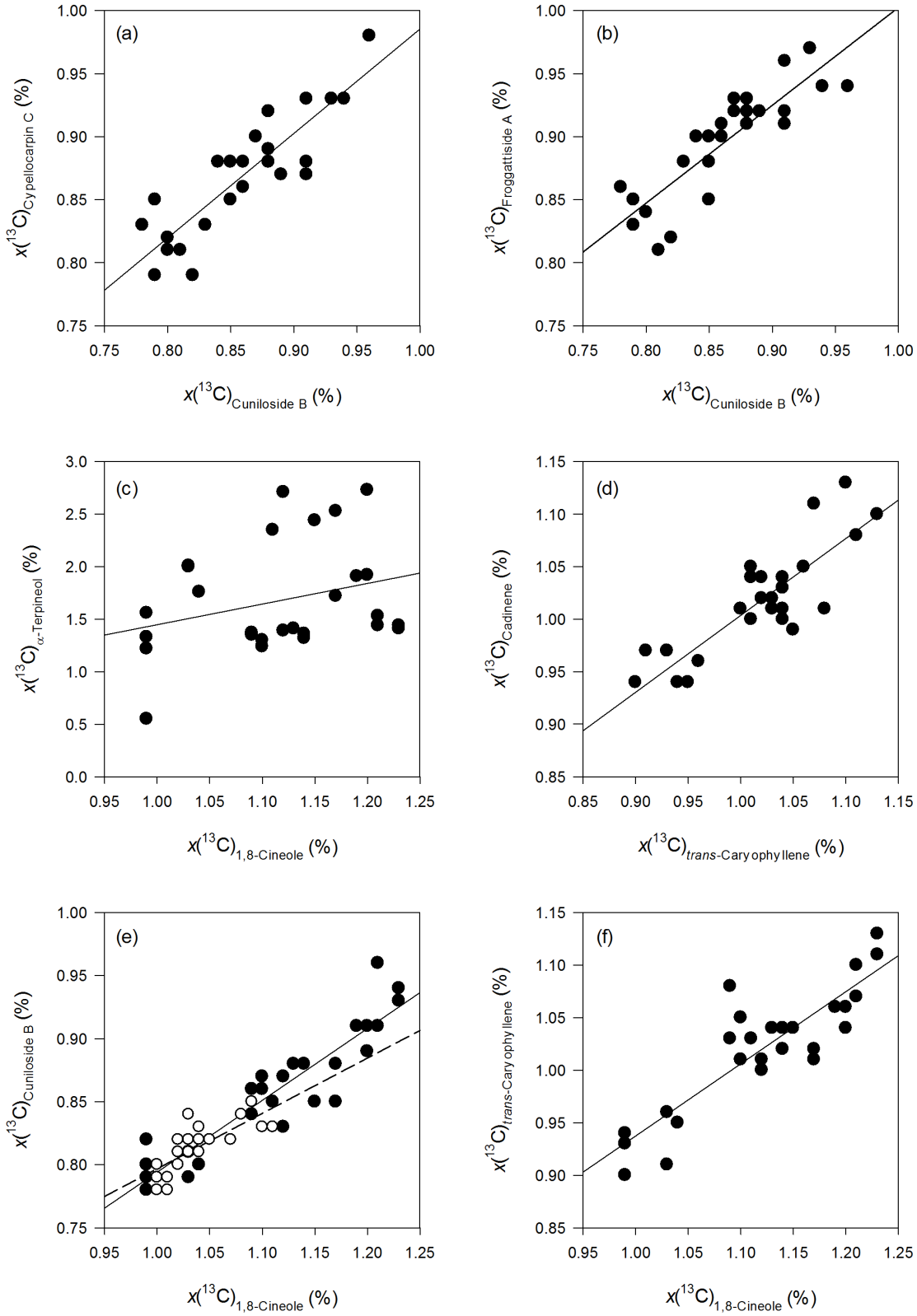

Figure 3.15: Relationship between ^{13}C enrichment of terpenoids in expanding leaves. Regression analysis statistics are reported in Table 3.2. Black circles: expanding leaves; open circles: mature leaves.

Table 3.2: Relationship between ^{13}C enrichment of terpenoids in expanding leaves. Regression coefficients and statistics for the linear regression analyses presented in Fig. 3.15. β = regression coefficient; SE = standard error of β; CI = 95% confidence interval for β.

Panel	Independent	Dependent	β	P	SE	CI	r^2
(a)	Cuniloside B	Cypellocarpin C	0.83	<0.01	0.09	0.64-1.02	0.75
(b)	Cuniloside B	Froggattiside A	0.78	<0.01	0.09	0.59-0.97	0.75
(c)	1,8-Cineole	α-Terpineol	1.97	0.13	-	-	-
(d)	*trans*-Caryophyllene	Cadinene	0.73	<0.01	0.09	0.54-0.92	0.73
(e)	1,8-Cineole (E)	Cuniloside B (E)	0.56	<0.01	0.05	0.46-0.66	0.84
	1,8-Cineole (M)	Cuniloside B (M)	0.45	<0.01	0.07	0.31-0.59	0.58
(f)	1,8-Cineole	*trans*-Caryophyllene	0.68	<0.01	0.07	0.54-0.82	0.78

Relationship between monoterpenes and evidence for a single synthase

Goodger *et al.* (2013b) showed that the concentrations of myrcene, sabinene, limonene and 1,8-cineole were all tightly correlated ($r^2 = 0.99$) in *E. polybractea* leaves. Such a fixed ratio of products most likely indicates they are synthesised by a single multi-product monoterpene synthase (Fähnrich *et al.*, 2011; Goodger *et al.*, 2013b). Evidence from characterised cineole/terpineol synthases suggest α-terpineol is also a product of the same synthase (Fähnrich *et al.*, 2011; 2012). In light of this and the differing labelling pattern of 1,8-cineole and α-terpineol it was of interest how the two would correlate. Pearson's correlations were run to determine the linear relationship between 1,8-cineole and the other major monoterpenes. Consistent with previous findings myrcene, sabinene and limonene were all strongly correlated with 1,8-cineole returning r values between 0.99 and 1 (Table 3.3). In addition, α-pinene and β-pinene showed the same tight positive correlation with 1,8-cineole giving r values of $\sim$1. Interestingly, the relationship between α-terpineol and 1,8-cineole was also one of strong positive correlation, although slightly more variable, returning an r value of 0.93 and 0.98 for expanding and mature leaves, respectively (Table 3.3). The ratios of monoterpene components to 1,8-cineole were found to be significantly different (with the exception of limonene) between expanding and mature leaves (Table 3.3). Although significant, the difference in ratio was small for all components with the exception of α-terpineol which increased from 0.66 to 1.44%.

Table 3.3: Correlation between 1,8-cineole concentration and related monoterpenes in expanding and mature leaves. Monoterpenes were compared on a μmol mL^{-1} hexane extract basis. r is the Pearson's correlation coefficient of a given monoterpene correlated against 1,8-cineole, where n = 27 and 20 for expanding and mature leaves, respectively. Percent is the mean ratio of a given monoterpene to 1,8-cineole expressed as a percentage $\pm$ 1 standard error (SE). P-values indicate whether mean ratios between expanding and mature leaves were significantly different as assessed with a Mann-Whitney U test.

	Expanding			**Mature**			
Monoterpene	r	%	$\pm$ SE	r	%	$\pm$ SE	P
β-Pinene	0.99	0.5	0.01	1.00	0.55	0.01	< 0.01
α-Terpineol	0.93	0.66	0.03	0.98	1.40	0.07	< 0.01
Myrcene	1.00	2.15	0.03	1.00	2.31	0.01	< 0.01
α-Pinene	0.99	2.94	0.07	1.00	2.46	0.02	< 0.01
Limonene	1.00	5.55	0.03	0.99	5.61	0.04	0.13
Sabinene	1.00	6.27	0.07	1.00	6.78	0.05	< 0.01

3.4 Discussion

3.4.1 MSE and terpene variation

Terpene concentration varied widely and continuously between individual plants in both study populations (Fig. 3.3). The variation in and also the domination of 1,8-cineole in the terpene profiles is consistent with a previous study carried out on a population of *E. polybractea* by King *et al.* (2004). In this study, terpene concentration ranged between 14 and 64 mg g^{-1} DW with an average concentration of 36 mg g^{-1} DW and percent 1,8-cineole ranged between 49 and 93% with an average of 78% (King *et al.*, 2004). The reported maximum and mean terpene concentrations are much lower than those reported in the present study where maxima of 161 and 151 mg g^{-1} and means of 90 and 77 mg g^{-1} DW were found for populations A and B, respectively. These contrasting results are consistent with the finding that oil yield reduces with coppice age (Goodger and Woodrow, 2009). The coppice regrowth sampled by King *et al.* (2004) was 14 years old compared to 18 months in the present study.

Only cuniloside B and froggattiside A were quantified in this study but cypellocarpin C is also present in this species at levels similar to froggattiside A (Table 2.3). Nevertheless, there was no evidence in chromatograms for significant levels of this or

any other MSE (data not shown), so it is reasonable to conclude that the combined concentration of cuniloside B and froggattiside A is a close approximation of total MSE concentration. Similarly to terpenes, MSE concentration was highly variable (Fig. 3.5) and, in addition, positively covaried with terpene concentration (Fig. 3.7). There was a strong relationship between the two groups of terpenoids with variation in terpenes accounting for some 80% of the variation in MSE concentration. In *E. polybractea*, where the oil profile is made up of >90% monoterpenes, it is not clear whether the MSEs are covaring with total terpenes or monoterpenes. Based on evidence from *E. froggattii*, it is likely to be the former as in this species the terpene profile was shown to be dominated by sesquiterpenes, but MSEs and terpenes still covaried (Goodger *et al.*, 2013a). Furthermore, total terpene concentration also explained more of the variation in MSE concentration than either monoterpene or sesquiterpene concentration alone in *E. froggattii*.

Terpene concentration is under strong genetic control in *Eucalyptus* (Barton *et al.*, 1991; Doran and Matheson, 1994). Therefore, the covariation of MSEs with terpenes observed in the population study suggests that, firstly, MSE concentration is also under strong genetic control and, secondly, the two are co-regulated. Co-regulation is likely to be occurring at multiple levels due to both the potential for biosynthetic links between monoterpenes (discussed in Section 3.4.2) and MSEs and also the fact that they are both localised to oil glands.

The genetic factors behind the quantitative variation in terpenes is only just starting to be explored in this genus. QTL studies have identified multiple loci which influence terpene concentration (Henery *et al.*, 2007; O'Reilly-Wapstra *et al.*, 2011), but the identity of the genes at these loci have not been established. Külheim *et al.* (2011) was able to associate allelic variation of genes in the pathways leading to terpenes with a small proportion of the variation in terpene concentration in *E. globulus*; however, in other species a far better predictor of terpene concentration is transcript abundance of these genes (Crocoll *et al.*, 2010; Webb *et al.*, 2013). Findings by Webb *et al.* (2013) in another myrtaceous species, *Melaleuca alternifolia*, support the hypothesis that the regulation of terpene yield is controlled at the transcriptional level in *Eucalyptus*. Strong correlations

were observed between the expression level of MEP pathway genes and monoterpene concentration in expanding leaves of this species. Overall, 87% of the variation in monoterpene concentration could be explained by variation in gene expression. The results from Webb *et al.* (2013) also indicate that the genes in both the MEP pathway and the MVA pathway are coordinately expressed and, furthermore, it was suggested that this may be due to common transcriptional regulators. Such a mechanism could explain the high level of coordination between monoterpene, sesquiterpene and MSE biosynthesis demonstrated in expanding leaves in the labelling study (Fig, 3.15, Table 3.2). Although, the apparent differential regulation of sesquiterpenes (Table 3.1) and also the possible slowing of froggattiside A and cypellocarpin C biosynthesis through ontogeny (Fig. 3.9) suggests that other, perhaps developmentally regulated factors, also seem to be determining terpenoid chemistry.

In species that accumulate metabolites in the cavities of specialised structures, such as oil glands, the genes controlling their size and density will ultimately determine the total amount that can be accumulated (Bouwmeester *et al.*, 1998; Goodger and Woodrow, 2012). Thus, MSE covariation with terpenes could be explained by the fact that the amount of both groups of terpenoids are constrained by total leaf cavity volume. However, it is surprising that the ratio between MSEs and terpenes showed little variation and was consistent across populations (Fig. 3.7). The lack of variation in this trait may indicate that the possible value this ratio can take in an individual of this species is tightly constrained. Without knowledge of function it is difficult to say what these constraining factors might be but could be either physiological or ecological.

In the labelling study there was a positive relationship detected between terpenes and MSEs in expanding leaves, however, there was no significant relationship detected in mature leaves (Fig. 3.10). This is surprising given the strong relationship observed in the population study and is inconsistent with findings from the study examining *E. froggattii* (Goodger *et al.*, 2013a). One possible explanation for the variability observed in the results is that these leaves were some of the first to emerge after coppicing of the plant and this may have affected their development. Ideally this experiment needs to be

repeated with true biological replication as opposed to the psuedo-replication used here in order to test the validity of this result.

3.4.2 ^{13}C enrichment of MSE and terpene pools

The pattern and magnitude of ^{13}C enrichment of MSEs, 1,8-cineole, *trans*-caryophyllene and cadinene in expanding leaves were remarkably similar given the multiple biosynthetic pathways involved in their synthesis, in particular, the additional enzymatic steps involved in the formation of MSEs, and differing pre-existing pool sizes. This is consistent with a model of regulation where metabolites are being added to existing pools at a steady rate that is reflective of their pool size with no or low rates of loss. For example, there was a 6 fold difference in the pool size of 1,8-cineole and cuniloside B in expanding leaves yet ^{13}C enrichment of their respective pools was comparable: 1,8-cineole had a maximum enrichment of $\sim$0.19% and cuniloside B a maximum of $\sim$0.12% (Fig. 3.12a & 3.13a). Nevertheless, as these numbers would suggest, the regression slopes within and between groups were less than one (Table 3.2). The pool of cuniloside B was slightly more enriched than froggattiside A and the pool of 1,8-cineole was more enriched than any other terpenoid with the exception of α-terpineol. Such difference are potentially the result of shifts in pathway activity through development and also, in the case of 1,8-cineole and to a lesser extent the sesquiterpenes, losses from foliar pools via volatilisation.

On the other hand if a metabolite pool is turned over rapidly (relative to the chase period) then it will both reach a higher percentage of enrichment and decline towards natural levels more quickly than metabolite pools with no or relatively slow turnover. Such a pattern was observed for phenylalanine, which rapidly increased in ^{13}C enrichment by $\sim$0.88% in the first 4 h and declined towards pre-pulse levels by 50 h (Fig. 3.11), and is consistent with the known rapid turnover of this amino acid in the cell (Kouchi *et al.*, 1985). The monoterpene α-terpineol also showed a pattern of enrichment consistent with turnover, reaching a maximum level of enrichment of $\sim$0.90% by 26 h before declining towards pre-pulse levels by 78 h (Fig. 3.13c).

The loss of label from α-terpineol could be due to a combination of factors including volatilisation, dilution with cold α-terpineol and further metabolism. *Eucalyptus* species emit relatively high levels of monoterpenes (Guenther *et al.*, 1991; He *et al.*, 2000), which are thought to originate from oil glands (Winters, 2010). However, monoterpene emissions from a diverse array of eucalypts have been measured and none were shown to contain detectable levels of α-terpineol (He *et al.*, 2000; Winters *et al.*, 2009). Instead, 1,8-cineole and α-pinene appear to be the major emitted species and their dominance is probably a reflection of stored terpene composition as well as relative vapour pressures (He *et al.*, 2000; Winters *et al.*, 2009). For this reason a similar loss of label in 1,8-cineole would be expected if volatilisation of α-terpineol is the main route of loss. In contrast to α-terpineol, the ^{13}C atom fraction of 1,8-cineole remained well above pre-pulse levels for the duration of the chase period, only beginning to decline after 98 h (Fig. 3.13a). It should be noted that two studies have localised α-terpineol and 1,8-cineole specifically to oil glands in *E. polybractea* (Goodger *et al.*, 2010; King *et al.*, 2006a), so it is unlikely that α-terpineol is being biosynthesised and emitted from mesophyll cells such as occurs in non-storing species (Staudt and Bertin, 1998).

An alternative explanation for α-terpineol's relatively rapid turnover is that a portion of this monoterpene is converted to oleuropeic acid, the monoterpenoid moiety in the majority of *Eucalyptus* MSEs, as suggested by Guo and Yang (2006). The conversion of α-terpineol to oleuropeic acid would require multiple oxidation steps at the C-7 position. Evidence from the biosynthetic pathway leading to sesquiterpene lactones in Asteraceae suggest these steps may be catalysed by a single enzyme (Cankar *et al.*, 2011; Nguyen *et al.*, 2010). Specifically, a cytochrome P450, CYP71AV8, has been shown to catalyse all three steps in the oxidation of germacrene A to germacranoic acid in multiple species from this family (Nguyen *et al.*, 2010). Alternatively, multiple enzymes could sequentially carry out the various hydroxylation and dehydrogenation steps such as in the biosynthesis of menthol from limonene (Croteau *et al.*, 2005).

The other major MSE in *E. polybractea*, froggattiside A, contains a second monoterpenoid, menthiafolic acid. Based on the structure of menthiafolic acid the most likely precursor to this compound is linalool. Unfortunately, linalool did not accumulate

to detectable levels in the genotype used in the labelling study so the ^{13}C incorporation could not be studied. However, it was detected in trace amounts in the population study (data not shown) and has been reported from this species previously (Goodger *et al.*, 2009). Recently, the pathway leading to a series of oxidised linalool derivatives, including menthiafolic acid was elucidated in *Arabidopsis* flowers. As for the formation of germacranoic acid, the oxidised derivatives of linalool were all found to be products of a single cytochrome P450 (Ginglinger *et al.*, 2013).

It should be noted that a recent publication has hypothesised that both menthiafolic acid and oleuropeic acid could be derived from linalool (Goodger and Woodrow, 2013). The apparent turnover of α-terpineol in the present study suggests this may be the precursor of oleuropeic acid but does not exclude the possibility that linalool also contributes to the pool of oleuropeic acid.

3.4.3 Regulation of MSE biosynthesis

Monoterpenes were found to be present in fixed ratios in accordance with previous findings from *E. polybractea* (Fig. 3.3; Goodger *et al.*, 2013b). This is strong evidence that these monoterpenes are derived from a single multi-product monoterpene synthase, a hypothesis further supported by the monoterpene product profile which is typical of characterised 1,8-cineole synthases (Fähnrich *et al.*, 2011). As 1,8-cineole is thought to be the result of further cyclisation of α-terpineol in the enzyme active site, it is argued that the efficiency of this reaction determines the ratio of α-terpineol to 1,8-cineole in the product profile of a given synthase (Fähnrich *et al.*, 2011; Fähnrich *et al.*, 2012). If a single 1,8-cineole/α-terpineol synthase is responsible for the production of both monoterpenes in *E. polybractea*, then the cyclisation efficiency could be an important determinant of the availability of oleuropeic acid for MSE biosynthesis. If the ratio of MSEs to terpenes is in fact an important trait, as suggested by the results of the population study, then the monoterpene synthase would be under strong selective pressure to maintain a minimum level of α-terpineol activity.

Consistent with α-terpineol being an intermediate, the ratio of this monoterpene to 1,8-cineole was shown to change between developmental stages whereas the other

monoterpenes were present in relatively constant proportions (Table. 3.3). Specifically, there was more α-terpineol relative to 1,8-cineole in mature compared to expanding leaves. This relationship could indicate that the production of MSEs is down regulated in later stages of development relative to monoterpene biosynthesis resulting in the accumulation of more α-terpineol in the oil gland cavity. Indeed, based on labelling results froggattiside A and cypellocarpin C were not being biosynthesised in mature leaves.

3.4.4 Loss of terpenoids from oil glands

The ^{13}C atom fraction of 1,8-cineole, MSE, and sesquiterpene pools all started to decline after $\sim$98 h. This is consistent with the dilution of labelled pools with newly synthesised metabolites that have natural abundance ^{13}C following the wash out of label ^{13}C from the system but could additionally be the result of gradual volatilisation and/or metabolism. Due to the experimental design of this study, including the choice of ^{13}C as label, it is not possible to separate out these factors. Nevertheless, it is worth commenting on the apparent ongoing biosynthesis in mature leaves which have presumably reached their cavity volume limit (Fig. 3.8). Pools of cuniloside B, 1,8-cineole and α-terpineol in mature leaves all incorporated appreciable amounts of pulse ^{13}C indicating these compounds were still being biosynthesised.

These findings are not congruent with the prevailing idea that foliar embedded oil glands, like those in *Eucalyptus*, are no longer biosynthetically active after leaves have reached maturity (Ciccarelli *et al.*, 2003; List *et al.*, 1995). This understanding is largely based on ultrastructural observations of oil glands and to a lesser extent terpene profile. For example, List *et al.* (1995) argue for a one-way developmental trajectory in *Melaleuca alternifolia*: oil glands develop with leaf ontogeny through a schizogenous/lysigenous mechanism, the terpene profile also matures through time and, at the conclusion of leaf maturation, the final terpene content is reached. This then remains stable for the remainder of the leaf lifetime. In glandular secreting trichomes (GSTs) this idea is supported by enzyme activity and gene expression studies which show a rapid decline

after maturation (Deschamps *et al.*, 2006; McConkey *et al.*, 2000). In addition, there is no evidence of catabolism or significant volatilisation over time (Gershenzon *et al.*, 2000).

In contrast to the short lived plant organs that carry GSTs, eucalypts have long lived leaves (Wright and Westoby, 2002) and, in addition, emit high levels of monoterpenes which are, at least in part, derived from oil gland cavities (Winters, 2010). Thus, it is conceivable that monoterpenes continue to be biosynthesised as replacements for those lost via gradual volatilisation from cavities. However, this explanation does not explain the continued biosynthesis of MSEs, which are not volatile. Given that there is a finite space available for the storage of terpenoids this continued biosynthesis may indicate that MSEs can be degraded. Continued tracking of leaf chemistry after full leaf expansion is reached will provide information on metabolite pool dynamics and how the relationship between the different terpenoid groups changes in the longer term.

3.5 Concluding remarks

This study examined the regulation of foliar terpenes and MSEs in *E. polybractea*. A high degree of polymorphism was observed, with terpenes and MSEs present in a wide range of concentrations, but the two groups were found to positively covary. To examine the factors regulating terpenoid composition, a ^{13}C labelling study was undertaken. Biosynthesis of monoterpenes, sesquiterpenes and MSEs was shown in developing leaves but only monoterpene and cuniloside B biosynthesis was detected in mature leaves. The pattern and magnitude of ^{13}C enrichment for each metabolite in developing leaves was consistent with a steady rate of accumulation that was reflective of the pool size of the measured metabolite and indicated that no or low rates of loss were occurring from oil glands. The exception to this pattern was α-terpineol which had a labelling pattern consistent with it being an intermediate. It is suggested that this monoterpene is a precursor to oleuropeic acid the main monoterpene-acid found in MSEs. The finding that oil glands are still metabolically active in mature leaves is contrary to our current understanding of oil gland physiology and raises questions about what the major factors are that influence terpenoid composition after leaf maturation.

In the present study a ^{13}C labelling protocol was developed which served to provide preliminary data on some of the terpenoids present in leaves; however, data for the majority of terpenoids could not be obtained. In addition, the use of ^{13}C precluded a clear analysis of oil gland pool dynamics because of the difficulty in deconvoluting the natural ^{13}C and supplied ^{13}C signals. The use of labelled substrate does show promise for elucidating terpenoid regulation in future studies but an alternative label, such as ^{14}C is recommended. Such work could provide information on how and when different terpene precursors are funnelled into the final terpenoid products and the rate of loss from each metabolite pool, thus creating a detailed picture of overall terpenoid metabolism in eucalypt oil glands.

Chapter 4

Multi-photon fluorescence lifetime imaging of *Eucalyptus* oil glands

4.1 Introduction

A defining feature of eucalypts is the presence of foliar oil glands. The glands consist of a central cavity lined by epithelial cells which are themselves encased by several layers of flattened thicker-walled parenchyma cells (Bohte and Drinnan, 2011; Carr and Carr, 1970). Oil glands are embedded in leaf mesophyll tissue and are present throughout the leaf lamina. They originate from either clusters of parenchyma cells or single epidermal cells and form and develop throughout organ expansion (Bohte and Drinnan, 2011; Carr and Carr, 1970). Historically *Eucalyptus* oil glands have been considered to only accumulate an essential oil rich in mono- and sesquiterpenes. With the recent discovery that cavities also contain an abundant, resinous non-volatile component (NVC), this list now extends to include monoterpene-acid sugar esters (MSEs) and flavonoids (Chapter 2, Goodger *et al.*, 2009).

Eucalyptus oil glands are difficult to study due to their embedded nature and as a consequence the presence of a NVC had been overlooked in previous investigations (King *et al.*, 2006a). A factor that aided in its discovery was the development of an oil gland isolation protocol, this enabled intact and living complexes to be isolated from surrounding tissue (Goodger *et al.*, 2010). Initial observations of isolated glands from *E. polybractea* using fluorescence microscopy indicated that the essential oil and NVC formed distinct phases in the cavity and that the NVC was the major source of fluorescence.

The presence of multiple phases is a relatively common observation in the metabolically similar essential oil bearing glandular secreting trichomes (GSTs) which are superficial in nature and thus easier to investigate (e.g. Appezzato-da Glória *et al.*, 2012; Majdi *et al.*, 2011; Turner *et al.*, 2000). Turner *et al.* (2000) proposed that such NVCs may form a protective barrier between secretory cells and the essential oil accumulating in the cavity. There is ample evidence that terpenes, particularly monoterpenes which are often components of essential oil, are capable of causing toxicity in plants (Abrahim *et al.*, 2003; Gog *et al.*, 2005; Nishida *et al.*, 2005; Yoshimura *et al.*, 2011). Multiple aspects of cell function appear to be affected and the effects are dosage dependent. These include the inhibition of DNA synthesis (Nishida *et al.*, 2005), increased membrane permeability (Maffei *et al.*, 2001) and altered respiration (Abrahim *et al.*, 2003).

Although the majority of tests have been carried out on species that do not naturally accumulate terpenes, the toxic effects appear to be present in accumulating species as well. Gog *et al.* (2005) examined the toxicity of monoterpenes towards the leaves of three species that accumulate terpenes in embedded cavities: *Pastinaca sativa*, *Petroselinum crispum* and *Citrus jambhiri*. The application of monoterpenes to leaves of all species resulted in the rapid reduction of photosynthetic activity and, in the long term, cell death. To compare these results to the impact of endogenously produced terpenes on cell viability, Gog *et al.* (2005) mechanically damaged areas of leaves that either did or did not contain oil glands. Only damaged areas where essential oil had been released from cavities showed a similar decrease in photosynthetic activity to that occurring when exogenous monoterpenes were applied. While cell wall modification has been suggested as a mechanism to isolate secretions from surrounding tissue (Bosabalidis and Tsekos, 1982a; List *et al.*, 1995), the mechanism proposed by Turner *et al.* (2000) would allow secretory cells in direct contact with the cavity contents to remain biosynthetically active.

The embedded nature of oil glands, like those found in *Eucalyptus* species, has hindered investigations of their structure and function (Turner *et al.*, 1998); however, the development of an isolation protocol has opened up the opportunity to investigate their internal structure using optical sectioning techniques. As such, multi-photon fluorescence lifetime imaging microscopy (MP-FLIM) was investigated as a tool to

visualise intact and living oil glands. MP-FLIM is a combination of two techniques. FLIM utilises the fluorescence decay properties of fluorophores to provide additional information about the sample at high spatial resolution. A fluorophore's lifetime is sensitive to the surrounding micro-environment which means this property can be used to measure diverse parameters such as viscosity (Suhling *et al.*, 2004), pH and ion concentration (Babourina and Rengel, 2009; Vroom *et al.*, 1999), and protein-protein interactions (Bücherl *et al.*, 2013).

The second aspect of this technique, MP excitation, uses near infrared (NIR) wavelengths to excite fluorophores in the sample instead of the usual UV and shorter visible wavelengths used in traditional fluorescence microscopy. NIR light is able to penetrate deeper into biological tissue than UV wavelengths due to the relative lack of endogenous absorbers and the reduced scattering of NIR light compared to UV (Helmchen and Denk, 2005). In addition, the non-linear dependence of multi-photon absorption on the excitation light intensity results in inherent optical sectioning (Denk *et al.*, 1990). This can often result in higher quality images obtained from deeper within materials, particularly biological tissue, than those obtained through conventional laser scanning confocal microscopy (LSCM; Centonze and White, 1998; Feijó and Moreno, 2004; Helmchen and Denk, 2005). Benefits have also been reported in terms of reduced photobleaching and increased cell viability due to both the limited excitation volume and less harmful NIR wavelengths used in multi-photon excitation (Feijó and Moreno, 2004).

In the botanical sciences MP-FLIM has been taken up relatively slowly compared to other areas of life science such as the biomedical field. The majority of studies on plant systems have used MP-FLIM to detect the close interaction of fluorescently labelled proteins in protoplasts and leaf epidermal cells via Förster resonance energy transfer (FRET) (Bernoux *et al.*, 2008; Boutant *et al.*, 2010). In this application the benefits of MP-FLIM are the increase in signal to noise ratio and the improvement in cell viability. However, as these cells are on the surface of plants and lack strongly absorbing pigments, the full benefit in terms of increased depth penetration of MP excitation has not been realised. Nonetheless, there are a few plant studies that have used this technology to obtain detailed lifetime information from fluorophores embedded deep within intact

plant tissue. For example, MP-FLIM has been used to successfully determine the excited state kinetics of light harvesting complexes in chloroplasts situated throughout the leaf lamina of *Alocasia wentii* (Broess *et al.*, 2009). This technique was also used to study the uptake of aluminium ions by *Arabidopsis* roots with high spatial resolution (Babourina and Rengel, 2009).

The aim of this chapter is to image the intact metabolome of eucalypt oil glands using MP-FLIM. Three species were selected for analysis based on both their chemistry and the isolability of glands. *Eucalyptus polybractea* was selected as a species whose NVC is dominated by the MSEs cuniloside B and froggattiside A (Goodger *et al.*, 2009). In addition, oil glands have previously been isolated from this species (Goodger *et al.*, 2010). *Eucalyptus spathulata* was chosen as a species with high levels of MSEs other than cuniloside B and froggattiside A, including the newly isolated gallic acid MSE, eucaglobulin B (Chapter 2). *Eucalyptus gregsoniana* was also selected for analysis as the non-volatile profile of this species is dominated by flavonoids (Chapter 2) and not MSEs. Neither of the major constituents of *E. polybractea* NVC are fluorescent. The origin of NVC fluorescence was speculated to be from phenolic glycosides also found in cavities (Goodger *et al.*, 2010). Eucalglobulin B, a phenolic glycoside, was available as a pure compound so its fluorescent properties were investigated as part of this study.

4.2 Materials and Methods

4.2.1 Plant material

Eucalyptus polybractea leaves were harvested from a micropropagated sapling (Goodger *et al.*, 2008). *Eucalyptus spathulata* and *E. gregsoniana* saplings were purchased from Kuranga Native Nursery (Mt Evelyn, Victoria, Australia). All plants were housed in a glasshouse with mean day/night temperature and relative humidity of $23.2 \pm 0.1^{\circ}C/19.8 \pm 0.1^{\circ}C$ and $55.5 \pm 0.2\%/63.4 \pm 0.1\%$, respectively. Plants were fertilized every 6 months with Osmocote slow release fertilizer (Scotts Australia, Bella Vista, New South Wales, Australia) and watered twice daily to field capacity. The plants were all between 1 and 2

years old during the experiment and all had adult foliage. Fully expanded leaves were sampled as needed and immediately used for either oil gland isolation or NVC extraction.

4.2.2 Sample preparation

Oil glands were isolated from leaf tissue using a pectinase leaf digestion protocol as described in Goodger *et al.* (2010). Briefly, leaves were sliced into 2 mm wide strips and placed in an Eppendorf tube with a 2:1 mixture of isolation buffer (500 mM sorbitol, 5 mM MES-KOH, 1 mM $CaCl_2$, pH 5.5) and pectinase in glycerol (P-4716, Sigma, St. Louis, MO, USA). Samples were incubated in a thermomixer (Eppendorf, Hamburg, Germany) at 25°C and 150 rpm. *Eucalyptus polybractea* tissue was incubated for 16 h and *E. spathulata* and *E. gregsoniana* tissues for 2 h. After pectinase digestion the glands were loosened from surrounding tissue and were manually removed with a pipette under a stereomicroscope (BH-2, Olympus, Centre Valley, PA, USA; Fig. 4.1). Glands were mounted on concave well glass microscope slides and covered with coverslips, which were then sealed around the edges with VALAP (Vaseline, lanolin and paraffin wax in 1:1:1 ratio). Non-enzymatically isolated glands were prepared from *E. polybractea* leaves by dissecting away as much surrounding leaf tissue as possible without rupturing cavities and mounting them as for enzymatically isolated glands. NVC was extracted from fully expanded leaves directly from cavities using a microprobe with 1 μm tip as described in Section 2.2.2 (World Precision Instruments Pty Ltd, Sarasota, FL, USA), applied to coverslips and imaged. Essential oil was steam distilled from a bulk leaf sample of *E. polybractea* (for details see Goodger *et al.*, 2007).

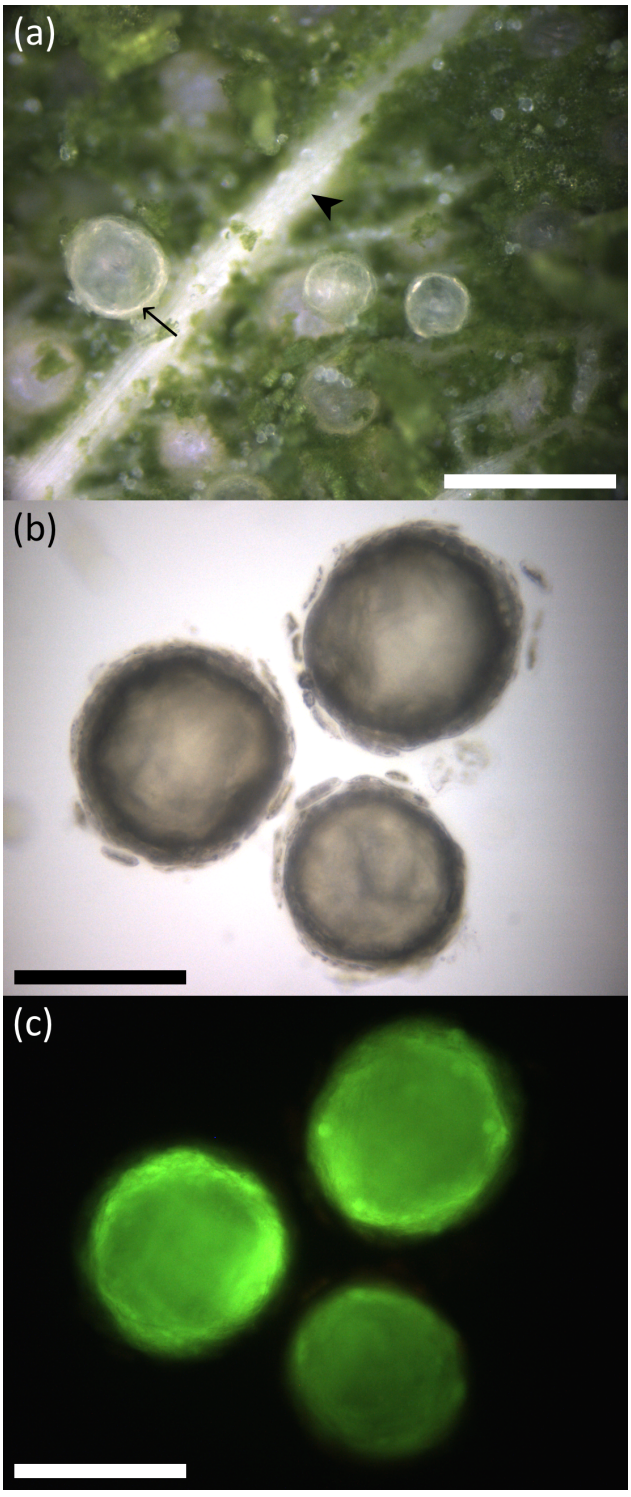

Figure 4.1: *Eucalyptus polybractea* oil gland isolation. (a) A leaf after petinase digestion with the cuticle removed and freed oil glands. Arrow = oil gland; arrowhead = midrib; scalebar = 200 μm. (b) Three isolated oil glands with flattened casing cells on the surface and (c) the same glands imaged under UV illumnation with GFP2 filter showing autofluorescence of the oil gland cavity. Scalebar = 100 μm.

4.2.3 Fluorescence spectrometry

Steady state excitation and emission spectra were collected with a Cary Eclipse fluorescence spectrophotometer (Varian Inc, Palo Alto, CA, USA) with a spectral bandwidth of 5 nm. NVC was extracted from cavities with a microprobe and applied to the surface of coverslips which were positioned in the light path of the spectrophotometer. Essential oil that had been steam extracted from *E. polybractea* and the purified phenolic glycoside eucaglobulin B were dissolved in 100% MeCN and placed separately in a 1 cm path length quartz cell. Eucaglobulin B was purified from *E. platypus* (see Chapter 2 for details).

4.2.4 Multi-photon fluorescence lifetime imaging microscopy

A schematic of the time-resolved, multi-photon fluorescence microscope is depicted in Figure 4.2. A mode-locked Ti:sapphire laser (Mira 900F, Coherent, Santa Clara, CA, USA) pumped by a 10 W Nd:vanadate laser (Verdi V10, Coherent) was used as the $\sim$800 nm illumination source. The laser produced optical pulses with a temporal pulse width of approximately 100 fs ($\sim$3 nJ pulse energy) at a repetition rate of 76 MHz. The laser beam was coupled to an inverted microscope (IX-71, Olympus) through a confocal scanning unit (FV-300, Olympus) and a transfer lens, which produced a focussed spot scanned across the normal focal plane of the imaging objective (Olympus 40$\times$ UPlanApo 1.0 NA oil, or 100$\times$ UPlanSApo, 1.4 NA oil). A dichromatic mirror (UV-Cold Mirror, TFI Inc., Greenfield, MA, USA) mounted at 45° in the rotating filter turret of the microscope efficiently allowed incident illumination to fill the back aperture of the imaging objective, while reflecting the emitted visible fluorescence from the sample to a PMT detector (PMC-1-100, Becker and Hickl, Berlin, Germany) masked with a blocking filter (BG39, TFI Inc.).

Time-resolved two-photon fluorescence images were obtained using a complete electronic system for recording fast light signals by time-correlated single photon counting (SPC-830, Becker and Hickl, Berlin, Germany). Synchronised data collection accumulating photon counts in each pixel following multiple scans was achieved with

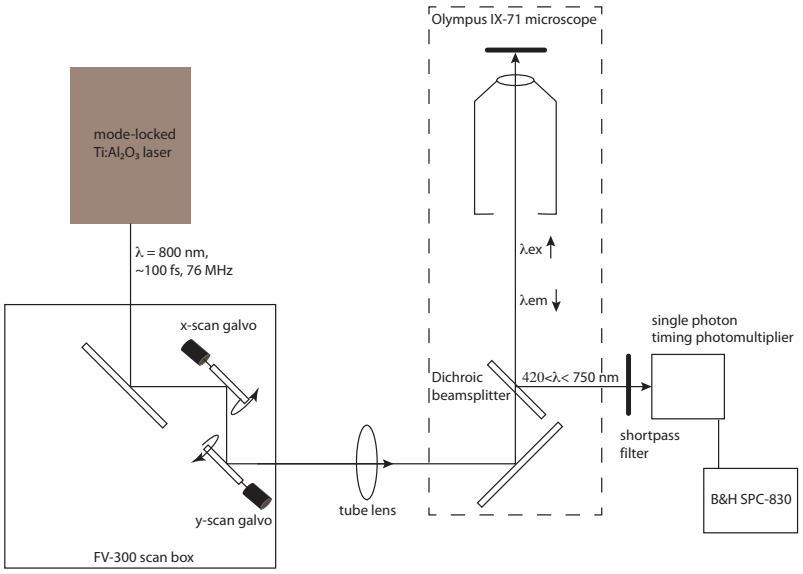

Figure 4.2: Schematic of the time-resolved multi-photon microscope.

the SPC-830 board using the frame, line and pixel clocks of the FV-300 scan unit following necessary hardware modifications. Each image was recorded as scans of 1024 $\times$ 1024 pixels that were binned by the SPC-830 data acquisition software to generate images of 256 $\times$ 256 pixels, comprising complete fluorescence decay information in each pixel. The temporal evolution of the emission probability after excitation was described by a histogram of these time spans whereby each counting event was allocated to a temporal bin for each pixel of the image. Intensity images were generated by summing all of the photons in the distribution histogram for each pixel individually using the separate off-line image analysis package SPCImage (Becker and Hickl). The fluorescence lifetime in each pixel was calculated using the same software. SPCImage was used to apply a Levenberg-Marquardt nonlinear least squares iterative re-convolution routine to individually fit the fluorescence decay data from each pixel, assuming that the fluorescence decay histogram for each pixel is well described by a multi-exponential decay (Equation 1):

$$I(t) = \sum_{i=0}^{n} a_i \exp^{(-t/\tau_i)} + c \tag{4.1}$$

where $I(t)$ is the fluorescence intensity at time t after the excitation pulse, τ_i and a_i are the fluorescence lifetimes and their fractional contributions, respectively, and c is a baseline parameter. The SPCImage software was used to derive the instrument response function (IRF) by approximating the IRF as a Gaussian function, the width of which was adjusted to give the best fit to the rising edge of the decays (Becker, 2005). Fluorescence lifetime images were generated by pseudo-colour mapping the average weighted fluorescence lifetime (τ_m) of each pixel over the intensity image. τ_m values are a weighted average of the different lifetime components and were calculated using the following:

$$\tau_m = \frac{\sum_{i=1}^{n} a_i \tau_i}{\sum_{i=1}^{n} a_i} \tag{4.2}$$

All fluorescence lifetime values were calculated for defined regions within an image with mean values being the average of 1000 pixels. In the specific case of oil gland cell walls, a triple, rather than a double exponential decay model, provided a better fit of the fluorescence decay data based on χ^2 values. It should be noted that in all cases the decay terms are not assigned to individual fluorescence species but are used in the calculation of the weighted average lifetime parameter.

4.2.5 Imaging parameters

The imaging parameters were optimised to obtain the strongest fluorescence signal from isolated oil glands whilst minimising the scanning time for each sample. The laser beam was focused to approximately the centre of the lumen and the wavelength tuned to achieve the strongest fluorescence signal. This was achieved with an excitation wavelength of 760 nm. A compromise between laser power and scan time was reached to minimise laser power yet acquire adequate photon counts in each pixel for accurate fluorescence decay curve fitting. This was achieved with a laser power of $\sim$14 mW at the sample through the 40 $\times$ objective ($\sim$180 pJ/pulse) and a total scan time of 3 min. These conditions did not visibly damage the oil glands or result in photobleaching. The extent to which oil glands could be optically sectioned was limited by the focussing depth of the

objective (80 μm). An image was taken of all oil glands at the focussing limit; this varied for different oil glands as it was dependent on where they were positioned relative to the coverslip. For selected oil glands, serial optical sections were imaged starting at the uppermost secretory cells with images taken every 10 μm along the z-axis to the focussing limit.

4.2.6 Non-linear excitation dependence of NVC fluorescence

The non-linear excitation power dependence was determined by varying the excitation light intensity and collecting successive fluorescence images using the Becker and Hickl photon counting software. NVC was extracted directly from oil gland cavities of *E. polybractea* and applied to a coverslip. The excitation light intensity was adjusted with a variable neutral density filter and the emission signal was measured over a range of laser powers from 6.2 to 100 mW, measured using an Ophir Nova power meter (Ophir Optronics, Jerusalem, Israel) just prior to the entrance to the scan box. The total emission photon counts in each image were integrated across all pixels (256×256) using a routine in MatLab (The MathWorks Inc, Natick, MA, USA) to give a representative emission intensity. The data acquisition parameters were the same as that used for oil gland imaging. To check for photo-degradation of the sample over the sampling period the emission signal resulting from the highest power tested (100 mW) was collected at the start and end of the experiment with no difference between the two measurements detected.

4.3 Results

4.3.1 Fluorescence spectroscopy

Steady state excitation and emission spectra were gathered for NVC extracts taken from the cavities of *E. polybractea*, *E. spathulata* and *E. gregsoniana*. The extract from *E. gregsoniana* was not fluorescent and so this species was not included in further analyses. *Eucalyptus polybractea* and *E. spathulata* extracts both had excitation/emission maxima of

345/490 nm (Fig. 4.3 a & c). The essential oil of *E. polybractea* was also found to be fluorescent with excitation/emission maxima of 290/350 nm (Fig. 4.3b). The phenolic glycoside, eucaglobulin B, had excitation/emission maxima of 275/343 nm (Fig. 4.3d).

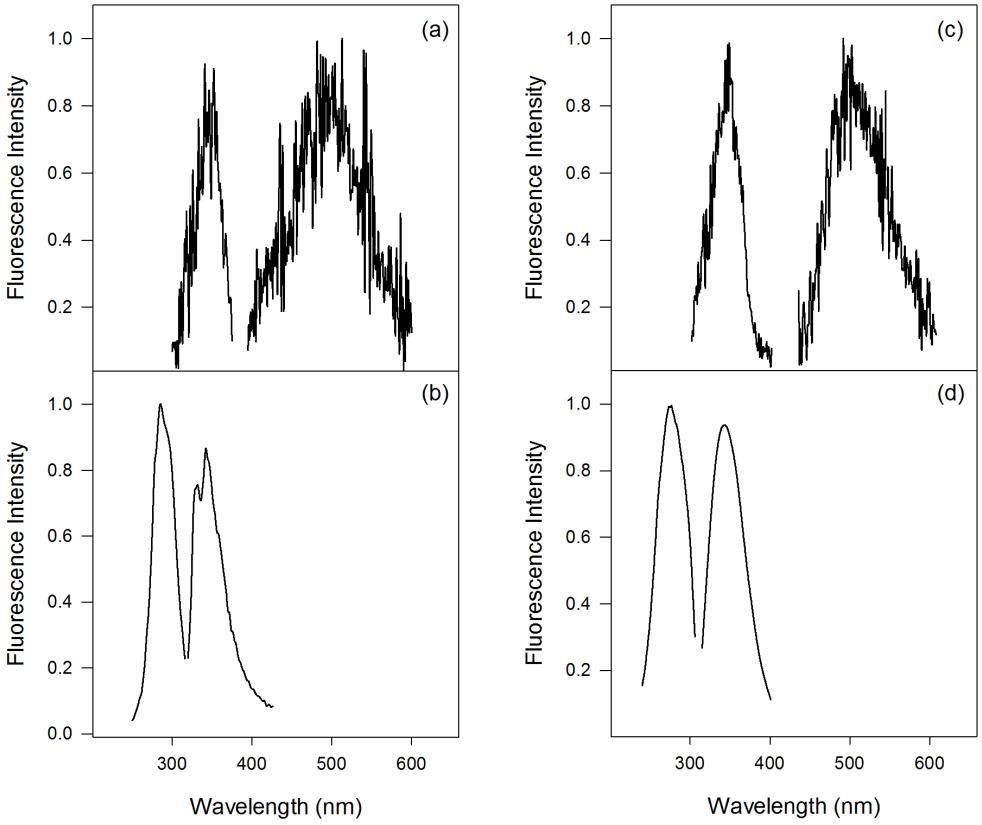

Figure 4.3: Fluorescence excitation and emission spectra of *E. polybractea* NVC (a) and essential oil (b), *E. spathulata* NVC (c), and eucaglobulin B (d).

4.3.2 Multi-photon fluorescence measurements

Eucalyptus polybractea extracts were used to ascertain whether non-volatile extracts would fluoresce under multi-photon excitation and to determine the non-linear excitation dependence of the emission signal. The strongest emission was achieved with 760 nm light. The emission signal was measured as a function of the excitation light intensity at

the sample. A linear regression of the log-log plot of this measurement gave a slope ($\pm$ 1 SE) of 2.06 $\pm$ 0.04 indicating that the emission is predominantly induced by two-photon excitation (Fig. 4.4).

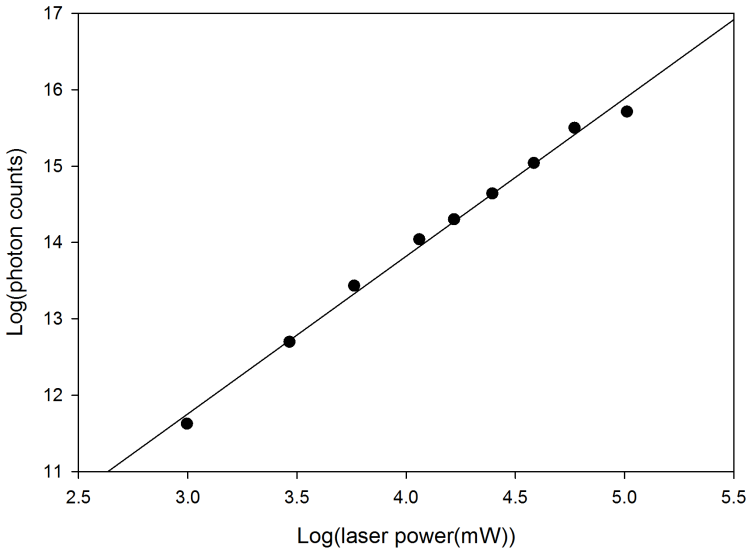

Figure 4.4: Log-log plot of the emission signal from *E. polybractea* NVC extracted from oil gland cavities as a function of excitation light intensity. A linear regression of this measurement gave a slope ($\pm$ 1 SE) of 2.06 $\pm$ 0.04 indicating that the emission is predominantly induced by two-photon excitation.

4.3.3 Fluorescence lifetime of extracted cavity components

The fluorescence decays of NVC extracts were well described by a double exponential decay model (Table 4.1). The NVC extracted from *E. polybractea* had a τ_m ($\pm$ 1 SE) of 1.12 $\pm$ 0.01 ns with a mean ($\pm$ 1 SE) χ^2 of 1.09 $\pm$ 0.01. This was dominated by a faster component (τ_1 $\pm$ 1 SE) of 0.51 $\pm$ 0.01 ns with a contribution to τ_m ($\pm$ 1 SE) of 66 $\pm$ 0.3%. *E. spathulata* gave a τ_m ($\pm$ 1 SE) of 1.03 $\pm$ 0.01 ns with a mean ($\pm$ 1 SE) χ^2 of 1.08 $\pm$ 0.01 and was also dominated by a shorter component (τ_1 $\pm$ 1 SE) of 0.6 $\pm$ 0.01 ns with a contribution to τ_m ($\pm$ 1 SE) of 68 $\pm$ 0.9%. Essential oil from *E. polybractea* was not found to exhibit

fluorescence under the excitation conditions used. This is consistent with the recorded single photon excitation spectrum for essential oil with minimal emission detected when excited with the corresponding single photon wavelength of 380 nm. Eucaglobulin B was also capable of undergoing mullti-photon excitation despite having an excitation maximum of 275 nm and had a τ_m ($\pm$ 1 SE) of 0.81 $\pm$ 0.003 ns with a mean ($\pm$ 1 SE) χ^2 of 1.15 $\pm$ 0.01.

4.3.4 Imaging *E. polybractea* oil glands

Imaging of oil glands that were dissected from fresh leaves was unsuccessful. Pigments in the chloroplasts of mesophyll cells that were adhered to the surface of oil glands strongly absorbed the excitation light. As a result no fluorescence from the underlying cavity was detected. Enzymatically isolated oil glands, free from all surrounding leaf tissue, could be imaged (Fig. 4.5). Clear images of cavities could be obtained up to the working distance of the high NA objectives (~80 μm) with only a minimal drop in fluorescence signal with depth (Fig. 4.6).

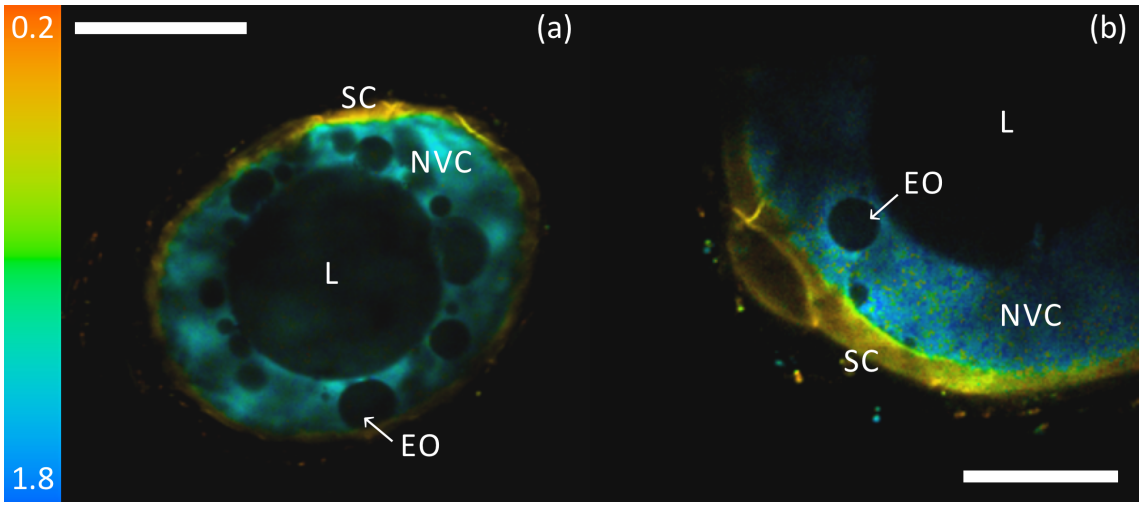

Figure 4.5: Fluorescence lifetime images of enzymatically isolated *E. polybractea* oil glands. Pseudo-colour mapping represents mean fluorescence lifetime (τ_m) in ns . Lumen (L); secretory cells (SC); non-volatile component (NVC); essential oil (EO). Panel (a) scalebar = 50 μm; panel (b) scalebar = 20 μm.

Table 4.1: Fluorescence lifetime values of *E. polybractea* (Ep) and *E. spathulata* (Es) oil glands and extracts, and a pure standard of eucaglobulin B.

Sample	τ_m (ns)	χ^2	τ_1 (ns)	a_1 (%)	τ_2 (ns)	a_2 (%)	τ_3 (ns)	a_3 (%)
Ep NVC (extracted)	1.12 ± 0.01	1.09 ± 0.01	0.51 ± 0.01	66 ± 0.3	2.33 ± 0.02	34 ± 0.4	-	-
Ep NVC (*in situ*)	1.38 ± 0.01	1.14 ± 0.01	0.56 ± 0.01	61 ± 0.2	2.65 ± 0.01	39 ± 0.2	-	-
Ep cell wall	0.54 ± 0.002	1.11 ± 0.004	0.2 ± 0.001	75 ± 0.1	1.04 ± 0.01	18 ± 0.1	3.11 ± 0.02	7 ± 0.1
Es NVC (extracted)	1.03 ± 0.01	1.08 ± 0.01	0.63 ± 0.01	68 ± 0.9	1.94 ± 0.03	32 ± 0.9	-	-
Es NVC cavity (*in situ*)	1.15 ± 0.01	1.09 ± 0.01	0.43 ± 0.01	57 ± 0.6	2.17 ± 0.02	43 ± 0.6	-	-
Es cavity oil (in situ)	0.98 ± 0.004	1.13 ± 0.01	0.52 ± 0.01	70 ± 0.5	2.08 ± 0.02	30 ± 0.5	-	-
Eucaglobulin B	0.81 ± 0.003	1.15 ± 0.01	0.44 ± 0.001	77 ± 0.1	2 ± 0.01	23 ± 0.1	-	-

Fluorescence lifetime imaging of enzymatically isolated oil glands revealed a complex pattern of lifetimes across secretory cells and cavity (Fig. 4.5 & 4.6). In particular, the cell walls of the secretory cells surrounding the lumen were highly fluorescent and where photon counts were high enough (greater than 1000), a triple exponential decay model was fitted to the data. This gave an average lifetime ($\tau_m \pm 1$ SE) of 0.54 $\pm$ 0.001 ns with a mean χ^2 ($\pm$ 1 SE) of 1.11 $\pm$ 0.004. Analysis of the components of τ_m revealed the fluorescence was dominated (75% $\pm$ 0.10) by a short component (τ_1) of 0.20 $\pm$ 0.01 ns.

Cavity fluorescence was heterogeneous with highly fluorescent regions (corresponding to longer lived emission) found between secretory cells and the centre of the lumen (pseudo-coloured blue; Fig. 4.5a). The centre of cavities emitted extremely weak fluorescence which, when present, was too low to calculate lifetime values. It was concluded that the fluorescent region was NVC based on the similarity of the calculated lifetime to extracted NVC lifetime (Table 4.1) and the region of non-fluorescence attributed to essential oil based on the similar lack of multi-photon fluorescence in extracted oil. *In situ* NVC had slightly longer τ_m values than extracted with an average of ($\pm$ 1 SE) of 1.38 $\pm$ 0.001 ns compared to 1.12 $\pm$ 0.01 ns. The lifetime was still dominated by a shorter component but the second component increased from 2.3 to 2.6 ns with an increased contribution of 39% as opposed to 33% in the extracted sample (Table 4.1).

Images show what appear to be oil droplets within the NVC (Fig. 4.5a & 4.6). These were generally towards the centre of cavities and appear to coalesce with the central pocket of essential oil, although smaller droplets were observed at the border of secretory cells (Fig. 4.5b). At the border between secretory cells and NVC a region exhibiting shorter fluorescence lifetimes is apparent with values between 0.7-1.3 ns (pseudo coloured green; Fig. 4.5b & 4.6).

Figure 4.6: Optical section along the *z*-axis of an enzymatically isolated *E. polybractea* oil gland. Pseudo-colour mapping represents mean fluorescence lifetime (τ_m). Depth along the *z*-axis relative to the surface from left to right: 20 μm, 40 μm, 60 μm, 80 μm. Secretory cells (SC); non-volatile component (NVC); essential oil (EO). Scalebar = 50 μm.

4.3.5 Imaging of *E. spathulata* oil glands

The oil glands of *E. spathulata* were not as amenable to isolation as those of *E. polybractea*. Mesophyll cells were more difficult to remove and isolated oil glands were more fragile. Despite this a small number were imaged and they also showed a similar pattern of fluorescence intensity. Lifetime values within cavities were shorter than in *E. polybraceta* and cell walls of secretory cells were only weakly fluorescent (Fig. 4.7). In contrast to *E. polybractea*, the centre of *E. spathulata* cavities was also clearly fluorescent, allbeit to a lesser extent than the region bordering secretory cells.

Based on the distribution of NVC in *E. polybractea* and fluorescent lifetime values it is suggested that the region of strong fluorescence bordering secretory cells is from constituents within the NVC. The fluorescence lifetime of this region was similar to extracted NVC but showed the same increase in lifetime observed for *in situ* compared to extracted NVC in *E. polybractea*. *E. spathulata in situ* NVC had an average ($\pm$ 1 SE) lifetime of τ_m of 1.15 $\pm$ 0.01 ns compared to 1.03 $\pm$ 0.01 ns for extracted NVC (Table 4.1). The central region of cavities was fluorescent with an average τ_m of ($\pm$ 1 SE) of 0.98 $\pm$ 0.00 ns. This region is likely to be essential oil, however, it can not be compared to extracted essential oil as the fluorescence of *E. spathulata* essential oil was not measured.

The pattern of lifetime values across *E. spathulata* cavities were more homogeneous than *E. polybractea* and lacked a region of short-lived fluorescence between secretory cells and NVC (Fig. 4.7). There was also no evidence of oil droplets within the layer of NVC.

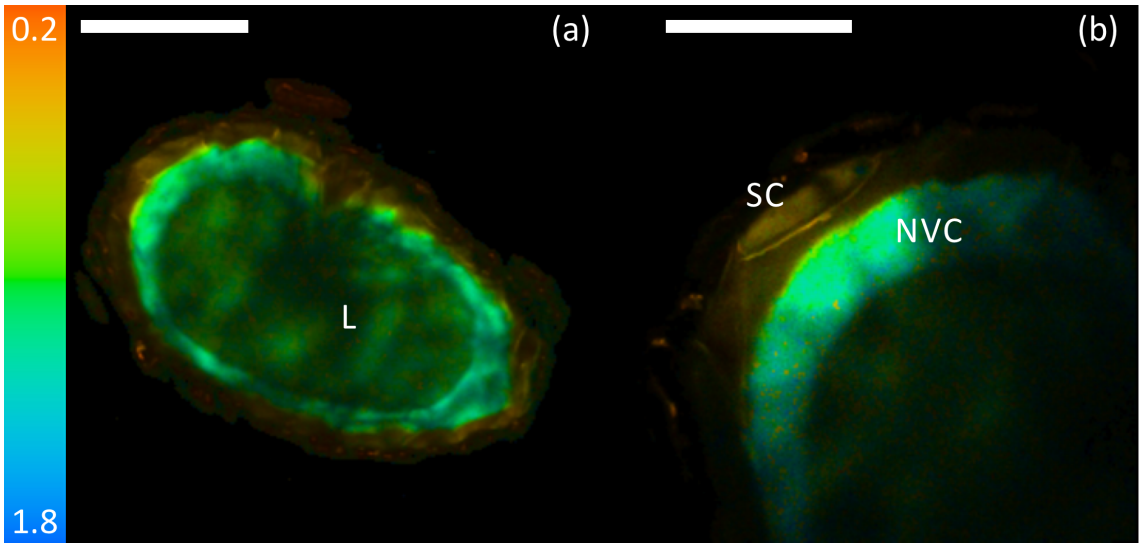

Figure 4.7: Fluorescence lifetime images of enzymatically isolated *E. spathulata* oil glands. pseudo-colour mapping represents mean fluorescence lifetime (τ_m) in ns. Lumen (L); secretory cells (SC); non-volatile component (NVC). Panel (a) scalebar = 50 μm; panel (b) scalebar = 20 μm.

4.4 Discussion

4.4.1 Spatial arrangment of cavity metabolites

The major finding of this research is the interesting spatial organisation of the oil gland metabolome as shown by different patterns of fluorescence from endogenous fluorophores. It must be noted that the interpretation of results is based on the assumption that the observed pattern of fluorescence is reflective of the underlying spatial distribution of essential oil and NVC in cavities. In *E. polybractea* the evidence in support of this assumption is the lack of MP-fluorescence of extracted essential oil and the fluorescence of NVC. The fluorescence lifetime of extracted NVC is also very similar to the fluorescence lifetime of the region identified as NVC in the images.

In *E. spathulata* the difference between the two phases present in cavities was less clear and the difficulty of interpretation is compounded by the fact that the fluorescent properties of the essential oil was not measured. Similarly to *E. polybractea*, there was a slight shortening of the fluorescence lifetime between extracted and *in situ* NVC. It is possible the shortening of NVC fluorescence lifetime of both species relates to the

difference in micro-environment experienced by NVC when extracted compared to *in situ* (Cser *et al.*, 2002; Suhling *et al.*, 2012).

Despite these limitations the results still present an interesting picture and raise questions about how oil glands function. In *E. polybractea* there appears to be a tendency for the NVC to localise to the peripheral region of the cavity with the essential oil localised to the centre (Fig. 4.5 & 4.6). A similar pattern was observed in *E. spathulata* although due to the fluorescence of both components this was less clear (Fig. 4.7). As the oil gland cavity is an extracellular space, the observed organisation must be due to non-active processes and is therefore the result of the innate chemical properties of each fraction.

An interesting question that has yet to be adequately addressed in the literature is: how do oil glands actually sequester accumulated metabolites? As discussed in Chapter 2, particular metabolites are stored extracellularly because they cannot be effectively stored intracellularly at required concentrations without toxic affects (Sirikantaramas *et al.*, 2007). It is unclear, however, what mechanism enables cells in direct contact with the sequestered material to avoid toxicity. Turner *et al.* (2000) have suggested that a non-volatile secretion observed between the secretory cells of mint GSTs and accumulated essential oil may serve a protective function by creating a barrier between secreted essential oil and the cells lining the site of accumulation.

Although this hypothesis was not tested directly, the distribution of NVCs in *Eucalyptus* cavities is consistent with this idea. Importantly, this function would enable secretory cells lining cavities to remain metabolically active whilst being protected from the accumulated essential oil that is known to cause auto-toxic effects when cavities are disrupted (Knight *et al.*, 2002). As described in Chapter 2 the non-volatile secretions of *E. polybractea* and *E. spathulata* contain MSEs. The structure of these compounds would give them amphiphilic properties provided by the presence of both polar sugar moieties and non-polar terpenoid groups (Goodger and Woodrow, 2011). Such properties would allow them to interact with the lipophilic essential oil within the gland cavity and the hydrated cell walls of epithelial cells bounding the cavity. Further testing of this proposed function is needed including gaining a fuller picture of the interaction between the essential oil and NVC.

One option to examine this relationship *in vivo* is to use fluorescent probes. The fluorescence lifetime of probes such as Nile red, BODIPY and fluorescein are all sensitive to their micro-environments and can report on parameters such as hydrophobicity and viscosity (Cser *et al.*, 2002; Suhling *et al.*, 2012). Much effort was applied in trying to infiltrate these fluorophores into cavities via petiole feeding experiments and incubation of isolated glands with fluorophores but unfortunately these attempts were unsuccessful (data not shown).

If successful infiltration into oil glands can be achieved, then the use of such probes in conjunction with MP-FLIM could provide a means to investigate the mechanism of terpene and MSE secretion. In *E. polybractea* cavities it is noteworthy that spherical, non-fluorescent regions of essential oil are apparent within the layer of NVC (Fig. 4.5 & 4.6) and at higher magnification small droplets at the boundary of the cavity can also be observed (Fig. 4.5 b). This may be indicative of transport of essential oil components from their site of synthesis in the epithelial cells into the cavity. Currently there is no conclusive evidence for the mode of secretion of essential oils into the extracellular spaces of either oil glands or GSTs. Both granulocrine mechanisms, where endoplasmic reticulum derived vesicles containing essential oil components fuse with the plasma membrane of secretory cells (Ascensao and Pais, 1998; Benayoun and Fahn, 1979; Bosabalidis and Tsekos, 1982a; Rodríguez *et al.*, 2011), and eccrine mechanisms, involving either diffusion or active transport via transport proteins, have been proposed (Bosabalidis and Tsekos, 1982b; Rodríguez *et al.*, 2011). MP-FLIM provides the opportunity to observe the process of secretion in real-time as actively secreting cells can be imaged in combination with *in vivo* lipid staining as demonstrated by Bago *et al.* (2002). In this example the fluorescent probe Nile red was used to stain lipid droplets in fungi which were then tracked in real-time through hyphae.

4.4.2 Origin of cavity metabolome fluorescence

Eucalyptus polybractea and *E. spathulata* NVC were both shown to be fluorescent and capable of MP-excitation (Fig. 4.3). The NVC from both species is chemically complex (Chapter 2) and it is likely the observed fluorescence is derived from multiple

fluorophores. Attempts to purify fluorescent compounds from extracted NVC by HPLC with fluorescence detection were not successful possibly because of the presence of many low abundant metabolites that contribute partially to the overall fluorescence (data not shown). Nonetheless, various phenolic containing compounds with the potential for fluorescence have been localised to oil gland cavities (Chapter 2). One such MSE with a phenolic moiety was eucaglobulin B, which had previously been purified from *E. platypus* and was shown to be present in extracts from *E. spathulata*. Although eucaglobulin B was shown to be fluorescent and capable of MP-excitation, the excitation and emission maxima were much lower than for *E. spathulata* NVC, 290/350 nm compared to 345/490 nm (Fig. 4.3d), so this compound may not be contributing greatly to the overall fluorescence.

4.4.3 Cell wall fluorescence

In addition to the proposed barrier function of NVC, wall modifications of the casing cells that surround epithelial cells are also likely to be involved in isolating cavity contents from surrounding tissue (Bennici and Tani, 2004; Carr and Carr, 1970; List *et al.*, 1995). Carr and Carr (1970) suggested that these thickenings were the result of either suberin or lignin deposition based on their resistance to acid hydrolysis. The shorter fluorescence lifetime values observed for *E. polybractea* casing cells have been attributed to wall bound phenolics in other species (Morales *et al.*, 2005), consistent with lignification of these walls.

4.5 Concluding remarks

The work presented in this chapter provides a first insight into the physical organisation of embedded oil glands in the living state, either from eucalypts or any other species. The imaging system successfully captured details of the oil gland cavity, and fluorescence lifetimes of gland components could be used to differentiate between different regions (Table 4.1). It was shown that the metabolome of oil glands is complex and possesses a surprising level of spatial organisation given that it is in an extracellular space (Fig.

4.5 and 4.7). The spatial organisation is consistent with the hypothesis that the NVC is acting as a region of low diffusivity between essential oil and secretory cells; however, this hypothesis needs to be directly tested before any conclusions can be made.

4.5.1 Appraisal of MP-FLIM system

Despite reports of the ability to image deep into photosynthetic tissue with MP-excitation (Broess *et al.*, 2009), oil glands could only be imaged once they were removed from leaves and cleaned of any surrounding tissue. Even a single layer of mesophyll cells attached to the surface of isolated oil glands inhibited the ability to image into cavities, presumably due to the re-absorbance of fluorescence by photosynthetic pigments. In addition, isolated oil glands were found to be extremely fragile (particularly those from *E. spathulata*) which made it more difficult to obtain intact and mesophyll free samples. Notwithstanding these difficulties, if used to visualise specific fluorescent probes this technique has the potential to help answer many pertinent questions about the physiology of embedded oil glands. It is hoped that questions relating to the sub-cellular localisation of biosynthetic pathways, secretory mechanisms and the localisation of metabolites within oil glands can be addressed in future work.

Chapter 5
Conclusions

The leaves of many species of eucalypts contain an abundance of oil glands. These oil glands accumulate an ecologically and economically important essential oil composed of mono- and sesquiterpenes. Until very recently it was believed oil glands were purely a repository of these terpenes. It was discovered that oil glands of a number of species also contain a group of non-volatile terpenoids, the MSEs (Goodger *et al.*, 2009). This discovery immediately raised questions about MSE function, oil gland physiology and eucalypt terpenoid metabolism more generally. Are non-volatile metabolites common constituents of oil glands in eucalypts? Is the occurrence of MSEs in eucalypts widespread? Why are MSEs accumulated in oil glands? What is their relationship with the co-stored essential oil? In asking these questions it also became clear how little is known about the physiology of embedded oil glands in *Eucalyptus* and also in other taxa. Fundamental questions remained unanswered not only about their biochemical organisation, but also how they contain concentrated pools of volatile terpenes in their cavities. The research presented in this thesis aimed to investigate these questions.

The prevalence of cavity localised non-volatiles was examined in Chapter 2, with a focus on MSEs. A high resolution tandem mass spectrometry approach was taken to enable the relatively rapid surveying of oil gland metabolites from a diverse selection of species. Through the combination of accurate mass measurements and the presence of a fragmentation pattern indicative of MSEs, many known and novel MSEs were putatively identified. MSEs were found to be widespread in *Eucalyptus* and, furthermore, present in the sister genus *Corymbia*. Several of the taxa contained complex mixtures of MSEs;

these species, such as *E. dielsii*, present prime targets for future investigations on the biochemistry of MSEs.

As this study was interested in the localisation of MSEs to oil glands, initial species choice was biased towards taxa with reported high oil yields or alternatively abundant oil glands. It was assumed this strategy would make the collection of cavity extracts more feasible. While this meant that cavity extracts could be collected from many species, it also meant that some phylogenetic groups were poorly sampled, such as the monocalypts. Nevertheless, the four species from this subgenus that were analysed had abundant NVCs. Contrary to all other species examined the extracts contained flavanones. MSEs with flavonoid moieties were also localised to cavities in this study but the presence of an unconjugated flavanone in eucalypt oil glands is the first observation of a non-terpenoid chemical accumulating in these structures.

In the first section of Chapter 3, the relationship between MSEs and terpenes was investigated in *E. polybractea*. This species was chosen for its well characterised MSE and terpene chemistry. Two natural populations were surveyed for their terpene and MSE variation. The major finding of this aspect of the study was that MSE and terpene concentrations were strongly and positively related, and no individual was identified that lacked or had very low MSE to oil levels. The reason for this relationship is unclear; it is likely to be driven in part by oil gland volume, but this does not necessarily explain the relatively fixed ratio in which the two groups were consistently found.

The aim of the second section was to investigate the biosynthetic connections between terpenes and MSEs and the different factors which determine oil gland composition. To achieve this, a *E. polybractea* plant was pulsed with $^{13}CO_2$ and the resulting ^{13}C enrichment of monoterpene, sesquiterpene and MSE pools was tracked over time. Leaves at two different stages of development were examined: developing leaves in which oil glands were still expanding and filling, and mature, fully expanded leaves. In expanding leaves 1,8-cineole, *trans*-caryophyllene, cadinene, cuniloside B, froggattiside A, and cypellocarpin C were found to follow a very similar pattern of label incorporation into their respective pools, despite different foliar pool sizes and biosynthetic origins. The similarity in enrichment of metabolite pools suggests a high level of co-regulation

between the different biosynthetic pathways at this stage of leaf ontogeny. In contrast, only monoterpene and cuniloside B biosynthesis was detected in mature leaves.

The other major finding from this study was that the ^{13}C kinetics of α-terpineol were consistent with it being an intermediate. Based on structural similarity and a plausible biosynthetic mechanism (Guo and Yang, 2006), it is proposed that this monoterpene is the precursor of oleuropeic acid, quantitatively the major monoterpenoid moiety of MSEs. The use of labelled precursors in future biochemical studies of MSE biosynthesis will be able to confirm whether or not this is the case.

How the non-volatile and volatile components in oil gland cavities are spatially organised in oil glands was examined in Chapter 4. This was achieved by using MP-FLIM, a technique that offered the possibility of imaging the undisturbed metabolome of unsectioned oil glands. The distribution of fluorescence in the cavities of *E. polybractea*, and to a lesser extent *E. spathulata*, presented a clear and reproducible pattern. Based on the fluorescence characteristics of extracted NVC and essential oil, the results suggested that the NVC was localised towards the periphery of cavities while the essential oil was localised towards the centre of the space. In addition, droplets of oil were apparent within the NVC and appeared to be in the process of coalescing with the central domain of oil. It was hypothesised that this spatial distribution of cavity components could function to minimise the contact between the toxic and volatile essential oil and secretory cells.

Several findings from both Chapters 2 and 3 are congruent with this hypothesised function. The abundance of NVCs in eucalypt oil gland cavities, the presence of MSEs in all individuals sampled from the two populations of *E. polybraceta* and also their presence in a relatively constant proportion to terpenes, are all results consistent with the proposed function. In addition, there is evidence from *E. froggattii* that these MSEs are present at all ontogenetic stages (Goodger *et al.*, 2013a). Despite this additional, indirect support, the proposed function of NVCs remains highly speculative. The observed spatial distribution could of course serve no such function, and the presence of these non-volatiles in oil glands, whether comprised of MSEs or flavanones, is purely the result of the toxicity of these metabolites. Nevertheless, these results will hopefully stimulate a discussion on how specialised structures that accumulate volatile terpenes (both

glandular secreting trichomes and embedded oil glands) are able to protect secretory cells from toxicity.

In addition to the proposed buffering hypothesis, arguments have been made in both Chapters 2 and 4 that MSEs may be involved in defence. Their sequestration away from sensitive cellular components in oil glands suggests the potential for toxicity (Sirikantaramas *et al.*, 2007) and their structures incorporate reactive chemical groups that have been implicated in defence responses of other plants (Alméras *et al.*, 2003). Interestingly, a recent investigation of *Arabidopsis* monoterpenoid metabolism revealed the presence of oxidised and conjugated linalool derivatives similar to the MSEs found in *Eucalyptus* species (Ginglinger *et al.*, 2013). These non-volatile compounds had a specific distribution in floral tissue leading the authors to speculate they had a defensive function. The results of experiments studying the resistance of knockout mutants deficient in these metabolites against chewing insects indicate that they may indeed be involved in defence (D. Werck-Reichhart, unpublished).

It is important to point out that a defensive function of MSEs is not necessarily at odds with their proposed involvement in creating a physical buffer between secretory cells and secreted essential oil. MSEs could serve both as defence chemicals and also participate in physically buffering secretory cells from accumulated terpenes because, unlike volatile terpenes, these compounds would not present the same containment issues.

5.1 Terpenoid regulation in *Eucalyptus* revisited

The results presented in this thesis add to an already existing body of research on oil gland metabolism in eucalypts. From this combined body of information a number of key facets of oil gland metabolism emerge. Drawing these results together we can summarise the current state of knowledge as follows: Oil glands can house a variety of monoterpenes and sesquiterpenes (Goodger *et al.*, 2010; King *et al.*, 2006a), MSEs (this thesis; Goodger *et al.*, 2009; 2010) and also non-terpenoid chemicals (this thesis). There is evidence suggesting that terpene-phloroglucinols are also housed in oil glands (Goodger, unpublished; Moore *et al.*, 2004a; Wallis *et al.*, 2011). In terms

of their biosynthetic organisation, we can conclude through both direct and indirect evidence that multiproduct mono- and sesquiterpene synthases produce the essential oil (this thesis; Goodger *et al.*, 2013b; Keszei *et al.*, 2010) and that some of the products of these terpene synthases are further metabolised into more complex terpenoids (this thesis, Moore *et al.*, 2004a; Wallis *et al.*, 2011). Both the oil glands and the biosynthetic pathways that produce the different terpenoids are under strong developmental control with different terpenoids biosynthesised at different stages of leaf development (this thesis, Goodger and Woodrow, 2012; 2013b). Finally, results from Chapter 3 show that oil glands remain biosynthetically active after full leaf expansion. Together, these results lay the foundation for addressing questions about how the diversity of terpenoids is generated and what regulatory mechanisms control their accumulation and composition.

Work in other essential oil producing species has shown that the temporal and spatial patterns of terpene synthase expression are important for their mono- and sesquiterpene composition (Crocoll *et al.*, 2010; Irmisch *et al.*, 2012; Wang *et al.*, 2008). This is also likely to be the case in eucalypts. In addition, these enzymes are potentially an important branch point in eucalypt terpenoid metabolism, assuming their products are being channeled into MSEs, euglobals and macrocarpals as well as directly contributing to the essential oil. How these terpene synthases are regulated through development could be an important factor controlling the formation of these more complex terpenoids. Furthermore, loss of function or even subtle changes in enzyme profile could have profound downstream effects on the overall terpenoid composition. Such shifts could result in chemotypes like the shared sesquiterpene/macrocarpal chemotypes found in a number of *Eucalyptus* species (Moore *et al.*, 2004a; Padovan *et al.*, 2012; Wallis *et al.*, 2011).

Other factors are also likely to be important in determining terpenoid composition. Evidence from peppermint, one of the few systems in which terpenoid regulation has been well studied, indicates that multiple factors interact to produce the observed oil composition. These include ontogenetic (McConkey *et al.*, 2000), environmental (Rios-Estepa *et al.*, 2008), and negative feedback loops in which oil components can inhibit the activity of pathway enzymes (Rios-Estepa *et al.*, 2008).

Precursors derived from different pathways are required for the biosynthesis of some of the more complex terpenoids, such as cypellocarpin C, which incorporates both monoterpenoid and phenolic moieties. How the biosynthesis of these end products is coordinated potentially has implications for the composition of oil glands through time. Do all of the pathways have to be coordinately expressed or is it possible that, like in other species, terpenes secreted into the oil gland cavity can be further modified at a later time? For example, evidence from peppermint suggests that menthone can re-enter secretory cells from the oil gland cavity where it is enzymatically converted to menthol (McConkey *et al.*, 2000; Turner and Croteau, 2004). Another possibility is that enzymatic conversion of terpenoids can occur in the oil gland cavity. In cannabis, tetrahydrocannabinolic acid synthase, the enzyme involved in tetrahydrocannabinol (THC) biosynthesis, is secreted into the storage cavity of GSTs where it catalyses the final step of the THC pathway (Sirikantaramas *et al.*, 2005). Both of these findings raise the possibility that, in eucalypts, enzymatic conversion of terpenoids can occur even after they have been secreted into the oil gland cavity.

5.1.1 MSE pathway discovery

Ultimately, answers to the questions raised in the previous section will only be found through the investigation of eucalypt terpenoid metabolism at the molecular level. In the case of MSEs, no specific genes involved in their biosynthesis have been reported. The biosynthesis of oleuropeic acid and menthiafolic acid from their monoterpene precursors, as well as the bonding of multiple moieties to the central sugar, will require multiple enzymatic steps. Such oxidative functionalisation of monoterpenes is typically catalysed by cytochrome P450-dependent monooxygenases (Ginglinger *et al.*, 2013; Höfer *et al.*, 2013; Mau and Croteau, 2006). In the case of phenolic glycoside-MSEs, glycosyltransferases are likely candidates for glycosylation of the phenolic moieties. Whereas acyltransferase are possible candidates for the addition of the ester linked monoterpene-acids. Where both moieties are ester linked, such as in cuniloside B and froggattiside A, both steps are possibly catalysed by acyltransferase.

The P450s, glycosyl- and acyltransferases involved in plant secondary metabolism are represented by large gene families within taxa (Gachon *et al.*, 2005; Nelson and Werck-Reichhart, 2011; Tuominen *et al.*, 2011). As such, the specific genes involved in the MSE pathway may be difficult to determine. The localisation of MSEs to oil glands and the finding that terpene and MSE biosynthesis is tightly coordinated in expanding leaves opens up the potential for systems biology type approaches for pathway discovery.

Firstly, the oil glands from eucalypts can be separated from surrounding tissue providing an enriched source of metabolites, enzymes and transcripts (Goodger *et al.*, 2010). The development of an analogous protocol for the isolation of GSTs has aided gene discovery efforts and led to the elucidation of the biosynthetic pathways of numerous secondary metabolites (for a recent review of this field see Lange and Turner, 2013). Secondly, genes involved in terpene biosynthetic pathways and many other secondary metabolite pathways are often co-regulated at the transcriptional level. Thus, the identification of a single gene in a pathway can, with co-expression analysis, lead to the identification of other pathway genes (Kliebenstein, 2012). Monoterpene synthases have already been identified in *Eucalyptus* species (Goodger *et al.*, 2010; Keszei *et al.*, 2010), and could provide such an entry point into the MSE pathway.

5.2 Conclusion

Through the investigation of the composition, prevalence, localisation, and regulation of oil gland metabolites, the work presented in this thesis provides new information on a major aspect of eucalypt chemistry. This research will hopefully pave the way for future investigations into terpenoid chemistry and regulation in this genus.

References

Abbott E, Hall D, Hamberger B, Bohlmann J (2010) Laser microdissection of conifer stem tissues: Isolation and analysis of high quality RNA, terpene synthase enzyme activity and terpenoid metabolites from resin ducts and cambial zone tissue of white spruce (*Picea glauca*). BMC Plant Biology **10:** 1–16

Abrahim D, Francischini AC, Pergo EM, Kelmer-Bracht AM, Ishii-Iwamoto EL (2003) Effects of α-pinene on the mitochondrial respiration of maize seedlings. Plant Physiology and Biochemistry **41:** 985–991

Akiyama K, Matsuzaki K, Hayashi H (2005) Plant sesquiterpenes induce hyphal branching in arbuscular mycorrhizal fungi. Nature **435:** 824–827

Alméras E, Stolz S, Vollenweider S, Reymond P, Mène-Saffrané L, Farmer EE (2003) Reactive electrophile species activate defense gene expression in Arabidopsis. The Plant Journal **34:** 205–216

Andrew RL, Keszei A, Foley WJ (2013) Intensive sampling identifies previously unknown chemotypes, population divergence and biosynthetic connections among terpenoids in *Eucalyptus tricarpa*. Phytochemistry **94:** 148–158

Andrew RL, Peakall R, Wallis IR, Wood JT, Knight EJ, Foley WJ (2005) Marker-based quantitative genetics in the wild? The heritability and genetic correlation of chemical defenses in *Eucalyptus*. Genetics **171:** 1989–1998

Anekonda TS, Criddle RS, Bacca M, Hansen LD (1999) Contrasting adaptation of two *Eucalyptus* subgenera is related to differences in respiratory metabolism. Functional Ecology **13:** 675–682

Appezzato-da Glória B, Da Costa FB, da Silva VC, Gobbo-Neto L, Rehder VLG, Hayashi AH (2012) Glandular trichomes on aerial and underground organs in *Chrysolaena* species (Vernonieae Asteraceae): Structure, ultrastructure and chemical composition. Flora - Morphology, Distribution, Functional Ecology of Plants **207:** 878–887

Ascensao L, Pais MS (1998) The leaf capitate trichomes of *Leonotis leonurus*: histochemistry, ultrastructure and secretion. Annals of Botany **81:** 263–271

Babourina O, Rengel Z (2009) Uptake of aluminium into Arabidopsis root cells measured by fluorescent lifetime imaging. Annals of Botany **104:** 189–195

Bago B, Zipfel W, Williams RM, Jun J, Arreola R, Lammers PJ, Pfeffer PE, Shachar-Hill Y (2002) Translocation and utilization of fungal storage lipid in the arbuscular mycorrhizal symbiosis. Plant Physiology **128:** 108–124

Barton AFM, Cotterill PP, Brooker MIH (1991) Short note: Heritability of cineole yield in *Eucalyptus kochii*. Silvae Genetica **40:** 37–38

Becerra JX, Venable DL (1990) Rapid-terpene-bath and "squirt-gun" defense in *Bursera schlechtendalii* and the counterploy of Chrysomelid beetles. Biotropica **22:** 320–323

Becker W (2005) Advanced time-correlated single photon counting techniques. Berlin: Springer-Verlag

Begum S, Farhat, Siddiqui BS (1997) Triterpenoids from the leaves of *Eucalyptus camaldulensis* var. *obtusa*. Journal of Natural Products **60:** 20–23

Begum S, Farhat, Siddiqui BS (2011) Chromenone glucosides acylated with monoterpene acids from the leaves of *Eucalyptus camaldulensis* var. *obtusa*. Helvetica Chimica Acta **94:** 238–247

Benayoun J, Fahn A (1979) Intracellular transport and elimination of resin from epithelial duct-cells of *Pinus halepensis*. Annals of Botany **43:** 179–181

Bennici A, Tani C (2004) Anatomical and ultrastructural study of the secretory cavity development of *Citrus sinensis* and *Citrus limon*: evaluation of schizolysigenous ontogeny. Flora - Morphology, Distribution, Functional Ecology of Plants **199:** 464–475

Benyahia S, Benayache S, Benayache F, León F, Quintana J, López M, Hernández JC, Estévez F, Bermejo J (2005) Cladocalol, a pentacyclic 28-nor-triterpene from *Eucalyptus cladocalyx* with cytotoxic activity. Phytochemistry **66:** 627–632

Bernoux M, Timmers T, Jauneau A, Brière C, de Wit PJGM, Marco Y, Deslandes L (2008) RD19, an Arabidopsis cysteine protease required for RRS1-R-mediated resistance, is relocalized to the nucleus by the *Ralstonia solanacearum* PopP2 effector. The Plant cell **20:** 2252–2264

Bick IRC, Brown RB, Hillis WE (1972) Three flavanones from leaves of *Eucalyptus sieberi*. Australian Journal of Chemistry **25:** 449–451

Bohte A, Drinnan AN (2011) Fruit development in eucalypts (Myrtaceae: Eucalypteae). Australian Systematic Botany **24:** 421–444

Boland DJ, Brophy JJ, Pennock APN (1991) *Eucalyptus* leaf oils: use, chemistry, distillation and marketing. Melbourne: Inkata Press

Bosabalidis A, Tsekos I (1982) Ultrastructural studies on the secretory cavities of *Citrus deliciosa* Ten. II. Development of the essential oil-accumulating central space of the gland and process of active secretion. Protoplasma **70:** 63–70

Bosabalidis AM, Tsekos I (1982) Ultrastructure of the essential oil secretion in glandular scales of *Origanum dictamnus* L. leaves. Aromatic Plants **7:** 3–12

Boughton BA, Callahan DL, Silva Cl, Bowne J, Nahid A, Rupasinghe T, Tull DedrejaL, Mcconville MJ, Bacic A, Roessner U (2011) Comprehensive profiling and quantitation of amine group containing metabolites. Analytical Chemistry **83:** 7523–7530

Boutant E, Didier P, Niehl A, Mély Y, Ritzenthaler C, Heinlein M (2010) Fluorescent protein recruitment assay for demonstration and analysis of in vivo protein interactions

in plant cells and its application to Tobacco mosaic virus movement protein. The Plant Journal **62:** 171–177

Bouwmeester HJ, Gershenzon J, Konings MCJM, Croteau R (1998) Biosynthesis of the monoterpenes limonene and carvone in the fruit of caraway I. Demonstration of enzyme activities and their changes with development. Plant Physiology **117:** 901–912

Broess K, Borst JW, van Amerongen H (2009) Applying two-photon excitation fluorescence lifetime imaging microscopy to study photosynthesis in plant leaves. Photosynthesis Research **100:** 89–96

Brooker MIH (2000) A new classification of the genus *Eucalyptus* L'Hér. (Myrtaceae). Australian Systematic Botany **13:** 79–148

Brophy JJ, Southwell IA (2002) *Eucalyptus* chemistry.In J J W Coppen , eds, *Eucalyptus*: the genus *Eucalyptus*, 102–160. London and New York: Taylor and Francis

Bücherl CA, van Esse GW, Kruis A, Luchtenberg J, Westphal AH, Aker J, van Hoek A, Albrecht C, Borst JW, de Vries SC (2013) Visualization of BRI1 and BAK1(SERK3) membrane receptor heterooligomers during brassinosteroid signaling. Plant Physiology **162:** 1911–1925

Cankar K, van Houwelingen A, Bosch D, Sonke T, Bouwmeester H, Beekwilder J (2011) A chicory cytochrome P450 mono-oxygenase CYP71AV8 for the oxidation of (+)-valencene. FEBS letters **585:** 178–182

Carr DJ, Carr SGM (1970) Oil glands and ducts in *Eucalyptus* L'Herit II: development and structure of oil glands in the embryo. Australian Journal of Botany **18:** 191–212

Centonze VE, White JG (1998) Multiphoton excitation provides optical sections from deeper within scattering specimens than confocal imaging. Biophysical Journal **75:** 2015–2024

Chen F, Tholl D, Bohlmann J, Pichersky E (2011) The family of terpene synthases in plants: a mid-size family of genes for specialized metabolism that is highly diversified throughout the kingdom. The Plant Journal **66:** 212–229

Ciccarelli D, Pagni AM, Andreucci AC (2003) Ontogeny of secretory cavities in vegetative parts of *Myrtus communis* L. (Myrtaceae): An example of schizolysigenous development. Israel Journal of Plant Sciences **51:** 193–198

Crisp MD, Burrows GE, Cook LG, Thornhill AH, Bowman DMJS (2011) Flammable biomes dominated by eucalypts originated at the Cretaceous-Palaeogene boundary. Nature Communications **2:** 1–8

Crisp MD, Cook LG, Steane D (2004) Radiation of the Australian flora: what can comparisons of molecular phylogenies across multiple taxa tell us about the evolution of diversity in present-day communities? Philosophical Transactions of the Royal Society of London. Series B, Biological Sciences **359:** 1551–1571

Crocoll C, Asbach J, Novak J, Gershenzon J, Degenhardt J (2010) Terpene synthases of oregano (*Origanum vulgare* L.) and their roles in the pathway and regulation of terpene biosynthesis. Plant Molecular Biology **73:** 587–603

Croteau RB, Davis EM, Ringer KL, Wildung MR (2005) (-)-Menthol biosynthesis and molecular genetics. Die Naturwissenschaften **92:** 562–577

Cser A, Nagy K, Biczok L (2002) Fluorescence lifetime of Nile Red as a probe for the hydrogen bonding strength with its microenvironment. Chemical Physics Letters **360:** 473–478

Danner H, Boeckler GA, Irmisch S, Yuan JS, Chen F, Gershenzon J, Unsicker SB, Köllner TG (2011) Four terpene synthases produce major compounds of the gypsy moth feeding-induced volatile blend of *Populus trichocarpa*. Phytochemistry **72:** 897–908

Denk W, Strickler JH, Webb WW (1990) Two-photon laser scanning fluorescence microscopy. Science **248:** 74–76

Deschamps C, Gang D, Dudareva N, Simon JE (2006) Developmental regulation of phenylpropanoid biosynthesis in leaves and glandular trichomes of basil (*Ocimum basilicum* L.). International Journal of Plant Sciences **167:** 447–454

Diaz Napal GN, Carpinella MC, Palacios SM (2009) Antifeedant activity of ethanolic extract from *Flourensia oolepis* and isolation of pinocembrin as its active principle compound. Bioresource Technology **100:** 3669–3673

Doran JC, Matheson AC (1994) Genetic parameters and expected gains from selection for monoterpene yields in Petford *Eucalyptus camaldulensis*. New Forests **8:** 155–167

Doran JC, Williams ER, Brophy JJ (1995) Patterns of variation in the seedling leaf oils of *Eucalyptus urophylla*, *E. pellita* and *E. scias*. Australian Journal of Botany **43:** 327–336

Dudareva N, Andersson S, Orlova I, Gatto N, Reichelt M, Rhodes D, Boland W, Gershenzon J (2005) The nonmevalonate pathway supports both monoterpene and sesquiterpene formation in snapdragon flowers. Proceedings of the National Academy of Sciences **102:** 933–938

Dudareva N, Negre F, Nagegowda DA, Orlova I (2006) Plant volatiles: Recent advances and future perspectives. Critical Reviews in Plant Sciences **25:** 417–440

Edwards PB, Wanjura WJ, Brown WV (1993) Selective herbivory by Christmas beetles in response to intraspecific variation in *Eucalyptus* terpenoids. Oecologia **95:** 551–557

Enfissi EMA, Fraser PD, Lois LM, Boronat A, Schuch W, Bramley PM (2005) Metabolic engineering of the mevalonate and non-mevalonate isopentenyl diphosphate-forming pathways for the production of health-promoting isoprenoids in tomato. Plant Biotechnology Journal **3:** 17–27

Eschler BM, Pass DM, Willis R, Foley WJ (2000) Distribution of foliar formylated phloroglucinol derivatives amongst *Eucalyptus* species. Biochemical Systematics and Ecology **28:** 813–824

Eyles A, Davies NW, Mohammed C (2003) Novel detection of formylated phloroglucinol compounds (FPCs) in the wound wood of *Eucalyptus globulus* and *E. nitens*. Journal of Chemical Ecology **29:** 881–898

Eyles A, Davies NW, Mohammed CM (2004) Traumatic oil glands induced by pruning in the wound-associated phloem of *Eucalyptus globulus*: chemistry and histology. Trees - Structure and Function **18:** 204–210

Fähnrich A, Brosemann A, Teske L, Neumann M, Piechulla B (2012) Synthesis of 'cineole cassette' monoterpenes in *Nicotiana* section *Alatae*: gene isolation, expression, functional characterization and phylogenetic analysis. Plant Molecular Biology **79:** 537–553

Fähnrich A, Krause K, Piechulla B (2011) Product variability of the 'cineole cassette' monoterpene synthases of related *Nicotiana* species. Molecular Plant **4:** 965–984

Faqueti LG, Petry CM, Meyre-Silva C, Machado KE, Cruz AB, Garcia PA, Cechinel-Filho V, San Feliciano A, Delle Monache F (2013) Euglobal-like compounds from the genus *Eugenia*. Natural Product Research **27:** 28–31

Feijó JA, Moreno N (2004) Imaging plant cells by two-photon excitation. Protoplasma **223:** 1–32

Freeman JS, O'Reilly-Wapstra JM, Vaillancourt RE, Wiggins N, Potts BM (2008) Quantitative trait loci for key defensive compounds affecting herbivory of eucalypts in Australia. New Phytologist **178:** 846–851

Fujimoto Y, Usui S, Makino M, Sumatra M (1996) Phloroglucinols from *Baeckea frutescens*. Phytochemistry **41:** 923–925

Gachon CMM, Langlois-Meurinne M, Saindrenan P (2005) Plant secondary metabolism glycosyltransferases: the emerging functional analysis. Trends in Plant Science **10:** 542–549

Gershenzon J, McConkey ME, Croteau RB (2000) Regulation of monoterpene accumulation in leaves of peppermint. Plant Physiology **122:** 205–213

Ghirardo A, Koch K, Taipale R, Zimmer INA, Schnitzler JP, Rinne J (2010) Determination of *de novo* and pool emissions of terpenes from four common

boreal/alpine trees by $^{13}CO_2$ labelling and PTR-MS analysis. Plant, Cell and Environment **33:** 781–792

Ghisalberti EL (1996) Bioactive acylphloroglucinol derivatives from *Eucalyptus* species. Phytochemistry **41:** 7–22

Gill AM (1997) Eucalypts and fires: interdependent or dependent?In Jann Williams and John Woinarski , eds, *Eucalypt* ecology: individuals to ecosystems, 151–167. Cambridge: Cambridge University Press

Ginglinger JF, Boachon B, Höfer R, Paetz C, Köllner TG, Miesch L, Lugan R, Baltenweck R, Mutterer J, Ullmann P, Beran F, Claudel P, Verstappen F, Fischer MJC, Karst F, Bouwmeester H, Miesch M, Schneider B, Gershenzon J, Ehlting J, Werck-Reichhart D (2013) Gene coexpression analysis reveals complex metabolism of the monoterpene alcohol linalool in Arabidopsis flowers. The Plant Cell **25:** 4640–4657

Gleadow RM, Haburjak J, Dunn JE, Conn ME, Conn EE (2008) Frequency and distribution of cyanogenic glycosides in *Eucalyptus* L'Hérit. Phytochemistry **69:** 1870–1874

Gobbo-Neto L, Gates PJ, Lopes NP (2008) Negative ion chip-based nanospray tandem mass spectrometry for the analysis of flavonoids in glandular trichomes of *Lychnophora ericoides* Mart. (Asteraceae). Rapid Communications in Mass Spectrometry **22:** 3802–3808

Gog L, Berenbaum MR, DeLucia EH, Zangerl AR (2005) Autotoxic effects of essential oils on photosynthesis in parsley, parsnip, and rough lemon. Chemoecology **15:** 115–119

Goodger JQD, Cao B, Jayadi I, Williams SJ, Woodrow IE (2009) Non-volatile components of the essential oil secretory cavities of *Eucalyptus* leaves: discovery of two glucose monoterpene esters, cuniloside B and froggattiside A. Phytochemistry **70:** 1187–1194

Goodger JQD, Connelly CA, Woodrow IE (2007) Examination of the consistency of plant traits driving oil yield and quality in short-rotation coppice cultivation of *Eucalyptus polybractea*. Forest Ecology and Management **250:** 196–205

Goodger JQD, Heskes AM, King DJ, Gleadow RM, Woodrow IE (2008) Research note: Micropropagation of *Eucalyptus polybractea* selected for key essential oil traits. Functional Plant Biology **35:** 247–251

Goodger JQD, Heskes AM, Mitchell MC, King DJ, Neilson EH, Woodrow IE (2010) Isolation of intact sub-dermal secretory cavities from *Eucalyptus*. Plant Methods **6:** 20

Goodger JQD, Heskes AM, Woodrow IE (2013) Contrasting ontogentic trajectories for phenolic and terpenoid defences in *Eucalyptus froggattii*. Annals of Botany **112:** 651–659

Goodger JQD, Mitchell MC, Woodrow IE (2013) Differential patterns of mono- and sesquiterpenes with leaf ontogeny influence pharmaceutical oil yield in *Eucalyptus polybractea* R.T. Baker. Trees **27:** 511–521

Goodger JQD, Woodrow IE (2008) Selection gains for essential oil traits using micropropagation of Eucalyptus polybractea. Forest Ecology and Management **255:** 3652–3658

Goodger JQD, Woodrow IE (2009) The influence of ontogeny on essential oil traits when micropropagating *Eucalyptus polybractea*. Forest Ecology and Management **258:** 650–656

Goodger JQD, Woodrow IE (2011) α,β-Unsaturated monoterpene acid glucose esters: structural diversity, bioactivities and functional roles. Phytochemistry **72:** 2259–2266

Goodger JQD, Woodrow IE (2012) Genetic determinants of oil yield in *Eucalyptus polybractea* R.T. Baker. Trees **26:** 1951–1956

Goodger JQD, Woodrow IE (2013) Oleuropeic and menthiafolic acid glucose esters from plants: shared structural relationships and biological activitiesIn A. Rahman , eds, Studies in Natural Products Chemistry, volume 40, chapter Oleuropeic. Oxford: Elsevier

Gras EK, Read J, Mach CT, Sanson GD, Clissold FJ (2005) Herbivore damage, resource richness and putative defences in juvenile versus adult *Eucalyptus* leaves. Australian Journal of Botany **53:** 33–44

Groll M, Schellenberg B, Bachmann AS, Archer CR, Huber R, Powell TK, Lindow S, Kaiser M, Dudler R (2008) A plant pathogen virulence factor inhibits the eukaryotic proteasome by a novel mechanism. Nature **452:** 755–759

Guenther B, Monson K, Fall R (1991) Isoprene and monoterpene emission rate variability: observations with *Eucalyptus* and emission rate algorithm development. Journal of Geophysical Research **96:** 10799–10808

Guo QM, Yang XW (2006) Cypellocarpin C and other compounds from the fruits of *Eucalyptus globulus* Labill. Biochemical Systematics and Ecology **34:** 543–545

Hakki Z, Cao B, Heskes AM, Goodger JQD, Woodrow IE, Williams SJ (2010) Synthesis of the monoterpenoid esters cypellocarpin C and cuniloside B and evidence for their widespread occurrence in *Eucalyptus*. Carbohydrate Research **345:** 2079–2084

Hampel D, Mosandl A, Wüst M (2005) Biosynthesis of mono- and sesquiterpenes in carrot roots and leaves (*Daucus carota* L.): metabolic cross talk of cytosolic mevalonate and plastidial methylerythritol phosphate pathways. Phytochemistry **66:** 305–311

Hanawa F, Yamada T, Nakashima T (2001) Phytoalexins from *Pinus strobus* bark infected with pinewood nematode, *Bursaphelenchus xylophilus*. Phytochemistry **57:** 223–228

Hasegawa T, Takano F, Takata T, Niiyama M, Ohta T (2008) Bioactive monoterpene glycosides conjugated with gallic acid from the leaves of *Eucalyptus globulus*. Phytochemistry **69:** 747–753

He C, Murray F, Lyons T (2000) Monoterpene and isoprene emissions from 15 *Eucalyptus* species in Australia. Atmospheric Environment **34:** 645–655

Helmchen F, Denk W (2005) Deep tissue two-photon microscopy. Nature **2:** 932–940

Hemmerlin A, Harwood JL, Bach TJ (2012) A raison d'être for two distinct pathways in the early steps of plant isoprenoid biosynthesis? Progress in Lipid Research **51:** 95–148

Henery ML, Henson M, Wallis IR, Stone C, Foley WJ (2008) Predicting crown damage to *Eucalyptus grandis* by *Paropsis atomaria* with direct and indirect measures of leaf composition. Forest Ecology and Management **255:** 3642–3651

Henery ML, Moran GF, Wallis IR, Foley WJ (2007) Identification of quantitative trait loci influencing foliar concentrations of terpenes and formylated phloroglucinol compounds in *Eucalyptus nitens*. The New Phytologist **176:** 82–95

Henery ML, Wallis IR, Stone C, Foley WJ (2008) Methyl jasmonate does not induce changes in *Eucalyptus grandis* leaves that alter the effect of constitutive defences on larvae of a specialist herbivore. Oecologia **156:** 847–859

Heskes AM, Goodger JQD, Tsegay S, Quach T, Williams SJ, Woodrow IE (2012) Localization of oleuropeyl glucose esters and a flavanone to secretory cavities of Myrtaceae. PloS One **7:** e40856

Höfer R, Dong L, André F, Ginglinger JF, Lugan R, Gavira C, Grec S, Lang G, Memelink J, Van der Krol S, Bouwmeester H, Werck-Reichhart D (2013) Geraniol hydroxylase and hydroxygeraniol oxidase activities of the CYP76 family of cytochrome P450 enzymes and potential for engineering the early steps of the (seco)iridoid pathway. Metabolic Engineering **20:** 221–232

Horn DHS, Lamberton JA (1964) The occurence of 11,12-dehydroursolic lactone acetatein *Eucalyptus* waxes. Australian Journal of Chemistry **17:** 477–480

Hou AJ, Liu YZ, Yang H, Lin ZW, Sun HD (2000) Hydrolyzable tannins and related polyphenols from *Eucalyptus globulus*. Journal of Asian Natural Products Research **2:** 205–212

Huang M, Sanchez-Moreiras AM, Abel C, Sohrabi R, Lee S, Gershenzon J, Tholl D (2012) The major volatile organic compound emitted from *Arabidopsis thaliana* flowers,

the sesquiterpene (E)-β-caryophyllene, is a defense against a bacterial pathogen. The New Phytologist **193:** 997–1008

Hyodo S, Etoh H, Yamashita N, Sakata K, Ina K (1992) Structure of resinosides from *Eucalyptus resinifera* as repellents against the blue mussel, *Mytilus edulis*. Bioscience, Biotechnology and Biochemistry **56:** 138

Irmisch S, Krause ST, Kunert G, Gershenzon J, Degenhardt J, Köllner TG (2012) The organ-specific expression of terpene synthase genes contributes to the terpene hydrocarbon composition of chamomile essential oils. BMC Plant Biology **12:** 84

Ito H, Iwamori H, Kasajima N, Kaneda M, Yoshida T (2004) Kunzeanones A, B, and C: novel alkylated phloroglucinol metabolites from *Kunzea ambigua*. Tetrahedron **60:** 9971–9976

Ito H, Koreishi M, Tokuda H, Nishino H, Yoshida T (2000) Cypellocarpins A-C, phenol glycosides esterified with oleuropeic acid, from *Eucalyptus cypellocarpa*. Journal of Natural Products **63:** 1253–1257

James SA, Bell DT (2000) Leaf orientation, light interception and stomatal conductance of *Eucalyptus globulus* ssp. *globulus* leaves. Tree Physiology **20:** 815–823

Jones TH, Potts BM, Vaillancourt RE, Davies NW (2002) Genetic resistance of *Eucalyptus globulus* to autumn gum moth defoliation and the role of cuticular waxes. Canadian Journal of Forest Research **1969:** 1961–1969

Jung JH, Pummangura S, Chaichantipyuth C, Patarapanich C, McLaughlin JL (1990) Bioactive constituents of *Melodorum fruticosum*. Phytochemistry **29:** 1667–1670

Kasajima N, Ito H, Hatano T, Yoshida T, Kaneda M (2005) Cypellogins A, B and C, acylated flavonol glycosides from *Eucalyptus cypellocarpa*. Chemical and Pharmaceutical Bulletin **53:** 1345–1347

Keszei A, Brubaker CL, Carter R, Köllner T, Degenhardt J, Foley WJ (2010) Functional and evolutionary relationships between terpene synthases from Australian Myrtaceae. Phytochemistry **71:** 844–852

King DA (1997) The functional significance of leaf angle in *Eucalyptus*. Australian Journal of Botany **45:** 619–639

King DJ, Gleadow RM, Woodrow IE (2004) Terpene deployment in *Eucalyptus polybractea*; relationships with leaf structure, environmental stresses, and growth. Functional Plant Biology **31:** 451–460

King DJ, Gleadow RM, Woodrow IE (2006) Regulation of oil accumulation in single glands of *Eucalyptus polybractea*. The New Phytologist **172:** 440–451

King DJ, Gleadow RM, Woodrow IE (2006) The accumulation of terpenoid oils does not incur a growth cost in *Eucalyptus polybractea* seedlings. Functional Plant Biology **33:** 497–505

Kirkpatrick JB (1997) Vascular plant-eucalypt interactions.In Jann Williams and John Woinarski , eds, Eucalypt ecology: individuals to ecosystems, 226–245. Cambridge: Cambridge University Press

Klayman DL (1985) Qinghaosu (Artemisinin): an antimalarial drug from China. Science **228:** 1049–1055

Kliebenstein DJ (2012) Plant defense compounds: systems approaches to metabolic analysis. Annual Review of Phytopathology **50:** 155–173

Knight TG, Klieber A, Sedgley M (2002) Structural basis of the rind disorder oleocellosis in Washington Navel orange (*Citrus sinensis* L. Osbeck). Annals of Botany **90:** 765–773

Konoshima T, Takasaki M (2002) Chemistry and bioactivity of the non-volatile constituents of *Eucalyptus*In J J W Coppen , eds, *Eucalyptus*: the genus *Eucalyptus*, 269–290. London and New York: Taylor and Francis

Kouchi H, Nakaji K, Yoneyama T, Ishizuka J (1985) Dynamics of carbon photosynthetically assimilated in nodulated soya bean plants under steady-state conditions 3: time-course study on ^{13}C incorporation into soluble metabolites and respiratory evolution of CO_2 from roots and nodules. Annals of Botany **56:** 333–346

Kulheim C, Webb H, Yeoh SH, Wallis IR, Moran G, Foley WJ (2011) Using the *Eucalyptus* genome to understand the evolution of plant secondary metabolites in the Myrtaceae. BMC Proceedings **5:** O11

Külheim C, Yeoh SH, Wallis IR, Laffan S, Moran GF, Foley WJ (2011) The molecular basis of quantitative variation in foliar secondary metabolites in *Eucalyptus globulus*. The New Phytologist **191:** 1041–1053

Ladiges PY (1997) Phylogenetic history and classification of eucalyptsIn Jann Williams and John Woinarski , eds, Eucalypt ecology: individuals to ecosystems, 16–29. Cambridge: Cambridge University Press

Ladiges PY, Udovicic F (2000) Comment on a new classification of the eucalypts. Australian Systematic Botany **13:** 149–152

Lange BM, Turner GW (2013) Terpenoid biosynthesis in trichomes- current status and future opportunities. Plant Biotechnology Journal **11:** 2–22

Lawler IR, Stapley J, Foley WJ, Eschler BM (1999) Ecological example of conditioned flavor aversion in plant-herbivore interactions: effect of terpenes of *Eucalyptus* leaves on feeding by common ringtail and brushtail possums. Journal of Chemical Ecology **25:** 401–416

Leivar P, Gonzalez VM, Castel S, Trelease RN, Lopez-Iglesias C, Arro M, Boronat A, Campos N, Ferrer A, Fernandez-Busquets X (2005) Subcellular localization of Arabidopsis 3-hydroxy-3-methylglutaryl-coenzyme A reductase. Plant Physiology **137:** 57–69

Li H, Madden JL, Potts BM (1995) Variation in volatile leaf oils of the Tasmanian *Eucalyptus* I. subgenus *Monocalyptus*. Biochemical Systematics and Ecology **23:** 299–318

Li H, Madden JL, Potts BM (1997) Variation in leaf waxes of the Tasmanian *Eucalyptus* species I. subgenus *Symphyomyrtus*. Biochemical Systematics and Ecology **25:** 631–657

Liang P, Ko T, Wang AHJ (2002) Structure, mechanism and function of prenyltransferases. European Journal of Biochemistry **269:** 3339–3354

List S, Brown PH, Walsh KB (1995) Functional anatomy of the oil glands of *Melaleuca alternifolia* (Myrtaceae). Australian Journal of Botany **43:** 629–641

Litvak ME, Monson RK (1998) Patterns of induced and constitutive monoterpene production in conifer needles in relation to insect herbivory. Oecologia **114:** 531–540

Loney PE, McArthur C, Potts BM, Jordan GJ (2006) How does ontogeny in a *Eucalyptus* species affect patterns of herbivory by Brushtail Possums? Functional Ecology **20:** 982–988

Loreto F, Förster A, Dürr M, Csiky O, Seufert G (1998) On the monoterpene emission under heat stress and on the increased thermotolerance of leaves of *Quercus ilex* L . fumigated with selected monoterpenes. Plant, Cell and Environment **21:** 101–107

Loreto F, Pinelli P, Manes F, Kollist H (2004) Impact of ozone on monoterpene emissions and evidence for an isoprene-like antioxidant action of monoterpenes emitted by *Quercus ilex* leaves. Tree Physiology **24:** 361–367

Loreto F, Schnitzler JP (2010) Abiotic stresses and induced BVOCs. Trends in Plant Science **15:** 154–166

Loreto F, Velikova V (2001) Isoprene produced by leaves protects the photosynthetic apparatus against ozone damage, quenches ozone products, and reduces lipid peroxidation of cellular membranes. Plant Physiology **127:** 1781–1787

Lucker, Schwab W, Hautum BV, Blaas J, van der Plas LHW, Bouwmeester HJ, Verhoeven HA (2004) Increased and altered fragrance of tobacco plants after metabolic engineering using three monoterpene synthases from lemon. Plant Physiology **134:** 510–519

Lücker J, Schwab W, Franssen MCR, Van Der Plas LHW, Bouwmeester HJ, Verhoeven HA (2004) Metabolic engineering of monoterpene biosynthesis: two-step production of (+)-trans-isopiperitenol by tobacco. The Plant Journal **39:** 135–145

Maffei M, Camusso W, Sacco S (2001) Effect of *Mentha* x *piperita* essential oil and monoterpenes on cucumber root membrane potential. Phytochemistry **58:** 703–707

Majdi M, Liu Q, Karimzadeh G, Malboobi MA, Beekwilder J, Cankar K, Vos RD, Todorović S, Simonović A, Bouwmeester HJ (2011) Biosynthesis and localization of parthenolide in glandular trichomes of feverfew (*Tanacetum parthenium* L. Schulz Bip.). Phytochemistry **72:** 1739–1750

Manns D, Hartmann R (1994) Monoterpene glucosides from *Cunila spicata*. Planta Medica **60:** 467–469

Martin DM, Aubourg S, Schouwey MB, Daviet L, Schalk M, Toub O, Lund ST, Bohlmann J (2010) Functional annotation, genome organization and phylogeny of the grapevine (*Vitis vinifera*) terpene synthase gene family based on genome assembly, FLcDNA cloning, and enzyme assays. BMC Plant Biology **10:** e226

Martins CBC, Zarbin PHG (2013) Volatile organic compounds of conspecific-damaged *Eucalyptus benthamii* influence responses of mated females of *Thaumastocoris peregrinus*. Journal of Chemical Ecology **39:** 602–611

Matsuki M, Foley WJ, Floyd RB (2011) Role of volatile and non-volatile plant secondary metabolites in host tree selection by Christmas beetles. Journal of Chemical Ecology **37:** 286–300

Mau CJD, Croteau R (2006) Cytochrome P450 oxygenases of monoterpene metabolism. Phytochemistry Reviews **5:** 373–383

McArthur C, Loney PE, Davies NW, Jordan GJ (2010) Early ontogenetic trajectories vary among defence chemicals in seedlings of a fast-growing eucalypt. Austral Ecology **35:** 157–166

McConkey ME, Gershenzon J, Croteau RB (2000) Developmental regulation of monoterpene biosynthesis in the glandular trichomes of peppermint. Plant Physiology **122:** 215–223

McDermitt DK, Welles JM, Eckles RD (1993) Effects of temperature, pressure and water vapor on gas phase infrared absorption by CO_2. LI-COR Technical Publication **116:** 1–5

Medina E, Garcia V, Cuevas E (1990) Sclerophylly and oligotrophic environments: relationships between leaf structure, mineral nutrient content, and drought resistance in tropical rain forests of the upper Rio Negro region. Biotropica **22:** 51–64

Merchant A, Richter A, Popp M, Adams M (2006) Targeted metabolite profiling provides a functional link among eucalypt taxonomy, physiology and evolution. Phytochemistry **67:** 402–408

Miller B, Madilao LL, Ralph S, Bohlmann J (2005) Insect-induced conifer defense. White pine weevil and methyl jasmonate induce traumatic resinosis, *de novo* formed volatile emissions, and accumulation of terpenoid synthase and putative octadecanoid pathway transcripts in Sitka spruce. Plant Physiology **137:** 369–382

Moore BD, Foley WJ (2005) Tree use by koalas in a chemically complex landscape. Nature **435:** 488–490

Moore BD, Wallis IR, Palá-Paul J, Brophy JJ, Willis RH, Foley WJ (2004) Antiherbivore chemistry of *Eucalyptus*- cues and deterrents for marsupial folivores. Journal of Chemical Ecology **30:** 1743–1769

Moore BD, Wallis IR, Wood JT, Foley WJ (2004) Foliar nutrition, site quality, and temperature influence folair chemistry of tallowood (*Eucalyptus microcorys*). Ecological Monographs **74:** 553–568

Morales F, Cartelat A, Alvarez-Fernández A, Moya I, Cerovic ZG (2005) Time-resolved spectral studies of blue-green fluorescence of artichoke (*Cynara cardunculus* L. var. *scolymus*) leaves: identification of chlorogenic acid as one of the major fluorophores and age-mediated changes. Journal of Agricultural and Food Chemistry **53:** 9668–9678

Mueller MJ, Berger S (2009) Reactive electrophilic oxylipins: pattern recognition and signalling. Phytochemistry **70:** 1511–1521

Mumm R, Schrank K, Wegener R, Schulz S, Hilker M (2003) Chemical analysis of volatiles emitted by *Pinus sylvestris* after induction by insect oviposition. Journal of Chemical Ecology **29:** 1235–1252

Nakanishi T, Iida N, Inatomi Y, Murata H, Inada A, Murata J, Lang FA, Iinuma M, Tanaka T, Sakagami Y (2005) A monoterpene glucoside and three megastigmane glycosides from *Juniperus communis* var. depressa. Chemical and Pharmaceutical Bulletin **53:** 783–787

Nelson D, Werck-Reichhart D (2011) A P450-centric view of plant evolution. The Plant Journal **66:** 194–211

Nguyen DT, Göpfert JC, Ikezawa N, Macnevin G, Kathiresan M, Conrad J, Spring O, Ro DK (2010) Biochemical conservation and evolution of germacrene A oxidase in Asteraceae. The Journal of Biological Chemistry **285:** 16588–16598

Nishida Nami, Tamotsu Satoshi, Nagata Noriko, Saito Chieko, Sakai Atsushi (2005) Allelopathic effects of volatile monoterpenoids produced by *Salvia leucophylla*: inhibition of cell proliferation and DNA synthesis in the root apical meristem of *Brassica campestris* seedlings. Journal of Chemical Ecology **31:** 1187–1203

O'Reilly-Wapstra JM, Freeman JS, Davies NW, Vaillancourt RE, Fitzgerald H, Potts BM (2011) Quantitative trait loci for foliar terpenes in a global eucalypt species. Tree Genetics and Genomes **7:** 485–498

O'Reilly-Wapstra JM, Humphreys JR, Potts BM (2007) Stability of genetic-based defensive chemistry across life stages in a *Eucalyptus* species. Journal of Chemical Ecology **33:** 1876–1884

O'Reilly-Wapstra JM, McArthur C, Potts BM (2004) Linking plant genotype, plant defensive chemistry and mammal browsing in a *Eucalyptus* species. Functional Ecology **18:** 677–684

O'Reilly-Wapstra JM, Miller AM, Hamilton MG, Williams D, Glancy-Dean N, Potts BM (2013) Chemical variation in a dominant tree species: population divergence, selection and genetic stability across environments. PloS One **8:** e58416

O'Reilly-Wapstra JM, Potts BM, McArthur C, Davies NW (2005) Effects of nutrient variability on the genetic-based resistance of *Eucalyptus globulus* to a mammalian herbivore and on plant defensive chemistry. Oecologia **142:** 597–605

Padovan A, Keszei A, Köllner TG, Degenhardt J, Foley WJ (2010) The molecular basis of host plant selection in *Melaleuca quinquenervia* by a successful biological control agent. Phytochemistry **71:** 1237–1244

Padovan A, Keszei A, Külheim C, Foley WJ (2013) The evolution of foliar terpene diversity in Myrtaceae. Phytochemistry Reviews **In Press**

Padovan A, Keszei A, Wallis IR, Foley WJ (2012) Mosaic eucalypt trees suggest genetic control at a point that influences several metabolic pathways. Journal of Chemical Ecology **38:** 914–923

Pass DM, Foley WJ, Bowden B (1998) Vertebrate herbivory on *Eucalyptus*- identification of specific feeding deterrents for common ringtail possums (*Pseudocheirus peregrinus*) by bioassay-guided fractionations of *Eucalyptus ovata* foliage. Journal of Chemical Ecology **24:** 1513–1527

Pereira SI, Freire CSR, Neto CP, Silvestre AJD, Silva AMS (2005) Chemical composition of the epicuticular wax from the fruits of *Eucalyptus globulus*. Phytochemical Analysis **369:** 364–369

Proksch M, Weissenböck G, Rodriguez E (1985) Flavonoids and phenolic acids in Adenostoma, a dominant genus of the californian chaparral. Phytochemistry **24:** 2889–2891

Ramsay JR, Suhrbier A, Aylward JH, Ogbourne S, Cozzi S, Poulsen MG, Baumann KC, Welburn P, Redlich GL, Parsons PG (2011) The sap from *Euphorbia peplus* is effective against human nonmelanoma skin cancers. British Journal of Dermatology **164:** 633–636

Rapley LP, Allen GR, Potts BM, Davies NW (2007) Constitutive or induced defences - how does *Eucalyptus globulus* defend itself from larval feeding? Chemoecology **243:** 235–243

Rasmann S, Köllner TG, Degenhardt J, Hiltpold I, Toepfer S, Kuhlmann U, Gershenzon J, Turlings TCJ (2005) Recruitment of entomopathogenic nematodes by insect-damaged maize roots. Nature **434:** 732–737

Rios-Estepa R, Turner GW, Lee JM, Croteau RB, Lange BM (2008) A systems biology approach identifies the biochemical mechanisms regulating monoterpenoid essential oil composition in peppermint. Proceedings of the National Academy of Sciences **105:** 2818–2823

Rodríguez Ana, San Andrés Victoria, Cervera Magdalena, Redondo Ana, Alquézar Berta, Shimada Takehiko, Gadea José, Rodrigo MaríaJesús, Zacarías Lorenzo, Palou Lluís, López MaríaM, Castañera Pedro, Peña Leandro (2011) Terpene down-regulation in orange reveals the role of fruit aromas in mediating interactions with insect herbivores and pathogens. Plant Physiology **156:** 793–802

Rodríguez-Concepción M (2006) Early steps in isoprenoid biosynthesis: multilevel regulation of the supply of common precursors in plant cells. Phytochemistry Reviews **5:** 1–15

Rodriguez-Concepcion M, Boronat A (2002) Elucidation of the methylerythritol phosphate pathway for isoprenoid biosynthesis in bacteria and plastids. A metabolic milestone achieved through genomics. Plant Physiology **130:** 1079–1089

Salleo S, Nardini A, Lo Gullo MA (1997) Is sclerophylly of Mediterranean evergreens an adaptation to drought? New Phytologist **135:** 603–612

Scarpati ML, Trogolo C (1966) 6-O-Oleuropeoylsucrose from *Olea europaea*. Tetrahedron Letters **46:** 5673–5674

Schnee C, Köllner TG, Gershenzon J (2002) The maize gene terpene synthase 1 encodes a sesquiterpene synthase catalyzing the formation of (E)-β-farnesene, (E)-nerolidol, and (E,E)-farnesol after herbivore damage. Plant Physiology **130:** 2049–2060

Schnee C, Köllner TG, Held M, Turlings TCJ, Gershenzon J, Degenhardt J (2007) The products of a single maize sesquiterpene synthase form a volatile defense signal that attracts natural enemies of maize herbivores. Proceedings of the National Academy of Sciences **103:** 1129–1134

Schneider CA, Rasband WS, Eliceiri KW (2012) NIH Image to ImageJ: 25 years of image analysis. Nature Methods **9:** 671–675

Shain L, Miller JB (1982) Pinocembrin: an antifungal compound secreted by leaf glands of eastern cottonwood. Phytopathology **72:** 877–880

Shepherd M, Chaparro JX, Teasdale R (1999) Genetic mapping of monoterpene composition in an interspecific eucalypt hybrid. Theoretical and Applied Genetics **99:** 1207–1215

Sidana J, Singh S, Arora SK, Foley WJ, Singh IP (2012) Terpenoidal constituents of *Eucalyptus loxophleba* ssp. *lissophloia*. Pharmaceutical Biology **50:** 823–827

Simkin AJ, Guirimand G, Papon N, Courdavault V, Thabet I, Ginis O, Bouzid S, Giglioli-Guivarc'h N, Clastre M (2011) Peroxisomal localisation of the final steps of the mevalonic acid pathway *in planta*. Planta **234:** 903–14

Singh IP, Bharate SB (2006) Phloroglucinol compounds of natural origin. Natural Product Reports **23:** 558–591

Sirikantaramas S, Taura F, Tanaka Y, Ishikawa Y, Morimoto S, Shoyama Y (2005) Tetrahydrocannabinolic acid synthase, the enzyme controlling marijuana psychoactivity, is secreted into the storage cavity of the glandular trichomes. Plant and Cell Physiology **46:** 1578–1582

Sirikantaramas S, Yamazaki M, Saito K (2007) Mechanisms of resistance to self-produced toxic secondary metabolites in plants. Phytochemistry Reviews **7:** 467–477

Staudt M, Bertin N (1998) Light and temperature dependence of the emission of cyclic and acyclic monoterpenes from holm oak (*Quercus ilex* L.) leaves. Plant, Cell and Environment **21:** 385–395

Steane DA, Nicolle D, McKinnon GE, Vaillancourt RE, Potts BM (2002) Higher-level relationships among the eucalypts are resolved by ITS-sequence data. Australian Systematic Botany **15:** 49–62

Stone C, Bacon PE (1994) Relationships among moisture stress, insect herbivory, foliar cineole content and the growth of River Red Gum Eucalyptus camaldulensis. Journal of Applied Ecology **31:** 604–612

Stone C, Simpson JA, Gittins R (1998) Differential impact of insect herbivores and fungal pathogens on the *Eucalyptus* subgenera *Symphyomyrtus* and *Monocalyptus* and genus *Corymbia*. Australian Journal of Botany **46:** 723–734

Street RA, Hewitt CN, Mennicken S (1997) Isoprene and monoterpene emissions from a *Eucalyptus* plantation in Portugal. Journal of Geophysical Research **102:** 875–887

Suhling K, Levitt JA, Chung PH, Kuimova MK, Yahioglu G (2012) Fluorescence lifetime imaging of molecular rotors in living cells. Journal of Visualized Experiments **60:** e2925

Suhling K, Siegel J, Lanigan PMP, Lévêque-Fort S, Webb SED, Phillips D, Davis DM, French PMW (2004) Time-resolved fluorescence anisotropy imaging applied to live cells. Optics Letters **29:** 584–586

Tanahashi T, Shimada A, Nagakura N, Inoue K, Ono M, Fujita T, Chen CC (1995) Structure elucidation of six acylated iridoid glucosides from *Jasminum hemsleyi*. Chemical and Pharmaceutical Bulletin **43:** 729–733

Tian LW, Zhang YJ, Wang YF, Lai CC, Yang CR (2009) Eucalmaidins A-E, (+)-oleuropeic acid derivatives from the fresh leaves of *Eucalyptus maidenii*. Journal of Natural Products **72:** 1608–11

Tucker DJ, Wallis IR, Bolton JM, Marsh KJ, Rosser AA, Brereton IM, Nicolle D, Foley WJ (2010) A Metabolomic approach to identifying chemical mediators of mammal plant interactions. Journal of Chemical Ecology **36:** 727–735

Tuominen LK, Johnson VE, Tsai CJ (2011) Differential phylogenetic expansions in BAHD acyltransferases across five angiosperm taxa and evidence of divergent expression among *Populus* paralogues. BMC Genomics **12:** 236

Turner GW, Berry AM, Gifford EM (1998) Schizogenous secretory cavities of *Citrus limon* (L.) Burm. F. and a reevaluation of the lysigenous gland concept. International Journal of Plant Sciences **159:** 75–88

Turner GW, Croteau RB (2004) Organization of monoterpene biosynthesis in Mentha. Immunocytochemical localizations of geranyl diphosphate synthase, limonene-6-hydroxylase, isopiperitenol dehydrogenase, and pulegone reductase. Plant Physiology **136:** 4215–4227

Turner GW, Gershenzon J, Croteau RB (2000) Development of peltate glandular trichomes of peppermint. Plant Physiology **124:** 665–679

Voo SS, Grimes HD, Lange BM (2012) Assessing the biosynthetic capabilities of secretory glands in *Citrus* peel. Plant Physiology **159:** 81–94

Vranová E, Coman D, Gruissem W (2013) Network analysis of the MVA and MEP pathways for isoprenoid synthesis. Annual Review of Plant Biology **64:** 665–700

Vroom JM, Grauw KJD, Gerritsen HC, Bradshaw DJ, Marsh PD, Watson GK, Birmingham J, Allison C, Grauw KJDE (1999) Depth penetration and detection of pH gradients in biofilms by two-photon excitation microscopy. Applied and Environmental Microbiology **65:** 3502–3511

Wallis IR, Keszei A, Henery ML, Moran GF, Forrester R, Maintz J, Marsh KJ, Andrew RoseL., Foley WilliamJ. (2011) A chemical perspective on the evolution of variation in *Eucalyptus globulus*. Perspectives in Plant Ecology, Evolution and Systematics **13:** 305–318

Wallis IR, Smith HJ, Henery ML, Henson M, Foley WJ (2010) Foliar chemistry of juvenile *Eucalyptus grandis* clones does not predict chemical defence in maturing ramets. Forest Ecology and Management **260:** 763–769

Wang G, Tian L, Aziz N, Broun P, Dai X, He Ji, King A, Zhao PX, Dixon RA (2008) Terpene biosynthesis in glandular trichomes of hop. Plant physiology **148:** 1254–1266

Wang H, Fujimoto Y (1993) Triterpene esters from *Eucalyptus tereticornis*. Phytochemistry **33:** 151–153

Wardell-Johnson GW, Williams JE, Hill KD, Cumming R (1997) Evolutionary biogeography and contemporary distribution of eucalyptsIn Jann Williams and John Woinarski , eds, Eucalypt ecology: individuals to ecosystems, 92–128. Cambridge: Cambridge University Press

Webb H, Lanfear R, Hamill J, Foley WJ, Külheim C (2013) The yield of essential oils in *Melaleuca alternifolia* (Myrtaceae) is regulated through transcript abundance of genes in the MEP pathway. PloS One **8:** e60631

Wiggins NL, Mcarthur C, Mclean S, Boyle R (2003) Effects of two plant secondary metabolites, cineole and gallic acid, on the nightly feeding patterns of the common bruxhtail possum. Journal of Chemical Ecology **29:** 1447–1464

Winters AJ, (2010) The composition and emission of volatile organic compounds in *Eucalyptus* spp. leaves. PhD Thesis. Sydney, University of New South Wales

Winters AJ, Adams MA, Bleby TM, Rennenberg H, Steigner D, Steinbrecher R, Kreuzwieser J (2009) Emissions of isoprene, monoterpene and short-chained carbonyl compounds from *Eucalyptus* spp. in southern Australia. Atmospheric Environment **43:** 3035–3043

Wollenweber E, Seigler DS (1982) Flavonoids from the exudate of *Acacia neovernicosa*. Phytochemistry **21:** 1063–1066

Wright GA, Lutmerding A, Dudareva N, Smith BH (2005) Intensity and the ratios of compounds in the scent of snapdragon flowers affect scent discrimination by honeybees (*Apis mellifera*). Journal of Comparative Physiology A **191:** 105–114

Wright IJ, Westoby M (2002) Leaves at low versus high rainfall: coordination of structure, lifespan and physiology. New Phytologist **155:** 403–416

Wu B, Yu L, Wu X, Chen J (2012) New $CuCl_2$-induced glucoside esters and other constituents from *Portucala oleracea*. Carbohydrate Research **351:** 68–73

Yoshimura H, Sawai Y, Tamotsu S, Sakai A (2011) 1,8-cineole inhibits both proliferation and elongation of BY-2 cultured tobacco cells. Journal of Chemical Ecology **37:** 320–328

Youngentob KN, Wallis IR, Lindenmayer DB, Wood JT, Pope ML, Foley WJ (2011) Foliage chemistry influences tree choice and landscape use of a gliding marsupial folivore. Journal of Chemical Ecology **37:** 71–84

Yuan Y, Yang QY, Tong YF, Chen F, Qi Y, Duan YB, Wu S (2008) Synthesis and enantiomeric resolution of (±)-pinocembrin. Journal of Asian Natural Product Research **10:** 999–1002

Zulak KG, Bohlmann J (2010) Terpenoid biosynthesis and specialized vascular cells of conifer defense. Journal of Integrative Plant Biology **52:** 86–97

Zwenger S, Basu C (2008) Plant terpenoids: applications and future potentials. Biotechnology and Molecular Biology Reviews **3:** 1–7

Appendix A

NMR and IR results are reproduced from Heskes *et al.* (2012).

IR, ^{1}H and ^{13}C NMR data for eucaglobulin B: $[\alpha]_D^{23}$ +8.9 (c 0.04, CHCl3); IR v 3380, 2937, 1703, 1599, 1462, 1426, 1337, 1257, 1216, 1185, 1070, 1035, 762 cm^{-1}; ^{1}H NMR (600 MHz, d_4-MeOH) δ 7.41 (s, 2 H, ArH), 7.03-7.02 (m, 1H, H2″), 5.68-5.67 (m, 1H, H1′), 4.45 (dd, J=12.0, 1.8 Hz, 1H, H6′), 4.27 (dd, J=12.0, 5.4 Hz, 1H, H6′), 3.90 (s, 6H, OMe), 3.70-3.67 (m, 1H, H5′), 3.54-3.49 (m, 2H, H2′,3′), 3.46-3.42 (m, 1H, H4′), 3.33 (m, 1H, H2′), 2.51-2.47 (m, 1H, H6″), 2.39-2.31 (m, 1H, H3″), 2.17-2.10 (m, 1H, H6″), 2.04-1.98 (m, 2H, H5″/ H3″), 1.56-1.51 (m, 1H, H4″), 1.20 (dd, J=12.6, 4.8 Hz, 1H, H5″), 1.17 (2 s, 2×3H, H9″,H10″); ^{13}C NMR (200 MHz, d_4-methanol) δ 167.33 (C7″), 165.13 (C7), 147.37 (C3), 141.18 (C4), 129.59 (C1″), 118.87 (C1), 107.18 (C2), 104.75 (C2″), 94.55 (C1′), 44.13 (C6″), 27.13 (C5″), 25.34 (C4″) (Note: Owing to the small amount of material available, the reported ^{13}C data was obtained from HMBC spectrum. Non-ambiguous data could not be obtained for the following carbons: C3″,C8″,C9″,C2′,C3′,C4′,C5′,C6′.). HR-FTMS-ESI gave a ions of m/z: 544.2378 $[M+NH_4]^+$ (calcd. 544.2399 for $C_25H_38O_12NH_4$) and m/z 549.1935 $[M+Na]^+$ (calcd. 549.1953 for $C_25H_34O_12Na$). MS^2 fragmentation of $[M+NH_4]^+$: 311.1488 (100); 509.2015 (53); 491.1909 (39); 329.1595 (21); 347.1490 (7); 275.1278 (6); 293.1383 (6); 167.1066 (6).

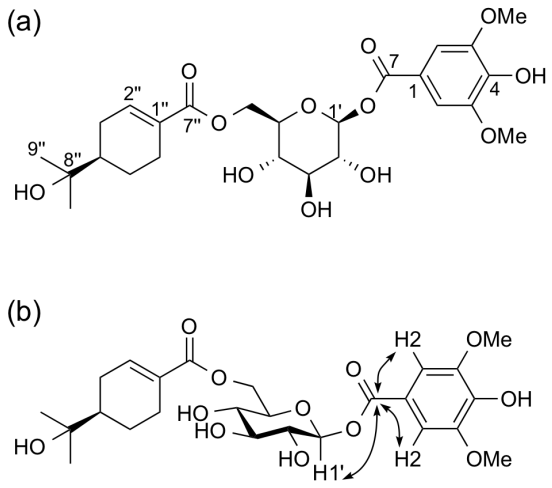

Figure A.1: Structure of the new monoterpene-acid sugar ester eucaglobulin B (a) with key HMBC correlations (b).

^{1}H and ^{13}C NMR data for pinocembrin: $[\alpha]_D^{22}$ –64.6° (c 0.025 in acetone). Lit. Yuan *et al.* (2008) −45.3° (c 0.9 in acetone, 15°C); lit. Jung *et al.* (1990) −45.6° (c 0.5 in MeOH); ^{1}H NMR ($CDCl_3$, 500 MHz) δ 12.04 (s, 1H, 5-OH), 7.47-7.38 (m, 5H, Ar), 6.00 (ABq, J = 2.5 Hz, 2H, H6 and H8), 5.43 (dd, J = 12.5, 3.0 Hz, 1H, H2), 3.09 (dd, J = 17.0, 13.0 Hz, 1H, H3b), 2.83 (dd, J = 17.0, 3.0 Hz, 1H, H3b). This data is consistent with that reported in Jung *et al.* (1990); ^{1}H NMR (d_6-acetone, 500 MHz) δ 12.19 (br s, 1H, 5-OH), 7.57-7.55 (m, 3H, Ar), 7.46-7.38 (m, 2H, Ar), 5.96 (d, J = 2.0 Hz, 1H, H8), 5.92 (d, J = 2.0 Hz, 1H, H6), 5.54 (dd, J = 12.5, 3.2 Hz, 1H, H2), 3.12 (dd, J = 17.0, 12.5 Hz, 1H, H3a), 2.77 (dd, J = 17.0, 3.2 Hz, 1H, H3b); 13C NMR (d_6-acetone, 150 MHz) δ 140.0 (C1′), 129.4 (C3′), 129.2 (C4′), 127.2 (C2′), 97.4 (C6), 96.5 (C8), 79.7 (C2), 43.6 (C3) (Note: No signals were observed for the quaternary carbons in the ^{13}C NMR spectrum due to the low concentration of the sample; however, the non-quaternary signals in the ^{13}C NMR spectrum and all the signals in the ^{1}H NMR spectrum were consistent with literature values Jung *et al.* (1990)). HR-FTMS-ESI gave an ion of m/z: 255.0661 $[M\text{-}H]^-$ (calcd. 255.0663 for $C_{15}H_{11}O_4$). MS^2 fragmentation of $[M\text{-}H]^-$: 213.0551 (100); 151.0032 (97); 187.0761 (48); 211.0760 (35); 169.0655 (30); 183.0813 (21).

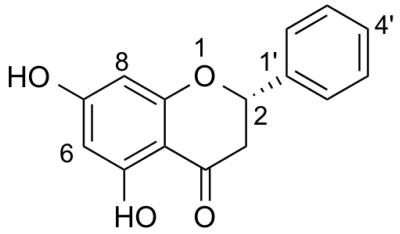

Figure A.2: Structure of pinocembrin: the flavanone localised to the oil glands of species from the subgenus *Eucalyptus*.